

UNIVERSIDADE DE LISBOA
FACULDADE DE CIÊNCIAS
DEPARTAMENTO DE ENGENHARIA GEOGRÁFICA, GEOFÍSICA E ENERGIA



Urban Load Optimization based on Agent-Based Model representation

Guilherme Pontes Luz

Mestrado Integrado em Engenharia da Energia e do Ambiente

Dissertação orientada por:
Professora Doutora Ana Estanqueiro (FCUL/LNEG)
Doutor Joaquim Duque (LNEG)

Agradecimentos

Quero, em primeiro lugar, agradecer ao Doutor Joaquim Duque e à Professora Ana Estanqueiro por me terem proposto este trabalho e aceitado a sua orientação. Em particular, às inúmeras sessões de discussão e trabalho com o Doutor Joaquim Duque sobre otimização e agentes mas também sobre o futuro do sistema energético bem como os sinuosos caminhos dos tempos que correm. De facto, é impossível pensar no futuro da energia sem pensar em tudo o resto.

Agradeço também ao professor Luis Moniz da FCUL que prontamente se disponibilizou para responder às minhas questões e me forneceu valiosas informações e reflexões para o trabalho. Quero ainda deixar um especial e grande agradecimento ao Carlos Jorge Luz (meu tio e professor) por se ter disponibilizado para discutir comigo não só o meu trabalho mas as inúmeras inquietações que correm na alma de quem se inicia no fantástico mundo da otimização matemática. Deixo ainda uma especial saudação e agradecimento ao professor Miguel Centeno Brito por ter estado presente e disponível durante todos os anos do curso que agora finda.

Agradeço ainda aos meus companheiros de viagem: Ricardo Moura, Vando Daniel, João Cravinho, Tomás Pedrosa e Ivo Félix.

À minha Mãe, aos meus irmãos, ao Samuelzinho, ao meu Pai e ao Rolandinho que havia de gozar comigo no dia de hoje. Ao Jorge Rodrigues e à Luisa Martins. Aos sempre presentes Coltrane e Bi-llevans, aos livres deste mundo e aos que sonham com um novo modelo e sistema energético. Por fim, agradeço à linda Inês, companheira de vida e audaz domadora de universos. Não só por caminharmos juntos mas por desenharmos caminhos e mapas.

Abstract

The energy system is expected to go through a phase change in coming years as distributed generation, demand flexibility and SmartGrid features gets implemented. The main driver for this process, climate change, imposes constraints on energy production and consumption making energy transition extremely urgent. Simultaneously, new players, entities and business models have emerged at almost all levels of the energy chain from production, transmission, distribution and commercialization down to power grid management driven by the unbundling process and the call for a more decentralized and horizontal energy system. The combined effect of this new *energy landscape* makes new system's architectures and functionalities desirable and possible, but poses huge physical, mathematical, engineering, economic and political questions and problems that need to be tackled. *Load Management* is one broad term depicting *Demand-Side Management* and *Demand Response* mechanisms and is one of the pressing problems on smart energy systems. To solve them, a plethora of computational and mathematical methods have been proposed in recent years. Distributed optimization and intelligence, software agents, agent-based systems and game theory are among the tools used to optimize load consumption and determine optimal device scheduling for residential, commercial and industrial power consumers

Following previous work found in literature, the present work proposes a general framework to treat the load optimization problem using agent-based architectures and models. We start by defining agents at critical points within the power grid as well as their internal reasoning process depicted by mathematical optimization models. We then proceed to model the cooperative interactions between agents as a Bi-level game between a grid entity and typified power consumers in order to coordinate the charging of several appliances and electrical vehicles and determine a feasible solution for the global system. We show the general functionality of the framework by implementing it in software and applying it to specific datasets. The framework is suitable for further refinement and development when applied to real world problems.

Keywords: Agents, Optimization, Bi-level game, Demand Response, Demand-Side Management

Resumo

O sistema energético atravessará uma profunda transformação nos próximos anos à medida que a produção renovável distribuída, a flexibilidade no lado do consumo e as funcionalidades de *SmartGrid* são implementadas. Este processo, conduzido em grande parte pelas imposições causadas pelos efeitos das alterações climáticas, implica profundas transformações na produção e consumo de energia e torna a transição energética extremamente urgente. Simultaneamente, novos *players*, entidades e modelos de negócio têm emergido em quase todos os níveis da cadeia energética desde a produção, a transmissão, distribuição e comercialização até à gestão da rede elétrica, num movimento conduzido pelo processo de particionamento (unbundling) do sistema elétrico e pela exigência de um sistema mais descentralizado e horizontal. O efeito combinado desta nova *paisagem energética* torna possíveis novas funcionalidades e arquiteturas de sistema na mesma medida em que coloca enormes problemas de natureza física e matemática mas também enormes questões económicas, sociais e políticas que terão, necessariamente, de ser abordadas e resolvidas. A *Gestão do Consumo* é um termo abrangente que representa tanto os mecanismos de *Resposta na Procura* (Demand Response) ou a *Gestão no Lado da Procura* (Demand-Side Management) e que se impõe como um dos problemas actuais mais importantes em sistemas energéticos inteligentes caracterizados por altas penetrações renováveis e mecanismos de mercado. Para resolver estes problemas, um conjunto de métodos matemáticos e computacionais têm sido propostos nos últimos anos. Otimização distribuída e sistemas inteligentes, sistemas baseados em agentes de software e teoria de jogos encontram-se entre algumas das ferramentas usadas para otimizar o consumo de energia e determinar o agendamento e a alocação ótima de equipamentos e máquinas para consumidores residenciais, comerciais e industriais.

Na sequência de trabalhos prévios disponíveis na literatura da especialidade, o presente trabalho propõe um modelo geral para abordar o problema da otimização de cargas através de arquiteturas e métodos baseados no paradigma dos *Agentes*. O trabalho começa por definir agentes em pontos críticos da rede elétrica e os seus processos internos de raciocínio representados por modelos de otimização matemática. Seguidamente as interações entre agentes são modeladas como um jogo de dois níveis (bi-level game) entre uma entidade gestora da rede e consumidores de energia tipificados de forma a coordenar o carregamento de diversos equipamentos, incluindo veículos elétricos, e determinar uma solução admissível para o sistema global. A funcionalidade geral do modelo proposto é demonstrada através da sua implementação em software proprietário e recorrendo a um conjunto de dados específicos. Está, então, pronto para ser complementado e refinado no futuro de forma a ser aplicado em problemas do mundo real, de grandes dimensões, mas também novas implementações em software *open source* de forma a ficar acessível a novos utilizadores.

Palavras-Chave: Agentes, Otimização, Jogos de Dois Níveis, Resposta da Procura, Gestão do Lado da Procura

Resumo alargado em Português

O sistema energético atravessará uma profunda transformação nos próximos anos à medida que a produção renovável distribuída, a flexibilidade no lado do consumo e as funcionalidades de *SmartGrid* são implementadas. Este processo, conduzido em grande parte pelas imposições causadas pelas medidas conducentes à mitigação dos efeitos das alterações climáticas, implica profundas transformações na produção e consumo de energia e torna a transição energética extremamente urgente. Simultaneamente, novos *players*, entidades e modelos de negócio têm emergido em quase todos os níveis da cadeia energética desde a produção à gestão da rede elétrica, passando pela transmissão, distribuição e comercialização num movimento conduzido pelo processo de particionamento (unbundling) do sistema elétrico e a exigência de um sistema mais descentralizado e horizontal. O efeito combinado desta nova *paisagem energética* torna possíveis novas funcionalidades e arquiteturas de sistema na mesma medida em que coloca enormes problemas de natureza física e matemática mas também enormes questões económicas, sociais e políticas que terão, necessariamente, de ser abordadas e resolvidas. A *Gestão do Consumo* é um termo abrangente que representa tanto os mecanismos de *Resposta na Procura* (Demand Response) ou a *Gestão no Lado da Procura* (Demand-Side Management) e que se impõe como um dos problemas atuais mais importantes em sistemas energéticos inteligentes caracterizados por altas penetrações renováveis e mecanismos de mercado. Para resolver estes problemas, um conjunto de métodos matemáticos e computacionais têm sido proposto nos últimos anos. Otimização distribuída, sistemas inteligentes, sistemas baseados em agentes de software e teoria de jogos encontram-se entre algumas das ferramentas usadas para otimizar o consumo de energia e determinar o agendamento e alocação ótima de equipamentos e máquinas para consumidores residenciais, comerciais e industriais. O presente trabalho propõe um modelo geral para abordar o problema da otimização de cargas através de arquiteturas e metodologias baseadas no paradigma dos *Agentes Inteligentes*, definidos como entidades computacionais estabelecidas num dado ambiente que são capazes de agir autonomamente de forma a atingir objetivos. Seguindo esta definição, grande parte da teoria de agentes centra-se na forma como são tomadas decisões e como são atingidos os objetivos. No entanto, a grande potencialidade dos Sistemas Baseados em Agentes (SBA) surge quando se estabelecem *interações* com outros agentes e se formam *sistemas multi-agente*. No contexto do presente trabalho a tónica é colocada nas potencialidades dos SBA para resolução de problemas de otimização e decisão reais e que normalmente são extremamente complexos quando formalizados na sua versão original e impossíveis de serem resolvidos por uma única entidade. Recorrendo a SBA, os problemas podem ser resolvidos de forma distribuída entre diversos agentes que interagem e cooperam para encontrar uma solução. Os agentes podem ser blocos de código que representam entidades em negociações de mercado ou leilões, sensores de temperatura numa rede ou nós numa rede de computadores que cooperam para chegar a um consenso. O presente trabalho começa por definir uma arquitetura *high-level* para um modelo geral onde se estabelecem as relações entre os diversos componentes tais como software, modelos matemáticos e conjuntos de dados. Através de uma representação deste tipo é possível visualizar a natureza escalável, modular e parametrizável do modelo como características fundamentais. Seguidamente, numa representação *low-level*, estes elementos de *high-level* são definidos univocamente. O problema da otimização de cargas é definido matematicamente e o modelo tem como objetivo determinar um conjunto de resultados numéricos e de design que

servam de base para um processo de decisão relativamente ao agendamento e controlo de cargas. Estas cargas são equipamentos de consumidores residenciais, máquinas em unidades industriais ou veículos elétricos mas também cargas agregadas que oscilam na ordem de grandeza entre o Watt e o MegaWatt. Esta multidimensionalidade remete para uma interpretação do sistema elétrico como um sistema complexo em que vários níveis interagem entre si e esta é base para a definição de agentes. Assim, diferentes níveis da rede elétrica terão os seus modelos físicos e matemáticos e os seus resultados numéricos que produzirão os seus diagramas de carga específicos.

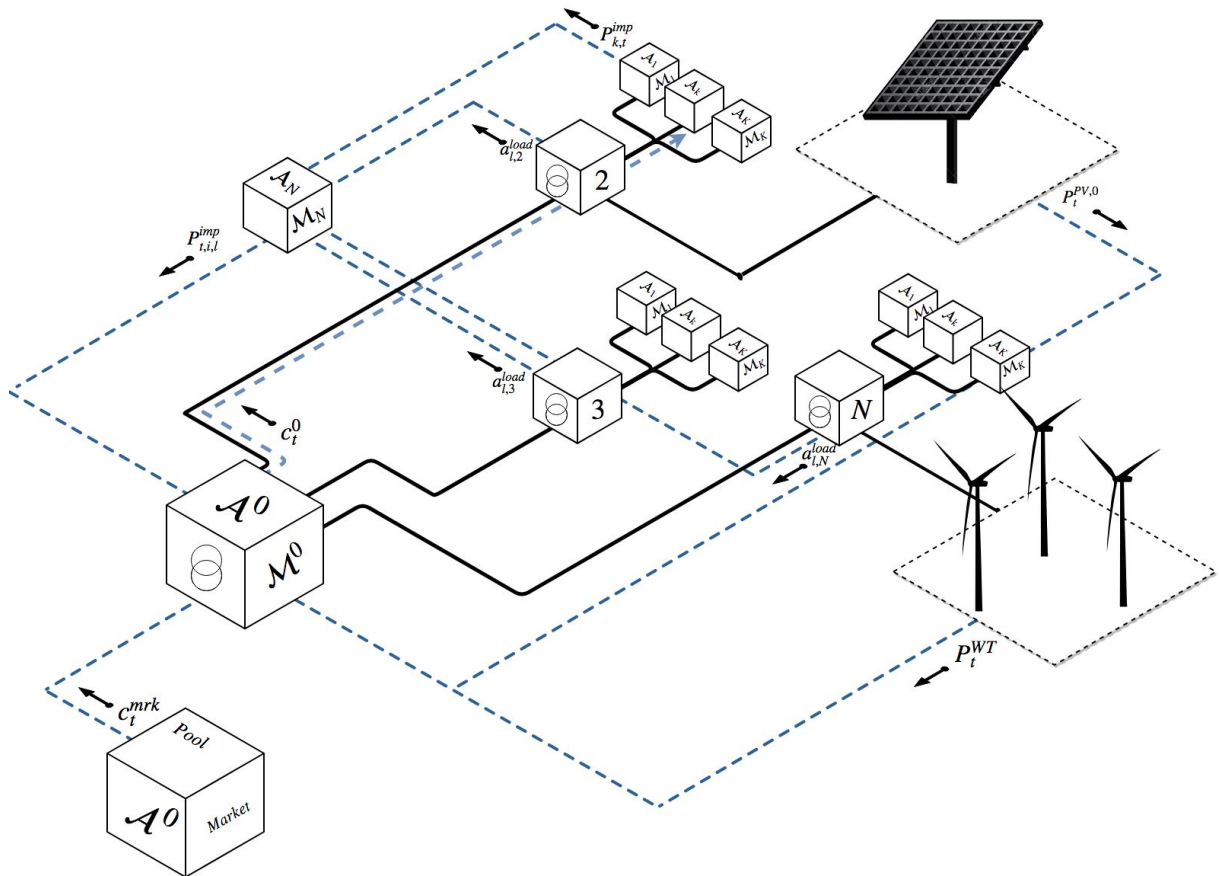
São então definidos três níveis principais. O *Nível das Tipologias*, o *Agregador* e o *Nodo Local*.

- No nível das tipologias são resolvidos modelos de DSM de forma a determinar os diagramas de carga ótimos e as necessidades de importação instantânea de potencia para consumidores residenciais, comerciais e industriais com o objetivo de minimizar o custo diário do consumo de eletricidade. A abordagem baseia-se na definição de k consumidores tipificados representados pelos agentes \mathcal{A}_k que têm a potencialidade de serem implementados em pontos de consumo (e.g *Smart Meters*). Cada agente é responsável por correr o seu modelo \mathcal{M}_k constituído por modelos físicos de eletrodomésticos, equipamentos residenciais e veículos elétricos mas também produção local de eletricidade de origem fotovoltaica ou eólica com base em previsões do recurso. A construção de \mathcal{M}_k segue uma abordagem *bottom-up* através da qual os equipamentos de cada unidade consumidora são inicialmente classificados em função do tipo de medida de DSM a que se submetem podendo ser de tipo *fixo*, que não estão submetidos a qualquer medida de gestão, *alocável* (shiftable), sujeitos a alocação temporal com um perfil fixo ou *elásticos*, equipamentos cujo perfil de consumo pode ser modelado. Seguidamente cada um dos equipamentos é modelado individualmente e posteriormente o diagrama de carga agregado de cada unidade consumidora é gerado sendo dado pela soma de todos os equipamentos consumidores. A potencialidade desta metodologia reside, no essencial, na possibilidade de gerar soluções individuais e ações de gestão para tipos específicos de equipamentos ou máquinas.
- No nível do agregador são resolvidos modelos de Fluxo de Potência Otimizado (Optimal Power Flow) de forma a estabelecer a correta operação da rede elétrica com o objetivo de minimizar o custo da produção de potência. Neste nível será definido o agente \mathcal{A}^0 que terá como função definir um preço dinâmico para a eletricidade ao longo do dia. O modelo \mathcal{M}^0 é constituído por uma representação da rede elétrica, pelas equações do fluxo de potencia, por modelos físicos para a produção eólica ou solar alimentada também por previsões de recurso e informação de preços da eletricidade no mercado do qual poderá ser importada potência. O agente \mathcal{A}^0 poderá ser implementado num transformador de uma subestação de distribuição, por exemplo.
- O nível do nó local tem como objetivo servir de intermediário entre os dois outros níveis e será representado por \mathcal{A}_N que tem como função agregar os consumos (operações algébricas) e intermediar as interações entre os outros níveis (algoritmos). Pode ser implementado num servidor em contacto com transformadores locais.

A dinâmica fundamental da interação entre agentes baseia-se na determinação, por parte de

\mathcal{M}^0 , de uma *tarifa dinâmica*, c_t^0 em €/kWh comunicada a cada \mathcal{A}_k . Estes, ao receberem o vetor de preços horários c_t^0 , respondem definindo os seus diagramas de carga ótimos e a energia a importar da rede P_t^{imp} em cada instante, ou seja, as estratégias que minimizam o seu custo. Estes valores são então comunicados a \mathcal{A}_N e seguidamente a \mathcal{A}^0 . O objetivo é que, através de um processo iterativo, se consiga obter uma solução global para o sistema, composta por um vetor de preços para a eletricidade no agregador e uma estratégia de alocação de cargas para cada um dos consumidores. Inevitavelmente, em problemas deste tipo os modelos são interdependentes entre si possuindo cada modelo as suas próprias variáveis independentes e objetivos locais mas havendo um subconjunto de variáveis comuns a \mathcal{M}^0 e a \mathcal{M}_k . O problema é formalizado como um problema de otimização de dois níveis (*bi-level problem*). Este tipo de problemas fazem parte de uma subclasse de problemas de otimização nos quais existe um problema no nível superior (*upper-level*) que admite um sub-problema (*lower-level*) como restrição. Essencialmente existe uma relação hierárquica entre a entidade que determina os preços da eletricidade no agregador, \mathcal{A}^0 , e as entidades que respondem aos preços, \mathcal{A}_k .

Uma visão geral e esquemática do modelo proposto pode ser vista na seguinte figura



As formas de resolver este tipo de problemas são também alvo de discussão no presente trabalho. Embora na literatura consultada existam metodologias de resolução deste tipo de problemas que consistem na sua redução a um só nível (*single-level problem*), a sua resolução exige grandes recursos e torna o problema reduzido mais complexo que os seus problemas

originais. Simultaneamente existe a necessidade de propor uma solução que preserve a privacidade dos agentes intervenientes garantindo que os modelos e as soluções locais não sejam do conhecimento global do sistema. Por estas razões é proposto um método de resolução *ad-hoc* em que o jogo de comunicação entre agentes é traduzido num algoritmo em que apenas o par (c_t^0, P_t^{imp}) circula no sistema de comunicação sendo privados os restantes parâmetros e variáveis locais. Esse jogo desenrola-se até ao ponto em que nenhum dos agentes envolvido no processo altera a sua estratégia, ou seja, a sua solução própria. O método proposto, embora tenha uma performance aceitável, levanta alguns problemas ao nível das soluções obtidas e desde logo é identificado o efeito "*ping-pong*" no qual as soluções são passadas iterativamente entre agentes e não há convergência para uma solução admissível. É ainda identificado o fenómeno de "*multidão*" (*herding effect*) que consiste na alocação simultânea e conjunta de cargas por parte dos \mathcal{A}_k nos mesmos *timeslots*. Este fenómeno é consequência do facto do mesmo vetor de preços ser enviado para os \mathcal{A}_k e perante composições semelhantes de \mathcal{M}_k ser um efeito espetável. É então proposto um mecanismo de DR entre os \mathcal{A}_k que consiste na resolução sequencial dos \mathcal{M}_k e na coordenação entre agentes através do *Factor de Carga Normalizado pela Média*, L_t^{ff} . Assim, o vetor de preços usado no mecanismo de DR passa a estar também indexado ao fator de carga tendo como efeito predominante a alocação sequencial de maquinas e equipamentos em *timeslots* de baixo fator de carga contribuindo desta forma para o alisamento do diagrama de carga agregado. Este mecanismo é também ele codificado num algoritmo construído a partir do algoritmo simples.

Os modelos e os métodos propostos foram implementados em código através do software *MATLAB* e do sistema *GAMS*. O *MATLAB* é usado para cálculos numéricos, tratamento de dados e operações matriciais e o sistema *GAMS* para a implementação e resolução dos \mathcal{M} 's. Os algoritmos são codificados em *MATLAB* que controla remotamente a execução dos modelos em *GAMS*. Para evidenciar a funcionalidade do modelo geral são construídos casos de estudo com o objetivo de representar possíveis problemas de decisão em contextos de mercados de energia para o dia seguinte (*day-ahead*) e grandes penetrações de produção renovável e veículos elétricos. Os resultados mostram que os modelos de \mathcal{M}_k são responsivos ao vetor de preços e que as tarifas dinâmicas são um mecanismo capaz de modelar os perfis de consumo. Conclui-se também que o mecanismo de DR é efetivo a induzir a coordenação entre agentes com especial relevância no caso em que estes possuem veículos elétricos como equipamentos. Mostram ainda que, através do mecanismo DR, é possível aumentar o fator de carga do diagrama de carga do agregador. No final identifica-se o modelo geral como um interessante ponto de partida para definir uma metodologia de gestão de redes baseada em agentes e sua posterior aplicação a problemas reais, de grande dimensão. O modelo está também apto para ser novamente implementado em software *open source* de forma a ficar acessível a novos utilizadores e ser, assim, complementado. No final apontam-se, ainda, direções de investigação a partir do presente trabalho.

Contents

List of Figures	XIII
List of Tables	XV
1 Introduction	1
1.1 SmartGrid as a cyber-physical complex system	1
1.2 Motivation	5
1.3 Objectives	5
1.4 Work Layout	6
1.5 Agents, optimization and game theory	7
1.5.1 From agents to multi-agent systems	7
1.5.2 Optimization	8
1.5.2.1 Bi-level problems	9
1.5.3 MAS and the power grid	10
1.5.4 MAS and DSM	10
1.5.5 Optimization and DSM	11
1.5.5.1 Bi-level models and DSM	11
1.6 Modeling and simulation of loads	12
2 Methodology	15
2.1 High-level architecture	15
2.2 Low-level models	17
2.2.1 General multi-level architecture	17
2.2.2 Communication	19
2.2.3 Data and information	20
2.3 Agent framework overview	22
2.4 Methodology - Development	23
2.4.1 Detailed Model - \mathcal{M}_k	23
2.4.1.1 Typologies creation	23
2.4.1.2 Demand Side Management as an optimization model	23
2.4.1.2.1 Fixed loads	24
2.4.1.2.2 Shiftable loads	25
2.4.1.2.3 Elastic Devices:	26
2.4.1.2.4 Confort-Based Elastic Devices	26
2.4.1.2.5 HVAC and AC system	26
2.4.1.2.6 Energy-Based Devices	27

2.4.1.2.7	Total load	28
2.4.1.2.8	Typology renewable energy production	29
2.4.1.2.9	Production - Photovoltaics	29
2.4.1.2.10	Residential storage	29
2.4.1.2.11	Exchanges with aggregator grid	29
2.4.1.2.12	Power balance	30
2.4.1.2.13	Objective function	30
2.4.2	Detailed Model - \mathcal{M}_N	31
2.4.2.1	Matrix representation of Load and production aggregation process	31
2.4.3	Detailed Model - \mathcal{M}^0	34
2.4.3.1	Aggregator renewable electricity production	34
2.4.3.2	Power Flow	34
2.4.4	Tariffs and pricing	38
2.4.5	Model's solution methods	39
2.4.5.1	Model as a bi-level model	39
2.4.5.2	Interaction and communication between agents	40
2.4.5.3	Demand Response mechanism	43
2.4.5.4	An heuristic <i>ad hoc</i> iterative algorithm for Demand Response .	44
2.5	Final considerations on methodology	46
3	Numerical implementation	47
3.1	Software and computacional Tools	47
3.2	Data	48
3.2.1	Simulation configurations	48
3.2.2	Convergence criteria	48
3.2.3	\mathcal{M}_k data	48
3.2.3.1	Photovoltaic system	48
3.2.3.2	Machine and devices characteristics	48
3.2.3.3	Modeling approach	52
3.2.3.4	Load vs Imported power	52
3.2.4	\mathcal{M}_N data	53
3.2.5	\mathcal{M}^0 data	55
4	Case Studies	59
4.1	Simple case	59
4.1.1	An individual solution	64
4.2	Production System Scenarios	65
4.3	Electric vehicle Schedules	71
4.4	DR vs No DR for highly renewable system configuration	75
4.5	Results discussion	78
5	Conclusion and future work	81
	Bibliography	85

6 Annexes	93
6.1 Fundamental Modeling Concepts	93
6.2 Abstraction layers	93
6.3 Information and privacy in agent-based systems	95
6.4 Thermal Models	96
6.4.1 HVAC characteristics	97
6.4.2 Refrigerator	97
6.4.2.1 Refrigerator parameters	98
6.5 Residential storage	98
6.6 Production - Wind power production	99
6.6.1 Wind Power Park	100
6.7 Line model	101
6.8 General Optimal Power Flow	102
6.9 Numerical implementation annexes	103
6.9.1 Software workflow algorithm	103
6.9.2 PV production	104
6.9.3 Meterological data	105
6.9.4 Wind speed scenarios	105
6.9.5 Typologies summary	107
6.9.6 Mean conductance for each typology	107
6.9.7 Adjacency and connection matrices	108
6.9.8 Aggregation bus example	109
6.9.9 Scenarios	110
6.9.9.1 Typologies mix matrices	110
6.9.10 Tariffs	111

List of Figures

2.1	Agent framework's general concept map	16
2.2	Agent framework's detailed concept map	17
2.3	General agent's framework multilevel structure	18
2.4	Agent framework's compositional structure block diagram	19
2.5	Agent framework's dynamic structure petri net	20
2.6	System wide vision on the framework's implementation	22
2.7	Top: An example load diagram. Down: Energy consumed per timeslot for $\Delta t=10$ minutes, $H=144$	24
2.8	Petri Net depicting communication between agents	41
2.9	Mean normalized price vector and production cost example	43
3.1	Shiftable devices output solution	49
3.2	On top: type $k = 6$ with ω_1^{EV} . Down: type $k = 5$ with ω_2^{EV}	50
3.3	HVAC load profile for Typology $k = 6$	51
3.4	Base Loads for all 6 typologies	52
3.5	Generic typology power balance with and without excess PV production	53
3.6	General star topology for the aggregator power grid	54
3.7	Power output for WPP with $n^{WT} = 20$ for high and low wind scenarios	56
3.8	PV Power Plant output	56
3.9	MIBEL prices in 29 th June 2017	57
4.1	Power balance at the aggregator	59
4.2	Original, filtered and hourly aggregator electricity production marginal cost plotted against market price vector and WPP LCOE	60
4.3	Bi-level variables and solutions for \mathcal{M}_k and \mathcal{M}^0 with and without DR mechanism	61
4.4	Solutions for \mathcal{M}_k with and without DR mechanism	62
4.5	Aggregated load with and without DR mechanism	63
4.6	Daily mean load factor along iterations	64
4.7	Type $k = 6$ example solution for EVs with and without DR mechanism	64
4.8	PVPP and WPP production	66
4.9	Bi-level variables and solutions for \mathcal{M}_k and \mathcal{M}^0 for SM, SMW and SMWP scenarios	67
4.10	Solutions for \mathcal{M}_k for SM, SMW and SMWP scenarios	67
4.11	\mathcal{M}_6 daily electricity bill, $C_{\gamma,6}$, along iterations	69
4.12	\mathcal{M}_6 Electric vehicle profile $P_{\omega,6,t}^{EVc}$ for SM, SMW, SMWP scenarios	69
4.13	Marginal cost of electricity production final solution, c_t^0 , for SM, SMW and SMWP scenarios	70

4.14	Daily mean Load factor L_γ^f final solution for SM, SMW and SMWP scenarios . . .	71
4.15	Bi-level variables and solutions for \mathcal{M}_k and \mathcal{M}^0 for F and C scenarios	72
4.16	Solutions for \mathcal{M}_k for F and C scenarios	73
4.17	Daily mean Load factor L_γ^f final solution for F and C scenarios	74
4.18	All typologies EVs final load profile $P_{\omega,k,t}^{EVc}$ for C scenario	74
4.19	All typologies EVs final load profile $P_{\omega,k,t}^{EVc}$ for F scenario	75
4.20	Bi-level variables and solutions for \mathcal{M}_k and \mathcal{M}^0 for F scenario with and without DR mechanism	76
4.21	Solutions for \mathcal{M}_k for F scenario with and without DR mechanisms	76
4.22	Daily mean Load factor L_γ^f final solution for F scenario with and without DR mechanismos	77
4.23	All typologies EVs final load profile $P_{\omega,k,t}^{EVc}$ for scenario F with DR mechanism . .	77
4.24	All typologies EVs final load profile $P_{\omega,k,t}^{EVc}$ for scenario F without DR mechanism	78
5.1	Holonic agent-based local electricity market where different \mathcal{A}^0 can exchange power and information between them and coordinate through negotiation by exploring cooperative or non cooperative strategies	83
6.1	Agent framework's compositional structure block diagram	94
6.2	NorthWind 100 Power Curve [77]	100
6.3	265 W Open Renewables PV module output	104
6.4	Temperature and irradiance time series for a day (font: [83])	105
6.5	Wind resource scenarios at hub height for a general day	106
6.6	Aggregated load at grid buses	109
6.7	Typologies mix for different scenarios	110

List of Tables

2.1	Abstraction layers summary	19
3.1	Shiftable devices parameters	48
3.2	Electric Vehicles characteristics	49
3.3	\mathcal{M}^0 power flow parameters	55
3.4	LCOE for Wind power in 2016 (€/kWh)	56
4.1	Base case devices assignment	59
4.2	Costs, Revenues and Profits for \mathcal{A}^0 (€)	65
4.3	LCOE in €/kWh Source: [64]	66
4.4	Data PEV (source: [56])	66
4.5	Electric vehicle schedule distribution	66
4.6	Percentage variations along iterations for C_γ^0 and c_γ^0	68
4.7	Percentage variations along iterations for $C_{\gamma,k}$	68
4.8	Electric vehicle scheduling distribution for Free and Constrained scenario	71
4.9	Percentage variations along iterations for C_γ^0 and c_γ^0	72
4.10	Percentage variations along iterations for $C_{\gamma,k}$	73
6.1	HVAC system characteristics	97
6.2	Fridge characteristics	98
6.3	NorthWind 100 characteristics [77]	100
6.4	PV module characteristics and model parameters [82]	104
6.5	Wind power law parameters(source: [75])	105
6.6	Typologies physical and thermal characteristics	107

Abbreviations

RES	Renewable Energy Sources
MAS	Multi Agent System
ABS	Agent Based System
GT	Game Theory
LP	Linear Programming
MILP	Mixed Integer Linear Programming
MINLP	Mixed Integer Non-Linear Programming
NLP	Non-Linear Programming
BLP	Bi-Level Problems
DR	Demand Response
DSM	Demand-Side Management
PEVS	Plug-In Electric Vehicles
EV	Electric Vehicle
WPP	Wind Power Plant
PVPP	Photovoltaics Power Plant
PV	Photovoltaics
RTP	Real-Time Pricing
TOU	Time-of-Use
KKT	Karush-Kuhn Tucker
ICT	Information and Communication Technology
HVAC	Heating, Ventilation, and Air Conditioning
COP	Coefficient of Performance
CBED	Comfort-Based Elastic Devices
EBED	Energy-Based Elastic Devices
VPP	Virtual Power Plant
DSO	Distribution System Operator
ISO	Independent System Operator
TSO	Transmission System Operator

GAMS General Algebraic Modeling System

GDX Gams Data Exchange

JADE Java Agents Development Framework

SPADE Smart Python Multi-Agent Development Environment

OPF Optimal Power Flow

MNLF Mean Normalized Load Factor

G2V Grid to Vehicle

V2G Vehicle to Grid

Symbols

K_b [$m^2 \text{ kg } s^{-2} \text{ K}^{-1}$] Boltzmann constant

q [Coulombs] Electron charge

Agents and sets

\mathcal{A}_k k -th Typology agent

\mathcal{A}_N Local Node agent

\mathcal{A}^0 Aggregator agent

\mathcal{M}_k k -th Typology agent's Model

\mathcal{M}_N Local Node agent's Model

\mathcal{M}^0 Aggregator agent's Model

Ω_k Appliances and devices set for the k -th typology/agent

ω Appliance or device element

F_k Fixed Devices set for the k -th typology/agent

S_k Shiftable Devices set for the k -th typology/agent

E_k Elastic Devices set for the k -th typology/agent

E_k^{cb} Elastic Confort-Based Devices set for the k -th typology/agent

E_k^{eb} Elastic Energy-Based Devices set for the k -th typology/agent

B_k Storage Devices set for the k -th typology/agent

G_k Renewable energy generators set for the k -th typology/agent

t [ts] Simulation and optimization timeslots

Δt [minutes] Model timestep

\mathcal{T} [minutes] Total day duration

H [ts] Total number of time-slots

k Typologies index

K Total number of typologies

γ iteration index

γ^{max} Maximum number of iterations

μ' [seconds] Watt to Joule conversion factor

μ^{kh} [kilo-hours] Watt to kilowatthour conversion factor

μ^h [hours] KilloWatt to kilowattHour conversion factor

Input Physical Parameters

$G_{k,t}$ [W/m^2] Global horizontal irradiation time series for the k -th typology/agent

$T_{k,t}^o$ [$^{\circ}C/K$] Environment temperatures time series for the k -th typology/agent

$v_{k,t}$ [m/s] Wind speed time series for the k -th typology/agent

Shiftable devices

$x_{\omega,k,t}^S$ [0-1] Activity binary variable for shiftable device ω at each timeslot for typology/agent k

$y_{\omega,k,t}^S$ [0-1] Operation ending binary variable for shiftable device ω at each timeslot for typology/agent k

$p_{\omega,k,t}^S$ [W] Load for shiftable device ω at each timeslot for typology/agent k

$P_{k,t}^S$ [W] Total Shiftable Load at each timeslot for typology/agent k

D_{ω}^S [ts] Cycle duration for shiftable device ω

l_{ω}^S [W] Constant load during cycle duration for shiftable device ω

$t_{k,start}^S$ [ts] Starting timeslot for shiftable devices for typology/agent k

$t_{k,end}^S$ [ts] Ending timeslot for shiftable devices for typology/agent k

t_{ω}^S [ts] Activity counter for shiftable device ω

Fixed Loads

$p_{\omega,k,t}^F$ [W] Load for fixed device ω at each timeslot for typology/agent k

$P_{k,t}^F$ [W] Total Fixed Load at each timeslot for typology/agent k

E_k^F [kWh] Daily fixed devices energy consumption for typology/agent k

Elastic Devices

$p_{\omega,k,t}^E$ Load for Elastic devices ω at each timeslot for typology/agent k

$p_{\omega,k,t}^{E^{cb}}$ [W] Load for Comfort-Based Elastic Device ω at each timeslot for typology/agent k

$p_{\omega,k,t}^{E^{eb}}$ [W] Load for Energy-Based Elastic Device ω at each timeslot for typology/agent k

$P_{k,t}^{E^{cb}}$ [W] Total load for Comfort-Based Energy Devices at each timeslot for typology/agent k

$P_{k,t}^{E^{eb}}$ [W] Total load for Energy-Based Energy Devices at each timeslot for typology/agent k

HVAC and thermal models

- $T_{k,t}^H$ [$^{\circ}C$] Household inside temperature time series for typology/agent k
- $p_{\omega,k,t}^H$ [W] Load for HVAC ω for at each timeslot for typology/agent k
- $p_{k,t}^{thH}$ [W] Extracted or injected thermal power at each timeslot for typology/agent k
- $p_{\omega,max}^H$ [W] Maximum electric power consumption for HVAC ω
- $\eta_{\omega,h}^H$ [ad] Coefficient of Performance of HVAC ω in Heat mode
- $\eta_{\omega,c}^H$ [ad] Coefficient of Performance of HVAC ω in Cooling mode
- ε_k^H [ad] Thermal inertia factor for typology/agent k
- β_k^H [K/W] Inverse of conductance for typology/agent k
- T_k^{Href} [$^{\circ}C$] Reference temperature for typology/agent k
- ΔT_k^H [$^{\circ}C$] Reference temperature variation for typology/agent k
- K_k^{thH} [W/K] Thermal conductance for typology/agent k
- U_k^H [W / m^2 $^{\circ}C$] Overall Heat Transfer Coefficient for typology/agent k
- C_k^H [J/ $^{\circ}C$] Thermal Mass for typology/agent k
- m_k^H [kg] Inner volume total mass for typology/agent k
- V_k^H Building total volume for typology/agent k
- A_k^H [m^2] Building Area for typology/agent k
- τ_k^H [s] Thermal Time-Constant for typology/agent k
- k^{th} [W/ m^2K] Thermal conductivity
- c_p [J/kg K] Specific Heat Capacity
- m_c [J/K] Heat Capacity
- ρ [kg/ m^3] Air Density

Electric Vehicles

- $p_{\omega,k,t}^{EVc}$ [W] Charging power for EV ω at each timeslot for typology/agent k
- $p_{\omega,k,t}^{EVd}$ [W] Discharging power for EV ω at each timeslot for typology/agent k
- $SOC_{\omega,k,t}^{EV}$ [kWh] Battery State-of-Charge for EV ω at each timeslot for typology/agent k
- $x_{\omega,k,t}^{EV}$ [0-1] Charge/Discharge binary variable for EV ω at each timeslot for typology/agent k
- E_{ω}^{EV} [kWh] Battery capacity for EV ω
- $p_{\omega,max}^{EVc}$ [W] Maximum charging power for EV ω

$p_{\omega,max}^{EVd}$ [W] Maximum discharging power for EV ω

$t_{\omega,k,end}^{EV}$ [ts] Fully charged delivering timeslot for EV ω for typology/agent k

$t_{\omega,k,start}^{EV}$ [ts] Charging starting time for EV ω for typology/agent k

V_{ω}^{EV} [V] Charging voltage for EV ω

I_{ω}^{EV} [A] Charging current for EV ω

η_{ω}^{EVc} [ad] Charging efficiency for EV ω

η_{ω}^{EVd} [ad] Discharging efficiency for EV ω

Storage System

$r_{b,k,t}^c$ [W] Charge rate for storage system b at each timeslot for typology/agent k

$r_{b,k,t}^d$ [W] Discharge rate for storage system b at each timeslot for typology/agent k

$SOC_{b,k,t}$ [kWh] State-of-Charge for storage system b at each timeslot for typology/agent k

$x_{b,k,t}$ Charge/Discharge binary variable for storage system b at each timeslot for typology/agent k

η_b^c Charging efficiency for storage system b

η_b^d Discharging efficiency for storage system b

$r_{b,max}^c$ [W] Maximum charge rate for storage system b

$r_{b,max}^d$ [W] Maximum discharge rate for storage system b

$SOC_{b,max}$ [kWh] Storage system capacity / Maximum State-of-Charge for storage system b

$SOC_{b,min}$ [kWh] Minimum State-of-Charge for storage system b

$SOC_{b,k,0}$ [kWh] Initial State-of-Charge for storage system b for typology/agent k

DOD_b [%] Depth of Discharge for storage system b

Photovoltaics

n_k^{PV} Number of PV modules for typology/agent k

P_k^{Wp} [Wp] Total installed renewable capacity for typology/agent k

$P_{k,t}^{PV}$ [W] Photovoltaic module power production time series for typology/agent k

η^{PV} [ad] PV modules efficiency

A^{PV} [m^2] PV module area

I_t^{MP} [A] MPP current profile

I^{rMP} [A] Reference MPP current

V_t^{MP} [V] MPP voltage

V_t^T [V] Thermal potential profile

V^{rT} [V] Reference Thermal potential

N_s Number of series cells in a module

I_0^r [A] Reference Diode reverse saturation current

I^{rcc} [A] reference short circuit current

T_t^c [°C] Cell temperature profile

$NOCT$ [°C] Normal Operating Cell Temperature

G^r [W/m²] Reference irradiance

m Diode ideality factor

ε [eV] Semiconductor band gap

Power and Energy balance variables

E_k^T [kWh] Total electrical energy consumption for typology/agent k

$x_{t,k}^{gr}$ Import/Export binary variable at each timeslot for typology/agent k

$P_{k,t}^L$ [W] Total load at each timeslot for typology/agent k

$P_{k,t}^G$ [W] Total generated power from RES at each timeslot for typology/agent k

$P_{k,t}^{imp}$ [W] Imported power from the grid at each timeslot for typology/agent k

$P_{k,t}^{inj}$ [W] Injected power to the grid at each timeslot for typology/agent k

$C_{k,t}$ [€] Electricity cost at each timeslot for typology/agent k

C_k [€] Total daily electricity cost for typology/agent k

$P_k^{LimGrid}$ [W] Contracted power for typology/agent k

Tariffs and economic parameters symbols

c_t^0 [€/kWh] Aggregator marginal cost of production at each timeslot

τ_t [€/kWh] Typologies level dynamic electricity tariff

c_t^{mkt} [€/kWh] Electricity Market energy cost at each timeslot

τ^{dist} [€/kWh] Normal Low Tension generic grid access tariff

τ_A^{com} [€/ kWh] Normal Low Tension Active Power Commercialization tariff

τ^{fix} [€] Normal Low Tension contracted power fixed tariff

c^b [€/kWh] Storage system LCOE

c^{PV} [€/kWh] Residential PV LCOE

π_t [€/kWh] Dynamic Selling price

τ^{HTpc} [€/kW.day] High tension contracted power tariff

τ_t^{HTpc} [€/kW.ts] High tension contracted power tariff per timeslot

τ_A^{HT} [€/kWh] High Tension grid access tariff for active power

c^{WT} [€/kWh] WPP LCOE

$c^{PV,0}$ [€/kWh] PVPP LCOE

Topology

n Local nodes set

l low level aggregation load mix set

i, j Grid Nodes set

g Generators or Electricity exchange nodes set

g^{wt} Wind generators / WPP set

g^{pv} PV generators / PVPP set

N Total number of grid nodes

L Total number of load mixes

N_g Total number of thermal generators or exchange nodes

N_g^{wt} Total number of WPP's

N_g^{pv} Total number of PVPP's

$\mathbf{a}_{l,i}^{load}$ Load connection matrix

$\mathbf{a}_{i,j}$ Electrical grid adjacency matrix

$\mathbf{a}_{i,g}^g$ generator connection matrix

$\mathbf{a}_{i,g^{wt}}^{wt}$ WPP connection matrix

$\mathbf{a}_{i,g^{pv}}^{pv}$ PVPP Power Plant connection matrix

$\mathbf{N}_{l,k}$ Aggregation load mix matrix

N_T^{mix} Total number of typologies agents in the aggregator

N_k^{mix} Total number of typology k agents in the aggregator

N_p^H Number of person per house in Portugal

Optimal Power Flow Symbols

$Z_{i,j}$ [Ω] Complex impedance

$Y_{i,j}$ [Siemens] Complex admittance

$R_{i,j}$ [Ω] Electrical Resistance

$\chi_{i,j}$ [Ω] Electrical Reactance

$L_{i,j}$ [Km] Line length between node i and j

$G_{i,j}$ [Siemens] Conductance matrix of line ij

$B_{i,j}$ [Siemens] Susceptance matrix of line ij

$V_{t,i}, V_{t,j}$ [kV] Voltage profile at node i / j

$P_{t,i,j}$ [kW] Active Power injected to or received from Power Line ij

$Q_{t,i,j}$ [kVAR] Reactive Power injected to or received from Power Line ij

V_b [kV] Base tension

S_b [kVA] Base apparent power

P^{SE} [kW] Installed capacity at distribution Sub-Station

$P_{t,i,j}^{max}, P_{t,i,j}^{min}$ [kW] Maximum and minimum active Power injected to or received from Power Line ij

$Q_{t,i,j}^{max}, Q_{t,i,j}^{min}$ [kVAR] Maximum and minimum reactive Power injected to or received from Power Line ij

$V_{t,i}^{max}, V_{t,i}^{min}$ [Volts] Maximum and minimum voltage profile at node i

$\delta_{i,j}^{max}, \delta_{i,j}^{min}$ Maximum and minimum Phase difference between node i and j

$x_{t,i,g}^{in}$ [kW] Active Imported Power at each timeslot at node i for exchange element g

$x_{t,i,g}^{out}$ [kW] Active Exported Power at each timeslot at node i for exchange element g

$P_{t,i,l}^{imp}$ [kW] Active imported aggregated load l at each timeslot at node i

$P_{t,i,l}^{inj}$ [kW] Active Injected aggregated power l at each timeslot at node i

$P_{t,i,g^{wt}}^{WT,0}$ [kW] Active Injected Wind Power from WPP g^{wt} at each timeslot at node i

$P_{t,i,g^{pv}}^{PV,0}$ [kW] Active Injected Wind Power from PV Power plant g^{pv} at each timeslot at node i

$\theta_{t,i}$ [degree] Power phase at each timeslot at node i

$\delta_{t,i,j}$ [degree] Phase difference at each timeslot between node i and j

$P_{t,i,j}$ [kW] Active Power injected to or received from Power Line ij at each timeslot

C_t^0 [€] Aggregator electricity production cost at each timeslot

C^0 [€] Aggergator daily electricity cost

E_t^0 [kWh] Aggregator Electrical energy total production at each timeslot

Re_t^0 [€] Aggregator total revenue at each timeslot

Pr_t^0 [€] Aggregator total Profit at each timeslot

x_t^{in} Aggregator imported Power at each timeslot

x_t^{out} Aggregator exported Power at each timeslot

P_t^{Timp} [kW] Total aggregator active power typologies level imports at each timeslot

P_t^{Tinj} [kW] Total aggregator active power typologies level injections at each timeslot

$P_t^{WT,0}$ [kW] Total aggregator active Wind Power injection at each timeslot

$P_t^{PV,0}$ [kW] Total aggregator active PV Power injection at each timeslot

$n^{WT,0}$ Number of Wind generators at WPP

$n^{PV,0}$ Number of photovoltaic modules at PVPP

Wind generator model

s Power curve velocities discretization set

p_s^{WTPC} [W/kW] Wind generator power curve

P_t^{WT} [W/kW] Wind generator active power output at each timeslot for one generator

v_s^{wtPC} [m/s] Power curve discretized wind speed values

v_{in}^{wt} [m/s] Wind generator cut-in speed

v_{out}^{wt} [m/s] Wind generator cut-out speed

v_t^{wt} [m/s] Wind speed profile at hub height

z_{wt} [m] Hub height

z_0 [m] Reference height

a, b, c wind profile power law coefficients

Bi-level and Demand Response

\mathbf{S}_γ Bi-level solutions pair at iteration γ

\mathbf{s}_γ Bi-level variable solutions pair at iteration γ

s_k \mathcal{M}_k 's variable solution

s^0 \mathcal{M}^0 's variable solution

- c_t^{init} [€/kWh] Initialization price vector
- c_γ^0 [€/kWh] Mean marginal electricity production cost at iteration γ
- $c_{\gamma,t}^0$ [€/kWh] Marginal electricity production vector at iteration γ
- C_γ [€] Mean typologies cost at iteration γ
- C_γ^0 [€] Aggregator cost at iteration γ
- P_{max}^{Timp} [kW] Maximum value in the P_t^{Timp} vector
- L_t^f [%] Load factor at each timeslot
- L_t^{ff} [%] Mean Normalized Load factor at each timeslot
- c_t^f [€/kWh] MNLF-based marginal cost vector
- τ_t^f [€/kWh] MNLF-based dynamic electricity tariff
- l_k Agents queue line for DR mechanism
- q_m Queue line random permutation for DR mechanism
- \mathcal{A}_{q_m} Agent on the line for DR mechanism
- \mathcal{M}_{q_m} Agent's model on the line for DR mechanism
- ϵ Convergence criteria

Chapter 1

Introduction

1.1 SmartGrid as a cyber-physical complex system

The present historical moment is characterized by two huge transformation processes occurring simultaneously. The first of these is the conceptual breakthrough in several technological and scientific domains driven by the rapid increase in computation capabilities and the multidisciplinary trend in research for all knowledge domains. The second is the phase shift that global climate and ecological systems are currently going through driven by anthropogenic climate change and general ecological breakdown. Inevitably, deep transformations in society, politics, economy and science will take place, independently of its direction. The energy network is one of the systems in which these processes have the bigger impacts. On one side it faces the need for decarbonization and adoption of renewable energy sources (RES). On the other it faces a process of digitalization that open up the conditions for new conceptual frameworks, ideas and methods in order to tackle the highly complex problems that come along. In fact, the way energy is produced, transmitted, stored and managed is changing and going through a deep transformation process with the adoption of distributed RES at its core. This transformation is mainly driven by the constraints imposed by climate change that, ironically, was caused by fossil fuel based power generation and transportation systems of the last 100 years. This dynamic context imposes the need to rethink the energy system by standards different from the business-as-usual ones that drove the climate system to chaos. Nonetheless, no one actually knows how future energy systems will look like, but there is a growing consensus over the need of a transition to an increasingly sustainable energy system that will impose a plethora of new technologies, systems and devices for which the scientific community and the energy sector must be prepared for. Along with it come new forms of organization rooted in increasingly democratic and participatory processes around the decisions and control of the energy system. Inevitably, this new paradigm calls for new tools to rethink the energy system.

Traditionally, the electrical system is a hierarchical structure in which power production flows, unidirectionally over big distances, from a few large thermal, hydroelectric or nuclear power plants to many passive consumers. This system is operated by centralized authorities that, having full knowledge of the whole grid, adapt production to the immediate demand while ensuring power system safety and stability. As a consequence there are big power losses and environmental impacts and, due to the unpredictability of demand, the need to meet peak loads lead to power overproduction [1]. However, in the last years the introduction of

distributed production near consumption points, mainly from different RES like wind or solar, have shifted the understanding of the energy system to a more distributed architecture [2]. These ongoing changes introduced several challenges and problems that need to be tackled. Local, decentralized production depends on *bidirectional flows* in the grid converting mere power consumers in active producers, i.e. *prosumers*. But the introduction of RES is characterized by *variability* and *randomness* in production, making it difficult to control. One solution to tackle this problem is that the classic fixed and static demand side should, progressively, evolve to a flexible, adaptable and manageable part of the system which surely demands for new conceptual frameworks and engineering procedures leading to *Demand Management*

Energy Management, Demand-Side Management and Demand Response Barbato and Capone in [3] present, for the residential level, a clear and precise definition of the terminology involved in *Demand Management*, a comprehensive term that represents the variety of measures and control methods that can be applied in order to adapt energy consumption to the resources available in order to meet some specific objective. These objectives may be technical, like peak shaving, or economical, like energy cost minimization. Therefore Energy Management represents *Demand-Side Management* and *Demand Response*. The former is defined as a proactive approach characterized by planning energy management in order to get efficient energy consumption in the long term. The latter constitutes reactive short term consumption management measures, driven by price signal or other signals. Although being different kinds of measures they may be used in coordination with each other. Soares, Gomes and Antunes in [4] present several conclusions about energy consumption for the residential sector in Portugal. Considering that appliance portfolio may be composed of fridge/freezer, HVAC system, electric heater, washing machine, dishwasher, electric oven, computers, lightning and microwave, they point out that, respectively, electric water heater are responsible for 5%, cold appliances 30% and HVAC systems 15% of the total annual electric consumption at the residential sector. According to [3] residential sector may become responsible for 40 % of the energy consumption in the near future.

Adding to load management, a wider new energy landscape is emerging as major key technology components and architectures are integrated in energy system as highlighted in [1].

Storage systems Batteries systems to store electric energy can be used to mitigate the variability of RES generators. Their decreasing costs over the last years give rise to commercial residential solutions for energy management along with larger community sized storage systems.

Plug-in electric vehicles EVs are expected to disrupt the present transportation model very soon and there is a consensus that they are, on one side, a manageable load and, on the other, a storage system. If EVs adoption fulfill the industry future expectations we can expect them to represent a huge future load that will assume stochastic charging profiles which can cause high demand peaks in local distribution grids with consequences such as voltage deviations, decrease in quality of supply, increase power losses or transformers overload [5]. This also makes EVs a prolific field of research in the DSM and DR field. Pathways for managing EV's load have

focused mainly on determining optimal scheduling for its charging or integrating them with RES by using them as storage through bi-directional power flows with the grid [1]. Smart charging and discharging approaches have been reviewed in [5] where two main modes of operation are pointed towards the interactions between EVs and the grid. These are Vehicle-to-Grid (V2G), when energy flows from EVs to the grid and Grid-to-Vehicle (G2V), the opposite mode. The combination of both modes makes bi-directional power flow a possible managing feature that highly increases complexity in energy management mechanism for EVs. V2G becomes important when EV's storage are managed through an aggregator. This source also reviews centralized and decentralized control architectures. The former stands for direct load control in which a central controller (e.g aggregator) manages the charge of all EVs in its region. The latter stands for a distributed control that places the decisions about charging strategies in the EV owner. However, much of the reviewed works in [5] show the need of *coordination* when considering decentralized control and points out that EVs must have some kind of intelligence

Microgrids Microgrids or mini-grid are distribution side sections of the grid that can operate in connected or isolated modes managing, internally, its resources and loads importing or exporting power with the main grid.

Virtual Power Plants VPPs are entities that virtually manage several RES power plants, load and storage systems in an aggregated manner. They can act as energy market agents managing in real time its RES. VPP are very tight to economics of power markets but they can be operated from a technical point of view for load balancing. Other architectures, such as *multi-energy systems* and *energy-hubs* are also reviewed by the authors in [1]

Blockchain and Smart Contracts technologies *Blockchain* is an emerging technology that allows decentralized computation and distributed consensus mechanisms using cryptography as a base mechanism and it is the base technology for the growing number of cryptocurrencies. *Smart Contracts* are computer protocols that allow for negotiation between parts. In practice, Blockchain is a traceable and distributed ledger that records information such as transactions and operations and uses cryptography to secure that data eliminating the possibility of adulteration and hacking. Both these technologies are being applied to energy system's problems and are expected to disrupt the energy system in the coming years due to their capacity to manage systems where several agents negotiate with each other, in a secure and scalable way [6]. It mainly applies as a secure database to register energy production and consumption using tokens as RES credits [7] without central authorities or intermediaries in an automated way. However the same authors highlight the potentiality of using blockchain technologies to solve decentralized optimization schemes.

Parallel to this changing technological context, since the beginning of the 90's a deregulation process has been developing in the organization of the power system through a mechanism called *unbundling*, meant to detach production, transmission, distribution, commercialization and operation. The establishment of the traditional centralized system during the 20th century is deeply connected with the fossil-fuel based corporate utilities organized as monopolies over the entire value chain of the power system. Unbundling, theoretically allows new players and stakeholders to assume fundamental roles at all levels of the power system. The model of the

vertical utility that controls all levels of the energy chain is being defied in the new energy landscape. Authors in [8] investigate the new opportunities that business model innovations are creating in electricity supply markets at the sub-national scale. They present several business model archetypes for electricity supply markets such as local white label archetype, organizations that partner with electricity suppliers using their own brand; Local Aggregator Archetype, entities that would propose DR participation mechanisms to match demand and local generation to groups of domestic properties. This archetype is specially designed to implement automated DR mechanisms and therefore move consumption into low price time periods. Local Pool and Sleeve archetype aggregates distributed generation from a local area and supplies the same quantity of energy to local consumers avoiding intermediaries with wholesale markets. Municipal utility archetype is a model where local authority runs a supply company for local market linking consume and generation within a geographical area. P2P archetype uses a software platform that allows commercial consumers to choose distributed generation to fulfill their energy needs but the concept may be easily expanded into residential consumers. In order to respond to new contexts in supply and demand, authors in [9] address the *Local Energy Management*, a solution for the coordination of decentralized supply, storage, transport, conversion and consumption in a given geographical area. As an example, they present a German village where a decentralized renewable energy system is fully operational. The organization that owns the electricity grid, retails and manages flexibility is a local cooperative that assumes the role of a local utility. There are 37 households, two businesses, two local government entities and three agricultural enterprises involved in the project. The cooperative direct-controls a lithium-ion battery, a biomass plant, a WPP and a solar PVPP. Energy is sold back to the grid and remunerated through feed-in tariffs. Prosumers are expected to become a major player in energy system since they constitute a big number of elements and are highly flexible [10]. Specifically its full potentiality arises when considered as an aggregated entity, i.e, when several electricity users are associated under the same RES system. Moura in [11] reviews several policy models and concepts for prosumer aggregation. Namely *community shared generation*, in which several entities share the output of a RES system, or *P2P energy trading*, in which producers and consumers in an energy network combine individual resources in to a large shared pool. When seen in conjunction, these architectural, technological, regulatory and organizational processes must give rise to an energy system perceived as a network of players. Specifically, the new energy landscape will introduce new technologies and entities in the form of *system modules* and, as a consequence, the power grid can no longer be regarded as a homogeneous entity but as a system-of-systems constituted by increasingly new and complex sub-systems. Therefore, studying and managing the whole system is a task that must take in to consideration interaction and the joint effects of the infinity of sub-system's modules, its individual rules and its interaction protocols. Its high-level operation comprise the low-level modules and the complex behavior of the system as a whole cannot be perceived by the behavior of its individual parts giving rise to *emergent phenomena* [12]. *SmartGrid* have been pointed out as a viable paradigm to deal with this new landscape and manage such a complex system. Although there is not a consensual definition, integration of ICT capabilities towards grid management and operation is at the center of the SmartGrid concept. In [13], it is defined as "*the integration of enabling ICT and other advanced technologies with the large-scale power networks to enable electric energy generation, transmission, distribution, and usage to be more efficient, effective, economical, and environmentally sustainable*". They further look at the power grid as a *cyber-physical system* defining it as "*a broad range of complex,*

multidisciplinary, physically aware next-generation engineered systems that integrate embedded computing technologies (cyber part) into the physical world". The existence of communication capabilities between the power system's sub-systems is the catalyst for several practical and theoretical approaches towards solving the plethora of emerging new problems. The authors in [1] identify the intersection of energy management and ICT technologies within the actual trend towards digitalization and point to the use of the *agency* and *distributed intelligence* paradigm towards this management.

1.2 Motivation

The new, emerging energy landscape in the context of SmartGrids and flexible demand poses different theoretical and practical problems in the domain of energy management and control. The specific form of that landscape calls for new theoretical and practical tools, approaches and paradigms with which these problems may be approached and solved. *Agency* is a computational paradigm that emerges from distributed and decentralized systems architectures and artificial intelligence and, therefore, applies to the emerging features of the SmartGrid as a network of distributed entities and modules. The main motivation behind the present work is to approach the load optimization of residential, commercial and industrial power profiles through DSM and DR mechanism using agent-based architectures and distributed optimization mechanisms.

1.3 Objectives

The present work objectives are the following

1. Review agency concepts and its applications to energy system's problems.
2. Review agency concepts and applications to DSM, DR and Load Management.
3. Apply agent-based architecture and principles to define a wide and general framework to optimize loads for power consumers.
4. Review distributed optimization models and its synergies with agent-based models for problem solving in energy systems and specifically to DR and DSM.
5. Design a general agent-based framework capable of determining a DR solution for day-ahead load scheduling in the context of energy markets and multi-entity interaction.
6. Implement the framework with computational platforms in order to demonstrate its functionality and to set it as a starting point towards an agent-based software tool for Load Management and optimization.
7. Apply the software implementation to specific datasets and produce solutions that test the performance of the general framework but also its optimization models, mechanisms and algorithms.
8. Outline work pathways for further development of the framework but also enumerate questions and problems for future reasoning about agent-based architectures applications to load optimization.

1.4 Work Layout

Chapter 1, from section 1.5 onwards, present the agency and GT concepts as well as the optimization BLP. It then moves on to reviewing some of the bibliography on the applications of these domains to energy system's problems and to load optimization, DR and DSM. This chapter constitutes a theoretical introduction to the ideas and approaches that will guide the general framework's design.

Chapter 2 presents the methodology and, specifically, the theoretical outline of the general framework. It uses a top down approach starting from a high-level description and move down to low-level models. It also presents the framework's hierarchical architecture, the general relation between levels and outlines the main functionalities and the involved agents. From section 2.4 onwards, the mathematical optimization models for the internal reasoning structure of each agent in the system are detailed. The communication dynamics between the agents is also detailed and a solution approach in the context of a bi-level model is proposed. At last, the coordination bottleneck is identified and an algorithm encoding a DR mechanism towards coordination between power consuming agents is proposed.

Chapter 3 presents the numerical implementation of the framework and describes the used software implementation. It also presents the used datasets (parameters and data series) and plots example output results for some of the system's variables and mechanisms.

Chapter 4 defines case studies from subsets of parameters and output simulation results. Simultaneously these results are analyzed, discussed and conclusions are presented about the performance of the mechanisms of the framework.

Chapter 5 critically review the framework and more conclusions about the used approaches are presented. It also outlines future work and possible research paths.

1.5 Agents, optimization and game theory

1.5.1 From agents to multi-agent systems

Agency is a paradigm of computation based on the concept of *agent*, an entity that, according to Michael Wooldridge, is defined as "a computer system, placed in an environment that is capable of acting autonomously in order to reach its objectives" [14]. A more conceptual definition is given to us by Helder Coelho stating that an agent "is an entity that operates autonomously in an environment where other processes and agents exist" [15]. Although there exist several other definitions of agents, the difference between these two lies in the fact that the latter identifies a practical application for agents (software) while the former defines an abstract entity. Agents can be specific elements in a software or computer system but also a conceptual framework from which systems are conceived. However, some fundamental characteristics are highlighted in the two presented definitions. First, *autonomy*, the capacity to act and reason without other agent's control and second, *objectives*, the goals that direct its actions. But also *reactivity*, the capability to sensor the environment and react to it in a way that satisfy their objectives, *practivity*, the capacity to take the initiative and exhibit goal-directed behavior and *social ability*, the capability to interact with other agents towards the satisfaction of its objectives [14]. These characteristics form the base of *intelligence* in agent-based systems (ABS). Therefore, a great part of agent theory is focused on how decisions are made, actions taken and how do agents reach their objectives. Several architectures have been proposed to formally address their internal process. These can range from purely *reactive*, i.e agents that act as a consequence of stimulus, to complex architectures based on *beliefs, desires and intentions*. There are also symbolic architectures in which the environment is symbolically represented, and also hybrid architectures. But *Social ability* is, perhaps, the most promising feature of the agent paradigm. It refer us to the notion of collective and *interaction* through *multi-agent system* (MAS). Groups of agents are quite important for distributed problem solving since solutions for real-world complex problems may be achieved through the cooperation between multiple agents. MAS may be defined as "a loosely coupled network of software agents that interact in an autonomous, collaborative and possibly synergistic way to solve problems that are beyond the individual capacities of a single problem solving agent" [16]. In this case theory focus on how agents communicate and negotiate between them, how they interact, how they compete or cooperate. *Interaction* and *negotiation* between agents constitutes a huge field within MAS theory and it relates directly to *game theory* (GT), the mathematics of negotiation and interactions between decision makers. GT is a wide knowledge domain that presents formal models for the strategy definition towards competition or cooperation between agents that participate, as example, in auctions or bargaining. Some of the original GT problems originate from economics and it has a wide applications to financial markets operations. However, as a computer science framework to model interactions, it has applications to fields that range from social science to physics and essentially to all real world problems that can be reduced to interactions and negotiation. The central piece of GT are self-interested agents that possess a description of the states that it wishes to assume. The outcomes of choosing such states may influence other agents or the environment in which all live. The dominant modeling approach for considering agent's preferences is based on quantifying some real *utility function* that represents its preference across a determined choice [17, pag. 17]. When several agents with different and, perhaps, conflicting utilities interact, games can become incredibly complex and GT describes the mathematics of these interactions. Games can be

noncooperative if the latter situation holds but they can also be *cooperative* if agents objectives are aligned between them. GT and MAS are closely linked and because of that in the present work, GT serves as a background and a line of thought in next chapters. However, its not our intention to describe extensively the theoretical formulations or results on GT. The work in [17] is a concise introduction on the field and [18] is a in-depth work about the topic. *Agent-based Modeling* focus "on the modeling of systems at a local level through the definition of their elementary units (called agents), as well as through their interactions" [12, pag. 53]. The same author points that ABM are a form of modeling MAS. The fact that agents may have the same internal architecture but its specific local environments may change, originates a situation in which agents with the same reasoning process and objectives make different decisions. As a consequence high level emergent phenomenon may result from agent interactions. These phenomenon are not possible to perceive from the agent individual behavior and moving from single to multi-agent systems is followed by an increase in the complexity of the problems. The search for new answers and tools made distributed intelligence an unavoidable field since complex applications are no longer constituted by its simple components. [19, pag. 4]

In practice, agents can be a block of code that represents an organization in negotiations with other organizations "living" in internet servers, a physical hardware component that controls a chemical process or a thermostat in a house with the capacity to disconnect an HAVC system. A MAS may be a group of distributed computers that work together to perform a task or a group of robots moving in the same space.

1.5.2 Optimization

Optimization and operations research are the mathematics fields that seeks to produce analytical methods for decision making. Having evolved from economic and industry problems it is nowadays a prolific field as more and more knowledge domains use it for solving complex real-world problems. A mathematical optimization problem is constituted by a set of equations, inequalities and parameters and can be written in the following generic form [20]

$$\begin{aligned} & \underset{\mathbf{x} \in R}{\text{minimize}} && f_i(\mathbf{x}), && (i = 1, \dots, m) \\ & \text{subject to} && \phi_j(\mathbf{x}) = 0, && (j = 1, \dots, n) \\ & && \psi_k(\mathbf{x}) \leq 0, && (k = 1, \dots, r) \end{aligned}$$

where $\phi_j(\mathbf{x})$ and $\psi_k(\mathbf{x})$ are functions of the decision vector $\mathbf{x} = (x_1, x_2, \dots, x_n)^T$ called *constraints*. x_n are the problems variables which can be continuous, discrete or binary. $f_i(x)$ are the *objective functions*. The domain of the decision variables is the *search space* while the values they may take, for which the problem have a solution, is called the *feasible space*. An analytical process for solving an optimization problem must be able to find the values of \mathbf{x}^* for which the $f_i(\mathbf{x})$ is minimized (or maximized). For the variable *optimal solutions* \mathbf{x}^* correspond the problem's optimal solution $f_i^*(\mathbf{x})$. Optimization is intended to solve theoretical or practical problems but can only be solved if its solutions are physically meaningful and if they can be represented in the given general form. If objectives and constraints are both linear and variables continuous it is a *Linear Programing* problem (LP). If one variable is integer and the remaining continuous, while objectives and constraints are linear, it is called a *Mixed Integer Linear Problem*. Problems are usually complicated if both objectives and constraints are

non-linear, i.e. *Non-Linear Problem* (NLP) and even more if they are *Mixed-Integer Non-Linear Problem* (MINLP). If problems have more than one objective function they are *Multi-Objective Problems*.

1.5.2.1 Bi-level problems

Bi-level problems (BLP) are a subclass of optimization problems in which a problem is nested in another. There are two levels of decision, an *upper level* containing the *leader* problem, and a *lower level* containing the *follower* problem. They are of special interest in problems that comprehend distributed decision making involving several entities with hierarchical relations [21]. The interest around BLP is increasing since its applications range from network design problems in transportation, combinatorial problem for facility location or policy decision in environmental economics and there are also extremely important applications to energy systems.

The general form of this kind of problems is as follows [22].

$$\begin{aligned} & \underset{x_u \in X_U, x_l \in X_L}{\text{minimize}} && F(x_u, x_l) \\ & \text{subject to} && G_k(x_u, x_l) \leq 0; \quad (k = 1, \dots, m) \\ & && x_l \in \underset{x_l}{\text{argmin}}\{f(x_u, x_l) : g_j(x_u, x_l) \leq 0, j = 1, \dots, n\} \end{aligned}$$

Where F and f , G_k and g_j , x_u and x_l , X_u and X_l are, respectively, the leader and follower objective function, constraints, decision variables and decision space. The *lower level reaction set* is defined as

$$\psi(x_u) = \{x_l \in \underset{x_l}{\text{argmin}}\{f(x_u, x_l) : g_j(x_u, x_l) \leq 0, j = 1, \dots, n\}\}$$

and it is comprised by the solutions for the lower level problem for an upper vector decision vector. A solution for the BLP is one that minimizes the leader objective constrained by the condition of being contained in the reaction set. This is one of the facts that make this problem computationally difficult. The upper level cannot find a solution for its problem without considering the lower level reaction set. Simultaneously, $\psi(x_u)$ can be seen as a non-linear constraint in the upper level problem making the whole problem non-convex [21]. Even if both level assume the simplest linear form, it is proven that an algorithm that find a solution in polynomial time doesn't exist [22]. In this sense metaheuristics have been used to solve the problem finding only a good solution. Other solution approaches have been used such as transforming the BLP in to a single-level problem and then solved using known methods like representing the lower level problem by its Karush–Kuhn–Tucker (KKT) conditions as a constraint for the upper-level problem. *Stackelberg games* are a class of strategy games named after the german economist Von Stackelberg that proposed it as a competition between firms in which they respond to each other moves sequentially. Stackelberg games and BLP are similar in many ways but they may differ when $\psi(x_u)$ is not a singleton set for some values of x_u . In that case a solution for the BLP may not be a solution for the Stackelberg game [23]. The authors in [21] present an extensive work on methods for solving BLP.

1.5.3 MAS and the power grid

The analysis of the power network from the MAS perspective is centered on the decomposition of its fundamental parts. Therefore, the mechanisms for managing such a system are being displaced away from the concepts of centralization on to full decentralized distributed management. In fact, the integration of large shares of DER in multiple points of the grid through PV or WPP, the approaches that focus on new typologies like energy-hubs, multi-energy systems, microgrids, Virtual Power plants, the adoption of PEVS, active loads and power markets immediately refer to a system-of-systems view that, inevitably, refers to the agent paradigm [1]. The potential of MAS applications to power systems can be understood through the common features between SmartGrid and agent-based architectures. First, MAS are *flexible* and *autonomous*, since they are able to react to dynamical situations and are able to choose the best action among a set of possible ones. Second they are *extensible* or *modular*, property that links with the capacity to add new functionalities to the systems in which it is integrated or update the existing ones. As an example, an agent responsible for grid parameters motorization may update its algorithm for computing power flow without the need to implement a new agent. In energy systems there is a growing concern with the ability for systems to be robust, i.e fault-tolerant and able to proceed with its operation when a part of the system fails.

The approach for using agent-based approaches to solve optimization problems is based on the decomposition of a global problem and the assignment of subproblems to agents or parts of the system. In this way large scale problems can be handled if the system under study shows characteristics of modularity like the SmartGrid paradigm does. An agent-based system for problem solving distributes the resources among a network of agents [16] and the determination of a good global solution depends, from there on, on the interaction among them [24]. The authors in [24] and [16] present an extensive review of agent-based systems applications to optimization problems. Specifically related to energy system problems, [25] and [12] present important reviews. Authors in [26] explore MAS energy markets and model the interaction between agents towards Bilateral contracts.

1.5.4 MAS and DSM

MAS approach to DSM and DR is of furthestmost interest when considering decentralized architectures not only for EVs. [27] and [28] both present decentralized strategies through game theory approaches or agent-based approaches. The authors point out that centralized mechanisms pose several privacy problems, namely detailed acquisition of data on user's consumption. On the other hand, using decentralized approaches, the involved devices optimize locally their consumption and only transmit reduced quantities of data and information to other points in the system. Authors in [29] presents a DSM program through a scheduling game among users. Authors in [30] propose an automatic DSM system for buildings. In [31] a MAS is applied to an electricity distribution grid. The system defines agents for the main grid components such as substations, buses, feeders and loads with the objective of dynamically balancing production and consumption and to maximize the use of locally produced renewable electricity. This work describes in detail the roles attributed to each agent and the rules that manage communication through messages as well as the sequence of steps that leads to demand management. In [32] a MAS is developed to allow for energy

exchange between microgrids incorporating DR as a way to reduce peak demand and minimize energy cost. The academic production in the domain of agent-based DSM mechanism is large. Concerning EVs management through agent-based approaches reference [5, pag. 724] makes an important review and clearly states that *"the experiments carried out by researchers show that MAS can manage PEVs charging task avoiding overloads in distribution networks"*. The authors in [33] design a resource management architecture for microgrids and implement it in a MAS specific software. Furthermore *GRIDLAB-D* [34] is an agent-based open source power system simulator to test new technology adopted and new management mechanisms. It has the particularity of modeling not only the power system but the underlying systems.

1.5.5 Optimization and DSM

About optimization methods for DSM, the authors in [3] point out three main classifications. First the demand management systems may be designed in order to optimize individual users energetic resources or a community of users. Second, optimization may be classified according to the techniques used to design the mechanism: stochastic or deterministic. The difference stands in the nature of data and parameters used, based on deterministic data or stochastic data based on random variables. A third classification divides problems according to the time-scale in which they are solved: day-ahead or real-time. The authors point-out the possibility of side-effects when consumption is displaced, in bulk, for the same timeslots for the cases in which the mechanism is controlled by price signals creating new load peaks. Possible solutions for this problem is the formation of user communities that manage their resources in a system-wide perspective. For these cases two approaches are proposed in order to solve the problem. optimization or game theory. Using optimization users may cooperate in order to solve the problem and optimize a common objective. However this does not solve possible conflicts making the use of game theory needed since it can model interactions between players in the power grid.

1.5.5.1 Bi-level models and DSM

Within this decade BLP have been used to solve DR and DSM problems in the context of SmartGrids. The common feature within these works is the interaction between upper level grid entities and lower level consumers. In [35] a 1-leader k -followers Stackelberg game between a utility company and multiple users is formulated towards the determination of an optimal strategy for balancing demand and supply and smooth the system's aggregated load. The authors present a DR mechanism using real time prices and propose an iterative algorithm to determine optimal power generation and demands. The numerical results show that the methods help to flatten the aggregated load and reduce mismatch between supply and demand. In [36] a similar situation is exploited with a greater focus on GT. A DR problem is formulated as a non-cooperative bi-level game between provider-level and consumer-level. They also exploit cases with information sharing among consumers and the algorithms presented are intended to serve as a starting point to study this question. Authors in [37] use a distributed algorithm to model the interactions between costumers willing to lower electricity bill and an electricity retailer willing to raise its profits. The problem is solved using a hybrid approach in which genetic algorithms are used to solve upper level problem and individual optimization algorithms for lower level. In [38] a DR model is presented that, again, solves a Stackelberg game between retailers and consumers. However, unlike the previous works the solution approach is to reduce the BLP to

a single-level MILP. This work considers uncertainties in data and compare the performance of the obtained solutions for RTP and TOU prices. In [39] the BLP is also reduced to a single-level MILP replacing the followers' problem by its KKT conditions using its linearity and the fact that a solution for the KKT system are also solutions for the followers' problem. This replacement can only happen when the lower level problem is convex and enough regular [22]. In [40] a distributed algorithm is also used to solve, in a distributed manner, the single-level problem. In [41] a different problem is solved. A Stackelberg game is formulated considering microgrids as followers, and generators as leaders with the objective of determine strategic generation planning of both levels.

BLP applied to specific energy system problems is a growing field of research with much to be explored. The ICT functionalities of the SmartGrid allows us to consider multi-level negotiation as viable control structures to manage the operation of energy systems. The reviewed papers served as a conceptual basis for the present work implemented within an agent-based framework. In [42, pag. 46] we can find an extensive review of game theory applications to SmartGrid problems.

1.6 Modeling and simulation of loads

Modeling and simulation of residential sector energy consumption profiles currently attracts enormous attention among modelers and energy systems analysts alike since results and outputs can be a major tool to analyze the impacts of social and technological changes in energy system and the adoption of new policies. However the residential sector electric structure is a complex and dense one that poses major challenges for the creation of numerical and computational models able to deliver profiles and forecasts. Levels of detail can start at individual home appliances and make up to the total load diagram of a household. It becomes clear that having insight onto a country, a city or even a neighborhood detailed energy consumption profile can become an impossible task with high computational and monetary costs. The residential sector is composed of a great quantity of typologies when it comes to buildings, thermal behaviors, appliances ownership and, much important, social and economical factors such as schedules of occupancy, patterns of appliances use or family structure. One major focus point is the influence of some of these factor on the general behavior of a profile and, here again, major computational issues arise. Different modeling techniques have been used to accomplish some of the later objectives and the work published in [43] reviews these techniques. It identifies two main approaches, namely, *Top-Down* and *Bottom-Up*, and points out its main strengths and weaknesses. The first difference that arise between modeling techniques is the kind of input data that must feed the models created, which can be obtained from physical building and appliances characteristics, social habits of inhabitants, historical energy consume data series, climate data and economic indicators. We can also have information about one appliance, one dwelling or an entire city and have different time resolutions going from one minute or one day up to a year of data.

Top-Down This class of modeling techniques looks at the residential sector as a whole. This means that there are no disaggregation in end-consumes at the household level and we can only look at the total aggregated consume. These techniques are used to analyze the effects of long-term measures in energy systems using data such as GDP, unemployment rates, climatic

conditions, energy prices, housing market data and estimates of appliance ownership.

Bottom-Up This class of modeling techniques represent all the techniques that model energy consumption at appliance or household level. The profiles can be extrapolated for groups of houses or regions in order to create aggregated profiles on upper levels. Input data for this kind of models are composed of building characteristics such as geometry, construction materials, thermal characteristics, climate data, appliances electrical characteristics and occupancy schedules. It is further divided into two kinds of techniques namely, *statistical methods* (SM) and *engineering methods* (EM). The former are based on historical data that is used to obtain end-use consumption through regression. The latter use dwelling thermal characteristic and power ratings of appliances to explicitly generate load profiles. One of its strengths is that there is no need for historical data, which poses big advantages when modeling the adoption of new technologies. EM is further divided in three techniques namely *distributions* technique, where appliance ownership distributions are used to calculate end-use energy consumption; *archetypes*, where housing is classified according to factors such as size, type or age. The archetypes are used as representative for house classes in a given zone and, using the number of houses belonging to each archetype, a regional consumption profile can be created. There is also the *sample* technique, where one sample house is determined to be used as reference.

António Sá, in [44], uses a *hybrid* approach between SM and EM bottom-up approaches where a synthetic data generator developed by Richardson *et al.* [45] is combined with EM for house appliances to develop an agent-based simulator for estimation of residential energy consumption and on-site renewable generation. The Richardson Model is used to simulate profiles that depend on occupancy patterns such as lights, and physical models are used to determine the consumption of HVAC, Water heater or refrigerator and production from PV modules and wind turbines.

The presented bibliographic review, crossing several domains was the theoretical base from where a solution for the *load optimization* problem, based on ABS, emerged.

Chapter 2

Methodology

Within next sections the complete description of the proposed framework will be presented. A top-down approach will be used starting from high-level concepts and move on to low-level models and methods. The general framework's main objective is *load optimization* in the context of day-ahead electricity markets. This means that it must be able to produce *solutions* for the stated problem which translate, specifically, into delivering *data* that constitutes the base for some *strategy* or a *decision-making process* about load optimization from an agent-based perspective. However, the physical meaning of *solutions* will be much clear as framework descriptions move from high to low level domains.

2.1 High-level architecture

High-level architecture stands for a general concept-based holistic description of a system. The presented framework must be built in the intersection between SmartGrid vision of the power grid and agent-based architectures. This intersection is explicitly defined in [13] where SmartGrids, if viewed as *cyber-physical systems*, may be treated as an agent-based system. Within this vision agents are interpreted as software entities that depict physical entities on the power grid. The framework must also assume characteristics such as *modularity*, *scalability* and *parameterizability* and agency concepts allows to do so like have been seen in Chapter 1.5. As can be seen in general concept map in Figure 2.1, the framework is composed of several modules in which some represent entities while others represent ideas, design characteristics or objectives. Departing from the top the framework's core is the *Optimization Agent Model* with the objective of solving the *Load Optimization problem*. For that it must, internally, depict the smart grid architecture as a cyber-physical system, namely through representations of cybernetic and physical subsystems. Software elements running on a computational system assume the agency characteristics depicting physical elements of the SmartGrid.

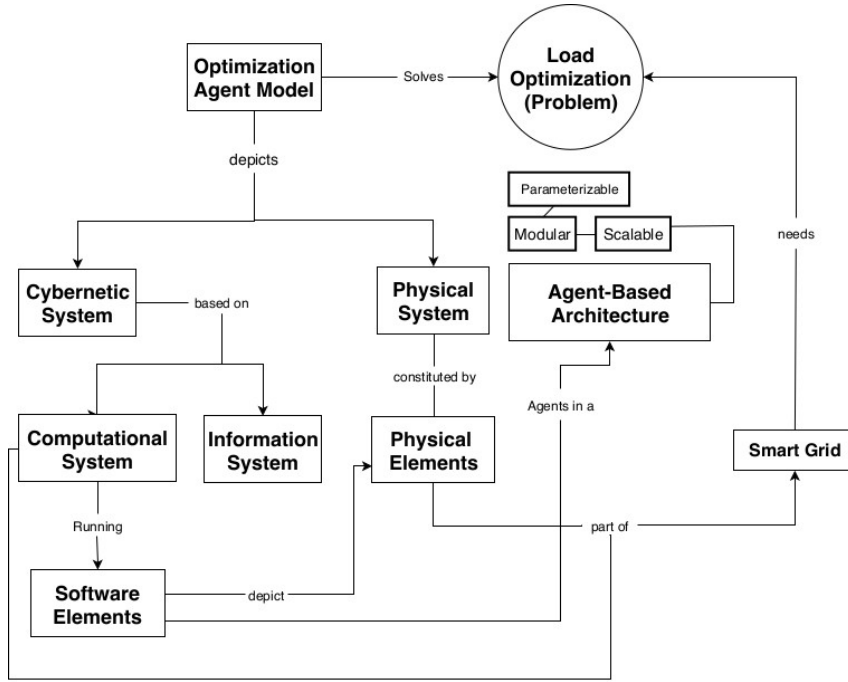


Figure 2.1: Agent framework's general concept map

Detailed concept map in Figure 2.2 takes a deeper look onto the framework's architecture. From an operational point of view, the model will be inputted with data that will travel along the communication system onto the sub-models where processing and computing takes place. This is already the domain of low-level models which will be described further ahead. Software elements such as code routines and applications are, internally, made up of mathematical models. Physical and optimization mathematical models are a special part of the framework since they simulate the behavior of smart-grid components in order to serve as a basis for a control and decision making process through the data they produce. Mathematical models will be the main focus of the present work and the fundamental part of the coming chapters. An important design architecture is the use of a *multi-level*¹ approach in which mathematical models, software and physical elements will have an equivalence to specially defined hierarchical levels. The different significance within the same level originate an abstraction layers. This multilevel hierarchical approach is the basis of the practical implementation of *agents* and of the dynamics for solving the load optimization problem. Mathematical models and data dynamics are two special points that are highlighted in the concept map in Figure 2.2 with red dashed rectangles enclosure and will be analyzed with great detail in further chapters.

Another important point is that this general framework is intended to be valid over several scales and formats of the power system such as Microgrids on the city scale, Virtual Power Plants, regional or national grids scale and to emergent organizations in future SmartGrid. The modular architecture makes it also possible to explore different internal contents of the models such as different mathematical models, different hardware components, communication systems or solution assessment processes. The agent-based architecture ensures that the operation dynamics fits those changes. This is the concept of modularity and what could be interpreted as *plug-and-*

¹One must not make confusion between Multi-Level agent architecture and High-Level/Low-Level descriptions. The former is a design characteristic and the latter a descriptive method

play modeling approach. If this view is extended into the multiplicity of data structures and formats the framework becomes a parameterizable one that can be applied to different contexts if fed with adequate data-sets.

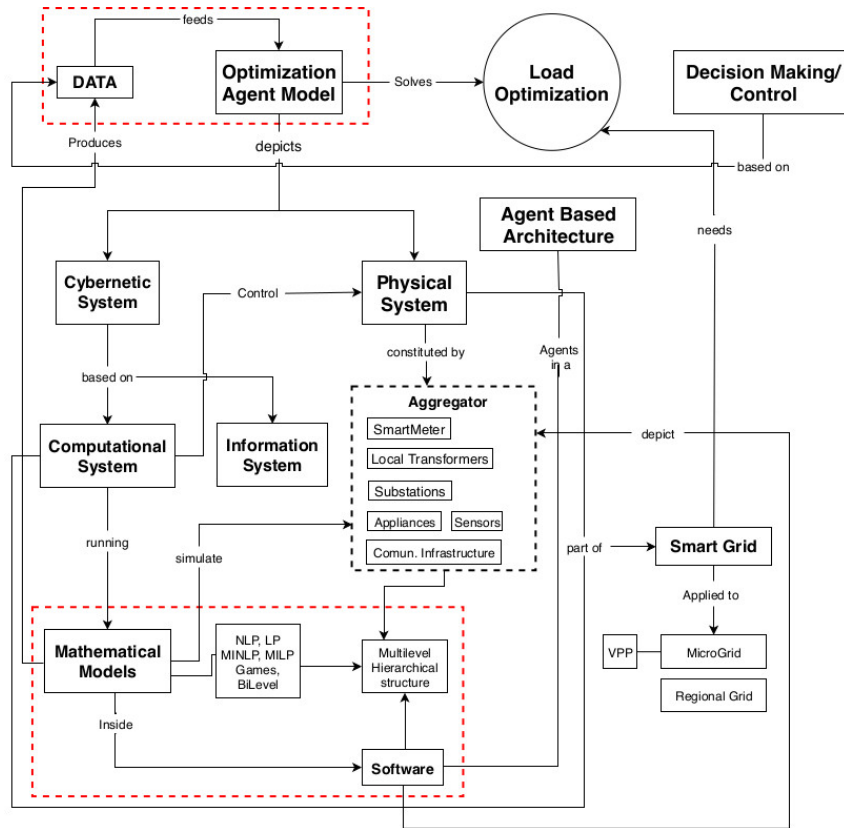


Figure 2.2: Agent framework's detailed concept map

2.2 Low-level models

Low-level architecture stands for a formal, detailed description of the mathematical, physical and algorithmic models used to compute a load optimization solution.

2.2.1 General multi-level architecture

Load optimization is defined as *the problem of determining a system's optimal load distribution when subjected to a specific objective*. With this definition in mind, the framework's main operation consists in determining *several different sets of numerical and design results with the purpose of serving as a base for control and decision making process on load scheduling and operation*. These loads range from individual household loads such as home appliances to industrial electric ovens or aggregated power consumption. Residential appliances load diagram, in the Watt scale, are different from household aggregated load diagrams, in the kilowatt scale, which in turn are very different from regional aggregated diagrams in the Megawatt scale. This is exactly the point where a multi-level architecture is of furthest interest. Different scales in the electrical system may be interpreted as *levels* and these have their specific optimization problems, i.e, they have level-specific numerical and design solutions

which produce different optimal load diagrams. The question that arise naturally is what kind of relations can be established between solutions from different levels or, specifically, what relations one may establish between the load diagrams and parameters of the different levels. This open up for a *complex-system* dynamics in which the system-wide aggregated behavior is the product of the joint activity of lower-level scales and these relations are rather obscure. Agent-based architecture is especially suitable for this problem since it uses the principle of dividing a system in its subsystems and through a bottom-up approach make the system-wide dynamics evident. Lower-level models are physical models that simulate the behavior of a set of power consuming appliances and devices at residential, commercial or industrial level, and higher-level models are power grid models such as power flow.

Three general levels will be defined named *Typologies Level*, *Local Node Level*, and *Aggregator Level*. On typologies level, *Demand Side Management* models are run in order to define the optimal load diagram for commercial, residential and industrial consumers with the objective of minimizing the users' electrical bill and from them demand information is sent to higher levels. The consumers load modeling approach is based on the definition of $K \in \mathbb{N}$ general consumers' typologies which allow for load diversity in users load profile. Local level will serve as an intermediary between typologies level and aggregator level. It will not be responsible for running optimization models but will act as an arbitration agent and data manager. In aggregator level, load flow models, such as *Optimal Power Flow* are run, in order to establish proper grid operation mode aiming at minimizing the aggregator's energy cost. This cost will be used to compute a *local energy tariff* for consumers. Agents are defined within levels and models are a part of agents. For the remainder of the present work, typologies, local node and aggregator agents will be referred as \mathcal{A}_k , \mathcal{A}_N and \mathcal{A}^0 , respectively. Each one of them integrates its own models, namely \mathcal{M}_k , \mathcal{M}_N and \mathcal{M}^0 . Agent's models are the central piece of its intelligence and they are part of their reasoning and decision process. The multi-level agent-based structure functionality demands that all agents communicate with each other and, through interaction, solve the load optimization problem in a distributed manner. These interactions will fall on the domain of a BLP model and GT approaches.

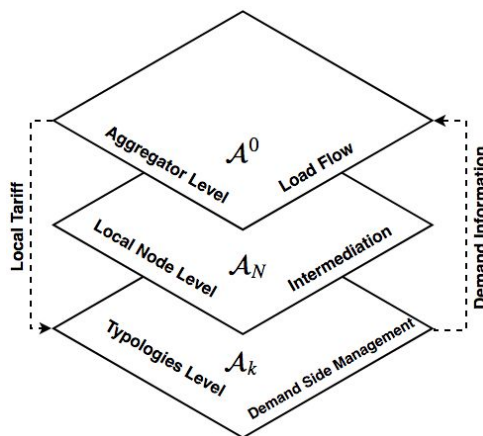


Figure 2.3: General agent's framework multilevel structure

Abstraction layers In Figure 2.2 multilevel based hierarchical structure is reached out from a number of other modules, namely physical system elements in the aggregator, software and

mathematical models. Those connections in the concept map highlight the fundamental idea that the levels depict specific physical critical points in the power grid such as smart-meters, local transformers or substations, but also the computing and data processors in a computer network. This equivalence between power grid nodes and computer network nodes is the corner stone of the SmartGrid concept and each of this nodes may be looked at from a functional, physical, or mathematical/software perspective or, as in the present work, as an *abstraction layer*. Agents are the abstract entities existing in these nodes that depict the levels. Abstraction layers are viewed through block diagrams, the *Fundamental Modeling Concepts* (FMC) static structure in Figure 2.4, since they only depict time-independent relations between agents. The notation needed to read FMC diagrams is given In Annex 6.1. Three abstraction layers will be considered, namely *functional layer*, which defines the model from a conceptual point of view, *physical layer* which identifies the physical components represented by each agent and *code layer* which identifies software, data types and mathematical models. In Table 2.1 a summary of the abstraction layers description is presented and in Annex 6.2 a more detailed description of compositional structure is presented.

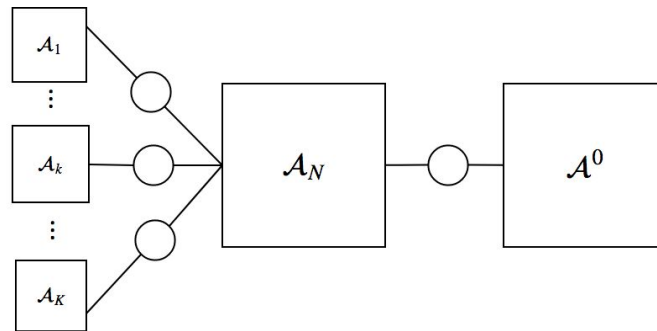


Figure 2.4: Agent framework's compositional structure block diagram

Agent/Layer	Depicting	Functional	Physical	Code
\mathcal{A}_k	Consumers	DSM Solutions	Power consumption points (Smart Meters)	Software and Models
\mathcal{A}_N	Intermediary	Aggregating solutions and mediation	Computational unit (Transformers)	Software and Models
\mathcal{A}^0	Price setting entity / Grid operator	Power Flow Solutions	Transformers	Software and Models

Table 2.1: Abstraction layers summary

As shown in Figure 2.4 there are K communication channels between \mathcal{A}_k and \mathcal{A}_N agents and one channel from \mathcal{A}_N to \mathcal{A}^0 .

2.2.2 Communication

Communication is a fundamental part of ABS. Using FMC petri-nets diagrams the proposed framework's dynamic structure can be analyzed. These diagrams express the system behavior over time issued from the dynamic operations contained in the channels between agents in the compositional structures. As can be seen from Figure 2.5, presenting a solution for load optimization is the consequence of an iterative process based on the information exchanged between agents, namely signals and solutions. Each agent has access to its own private data-sets, computes his own solutions and sends partial sets of data onto other agents. An important role

is assumed by \mathcal{A}_N since it is responsible for moderation, negotiation and aggregation processes but also evaluation of criteria for ending the iterative process.

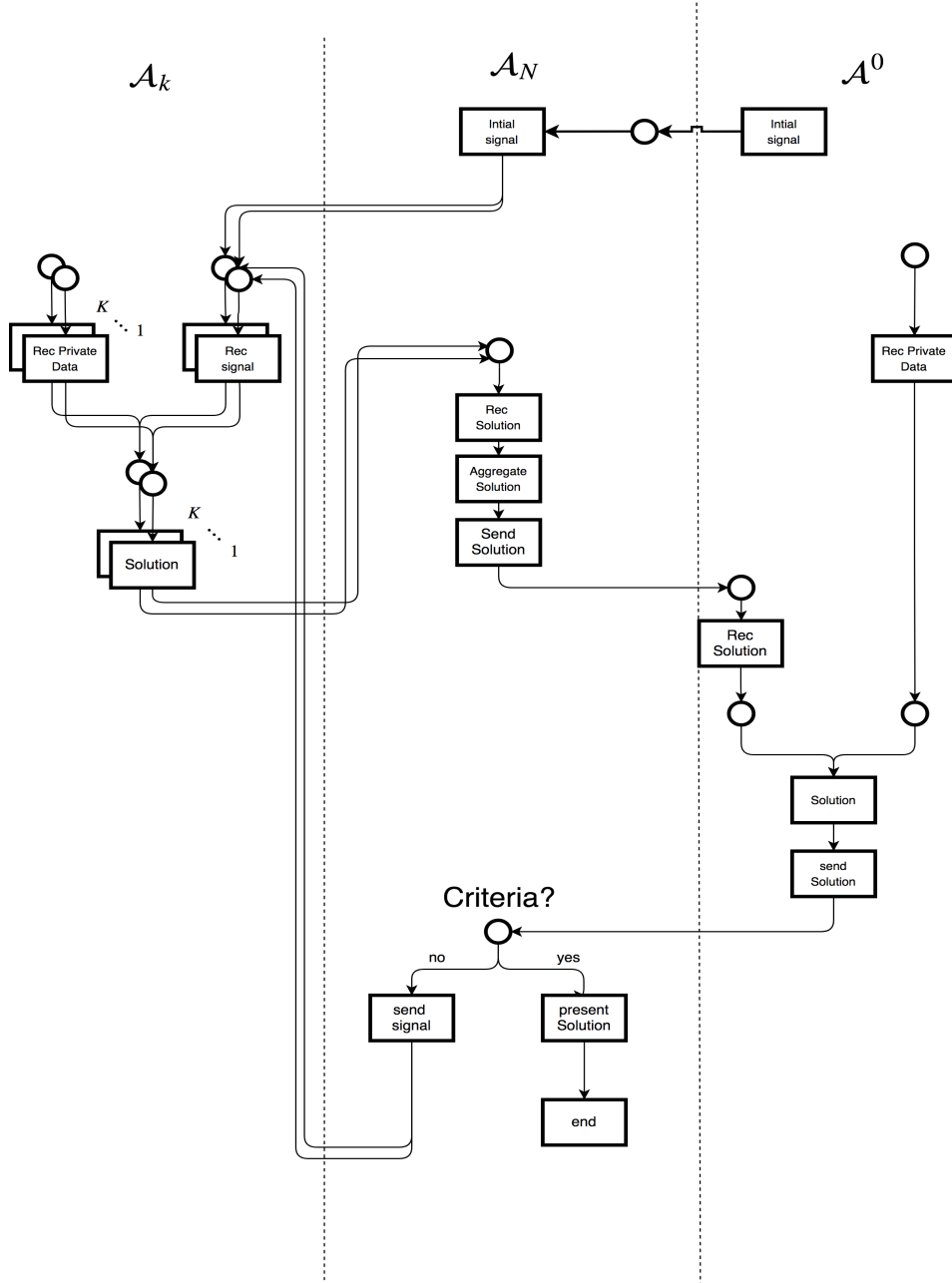


Figure 2.5: Agent framework's dynamic structure petri net

2.2.3 Data and information

In the present framework all input data series are available real data that can be obtained in various ways. This is the case of some device load profiles or climate data forecasts like wind speed or temperature data sets. The model needs a determined set of data to work, whether this data is generated through algorithms, obtained through sensors or from Internet servers. Another important issue is the time domain of input data and solutions. Since the model's specific context are *Day-Ahead Energy Markets and Demand Response*, the data series,

independently of its time discretization, must have a time horizon of 24 hours. All data will have the format and structure that better fits the models. The present framework is designed considering privacy as a fundamental feature. This means that the agents will not have access to all data and models will work with only subsets of all the data available reducing in this way the quantity of information exchanged between agents. In Annex 6.3 further notes about this specific issue are presented.

2.3 Agent framework overview

A possible implementation of the general framework is presented in Figure 2.6 where the most important elements of the proposed frameworks, as well as the the static relations between them, can be seen. It also depicts a possible geographical disposition for the physical elements. Dark lines are power connections and dashed blue lines are communication channels (not necessarily physical, may be wireless). Cubes depict agents and each cube face highlights abstraction layers. In the beginning of each communication channel a dark arrow points the direction of the communication act and what information is sent. Figure 2.6 has the particularity of showing the intersection and relation between the multiple knowledge zones where the framework exists: between computer science, agent theory, communication and information science, power-grid engineering, innovation, changes in energy system organization, physics of complex systems, optimization and GT. The different disciplines only enforces the idea that smart-grid applications exist in the intersection of several different knowledge areas.

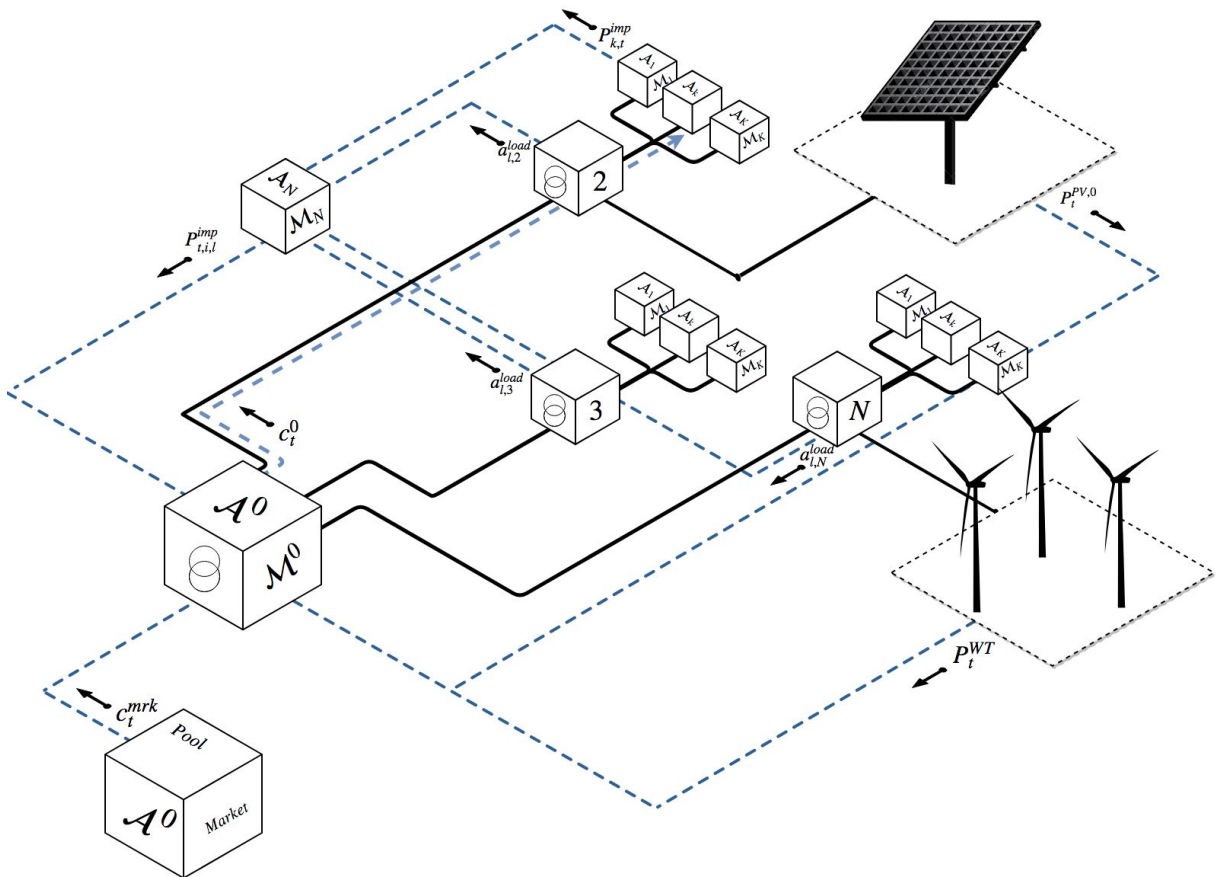


Figure 2.6: System wide vision on the framework's implementation

2.4 Methodology - Development

2.4.1 Detailed Model - \mathcal{M}_k

2.4.1.1 Typologies creation

The approach used at typologies level consist in modeling aggregated load diagrams for a residential or commercial elements such as households, workshops or small industrial units. This translates into modeling its appliance individualized loads and then aggregate them through Bottom-Up Engineering Methods. However one element, by itself, don't allows us to represent aggregated load from one building, neighborhood block, city or region unless it is a reference sample dwelling [46]. To tackle that problem the modeling approach used is based on the creation of *typologies*, or archetypes, that represent variety and diversity in the elements structure and the characteristics for a specific region or zone. The variety of input parameters that influence household load profile may be building constructions insulations, geometry, climate profiles, appliances settings and much more. Typologies will be created defining K parameter sets to serve as reference for dwelling types. This means that dwelling diversity will be reduced to K types, which obviously heavily limits the capacity to represent urban or rural dwelling diversity in that way. Anyway the complex nature of the energy system imposes the need for major simplifications. One can construct a very large quantity of typologies in order to have much references but a typifying procedure is inevitable, since simulation models simplify reality for feasibility sake. Archetype based methods can also serve as a more general approach into electricity consumption modeling since one can set them to represent higher or lower aggregation levels like households or commercial installations. Archetypes may be easily adapted into modeling an individual machine, like a specific machine inside an industrial plant or a PEV charging station. In this sense, typologies based load modeling is a general methodology that allows for diversity. The effort in this work will be placed in determining typologies that models, mostly, urban or rural dwellings.

2.4.1.2 Demand Side Management as an optimization model

To formulate \mathcal{M}_k the models presented in [3] will be used. With the appliance specific solutions it is possible to compose a load profile, or load diagram, for each typology. Since solutions must be determined for a full day, the problem must be solved recursively for each **timeslot** t of a time discretization of the full day duration \mathcal{T} . Each timeslot must have a specific duration **timestep** Δt . Independently of the time unit (seconds, minutes or hours) in which \mathcal{T} is expressed, it must be verified that $t = 1, 2, \dots, H$ and $H = \frac{\mathcal{T}}{\Delta t}$. Several modeling applications use minutes as base unit for time ($\mathcal{T} = 1440$) and typical settings for timesteps are $\Delta t = 1, 5, 10, 15$ minutes. A smaller Δt means more computational time used to solve the model since the problem will have to be solved coherently for H time intervals in order to construct a full day optimal load profile. Typologies load profiles will be expressed in terms of the instant electrical power P_t in units of Watts at each timeslot t . Each typology load profile is a sum of the individual appliances load profiles and for each appliances it is considered that its specific power consumption at each timeslot p_t is constant during that timeslot so the total load profile at each timeslot is given by

$$P_t = \sum_{\text{appliances}} p_t, t \in H \quad (2.1)$$

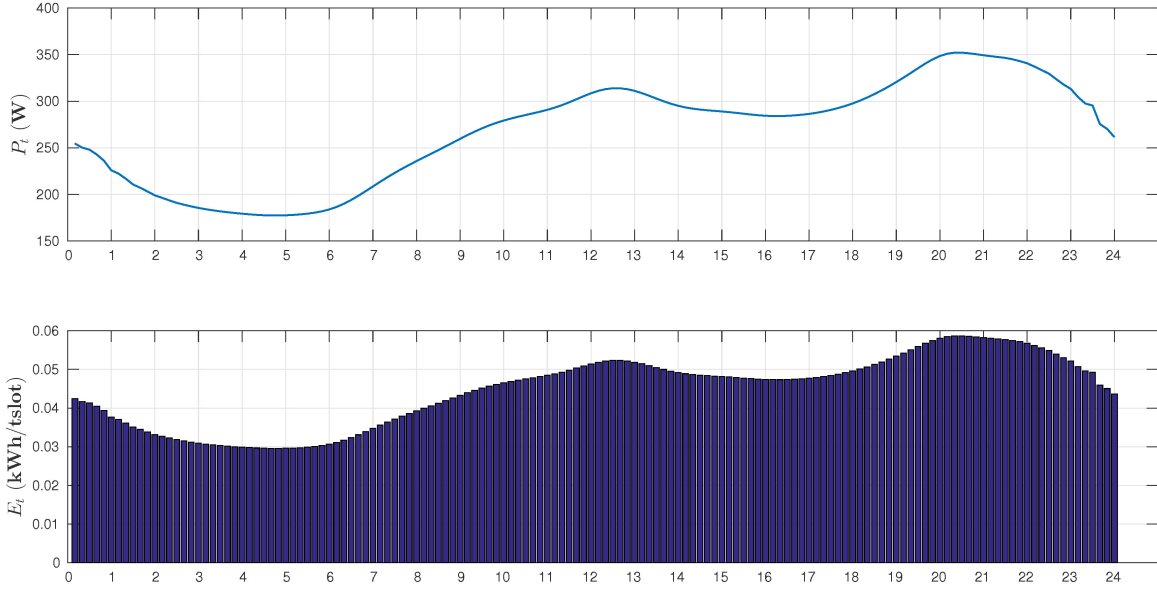


Figure 2.7: Top: An example load diagram. Down: Energy consumed per timeslot for $\Delta t=10$ minutes, $H=144$

This expression gives the typology consumption at each time timeslot t , a constant quantity of power P_t in Watts during one timeslot. During that time the quantity of energy consumed is just $E_t = P_t \mu$ where μ is a conversion factor between power and energy that is used to convert from W to J ($\mu' = 60\Delta t$ in seconds) or from W to kWh ($\mu^{kh} = \frac{\mu'}{3.6 \times 10^6}$) or, since timesteps will have less than an hour duration, from kW to kWh ($\mu^h = \Delta t/60$). The size of Δt is a consequence of the type of appliances present in a typology since small machines or even HVAC systems have reaction times less than an hour. Ω_k is the set of all appliances and power consuming devices present at typology k , represented by agent \mathcal{A}_k running model \mathcal{M}_k . The method to implement a DSM strategy consists in classifying the typology appliances $\omega \in \Omega_k$ in terms of the specific actions they can be submitted to and define their physical operation accordingly. These actions may be allocating the operation of an appliance during a specific subset of timeslots or resetting the limits of operation for others. To clear the language we say that defining the DSM strategy for typology k means computing a solution s_k , the output of \mathcal{M}_k . The appliances will be classified as *Fixed*, *Shiftable* and *Elastic*, respectively depicted by sets F_k , S_k and E_k , but the model will also include *Storage* and *Production* devices depicted by sets B_k and G_k with $k = 1, \dots, K$. For each k , the set of all appliances is just $\Omega_k = F_k \cup S_k \cup E_k$. In the next paragraphs detailed descriptions of appliance specific modeling is presented. These models are part of \mathcal{M}_k that is a general model with the same structure for all \mathcal{A}_k . So, for the purpose of presenting the models we may drop index k for variables and parameters keeping the index for the remaining symbols without any lack of generality. As an example, variables like $x_{\omega,k,t}$ will be considered just $x_{\omega,t}$

2.4.1.2.1 Fixed loads These are loads that cannot be submitted to any kind of DSM action. These loads account for lights, entertainment equipment such as TV's, laptops and other devices

with operating schedules determined by individual behaviors. These appliances may be modeled individually or aggregated but in any case the specific output of such models constitutes a parameter in the general model. On some cases the fixed load contribution to total load may be obtained from real measured data. Each $\omega \in F_k \subseteq \Omega_k$ is characterized by its instant power consumption $p_{\omega,t}^F$. The total fixed load is the sum of all fixed appliances

$$P_t^F = \sum_{\omega \in F} p_{\omega,t}^F \quad (2.2)$$

2.4.1.2.2 Shiftable loads These are devices whose load profile is set at a fixed rate during a given number of timeslots and the only possible DSM action consists on choosing its starting timeslot over the time horizon H , i.e, scheduling its operation. They operate in cycles, for example washing machines, dishwashers and many other home, commercial or industrial appliances fit in this representation. Each $\omega \in S_k \subseteq \Omega_k$ is characterized by D_ω^S , the duration (in number of timeslots) of its operation cycle, and l_ω^S , its constant load profile during its operation timeslots. \mathcal{M}_k must output the optimal timeslots in which a certain shiftable device must start and end its functioning cycle. For that the following binary variables are used.

$$x_{\omega,t}^S = \begin{cases} 1 & \text{if } \omega \in S_k \text{ is active at } t \\ 0 & \text{else} \end{cases} \quad (2.3)$$

$$y_{\omega,t}^S = \begin{cases} 1 & \text{if } \omega \in S_k \text{ starts its operation at } t \\ 0 & \text{else} \end{cases} \quad (2.4)$$

$x_{\omega,t}^S$ and $y_{\omega,t}^S$ are defined for each timeslot, each $\omega \in S_k$ and each typology (hidden for now) . These devices' operation is also subjected to the following constraints

$$\sum_{t=t_{start}^S}^{t_{end}^S} y_{\omega,t}^S = 1 \quad (2.5)$$

$$\sum_{t_\omega^S=1}^{D_\omega^S} x_{\omega,t+t_\omega^S}^S \geq D_\omega^S y_{\omega,t}^S \quad (2.6)$$

Constraint (2.5) guarantees that each device only starts working once during for $t_{start}^S \leq t \leq t_{end}^S$, where t_{start}^S and t_{end}^S are the \mathcal{A}_k preferences regarding shiftable devices operation and they can be used to set the time interval in which a shiftable device can operate. Constraint (2.6) guarantees that if a device starts working at a certain timeslot it stays active for exactly D_ω^S timeslots and completes its cycle. $1 \leq t_\omega^S \leq D_\omega^S$ is a parameter used as a counter towards that end. Since D_ω^S is a fixed parameter for every $\omega \in S$ the problem of determining when a certain device starts is equivalent to determining when it stops. The consumed power at each timeslot, for each shiftable device, is given by

$$p_{\omega,t}^S = l_\omega^S x_{\omega,t}^S \quad (2.7)$$

And the total shiftable power is given by the sum of all the shiftable devices.

$$P_t^S = \sum_{\omega \in S} p_{\omega,t}^S \quad (2.8)$$

$$\sum_{t=1}^H P_t^S = \sum_{\omega \in S} D_{\omega}^S I_{\omega}^S \quad (2.9)$$

The essential result of this approach for shiftable devices is that load profile becomes a succession of square steps that the optimization solver will place in the most convenient point in time. Typologies may have as much of these kind of devices as needed and they may be used to model more complex machines through the definition of a machine cycle as composed of a sequence of cycles. Further restrictions would have to be considered if we wish to impose that machines do not superpose they're operation.

2.4.1.2.3 Elastic Devices: Elastic devices are those whose instant power $p_{\omega,t}^E$ may be modeled or controlled by other model variable. They will be divided into two subsets, namely *Energy-Based* and *Comfort-Based* elastic devices. The main difference between subtypes is that Energy-Based devices need to consume a fixed quantity of energy during a certain time period and Comfort-Based devices are controlled by some comfort physical variable.

2.4.1.2.4 Comfort-Based Elastic Devices Let $E_k^{cb} \subseteq E_k \subseteq \Omega_k$ be the set that contains all Comfort-Based Elastic Devices (CBED) present in a given typology. CBED devices control some comfort variable but its operation also depends on physical external variables. Examples of such devices are different thermal devices such as building HVAC systems, whose power consumption depends on air temperature but, at the same time, controls the temperature value inside. But also refrigerators, that are controlled by household room temperature but control the temperature inside it. Electric water heaters that control the water temperature inside a tank also fit CBED category. For refrigerators and HVAC systems there are adjustable control parameters that determine their operation such as user-defined temperature setpoints or maximum power output. \mathcal{M}_k must determine CBED devices power consumption $p_{\omega,t}^{E^{cb}}$ for all timeslots

2.4.1.2.5 HVAC and AC system For HVAC $\omega \in E_k^{cb} \subseteq \Omega_k$, thermal power p_t^{thH} and electric power $p_{\omega,t}^H$ are related through efficiency's or Coefficients of Performance (COP), η , with the following expression

$$p_t^{thH} = \eta p_{\omega,t}^H$$

The temperature inside a given dwelling at a given timeslot will be introduced as a constraint and is recursively given by

$$T_{t+1}^H = \varepsilon^H T_t^H + (1 - \varepsilon^H)(T_{t+1}^o \pm \beta^H \eta_{\omega}^H p_{\omega,t}^H) \quad (2.10)$$

The deduction of the general form of this expression can be found in Annex 6.4. External temperatures T_t^o are input parameters, ε^H and β^H are, respectively the thermal inertia and the inverse of thermal conductance K^{thH} . T_t^H and $p_{\omega,t}^H$ are variables. The \pm sign means that there are two modes of HVAC operation, namely transferring heat into the household or taking heat

out of the household therefore raising, or lowering, its internal temperature T_t^H . HVAC operation mode will be controlled by reference temperature for household comfort, T^{Href} . Heating mode will operate when $T^{Href} \geq T_t^o$ and Cooling Mode when $T^{Href} \leq T_t^o$. Therefore, HVAC COP will also assume two values

$$\eta_\omega^H = \begin{cases} \eta_{\omega,h}^H & \text{Heating mode} \\ \eta_{\omega,c}^H & \text{Cooling Mode} \end{cases} \quad (2.11)$$

The objective of HVAC is to maintain household internal temperature as close as possible to user-defined reference temperature T^{Href} .

$$T^{Href} - \Delta T^H \leq T_t^H \leq T^{Href} + \Delta T^H \quad (2.12)$$

ΔT^H is an allowed temperature displacement from reference which will allow for a bigger feasibility region for T_t^H if set into bigger values. ΔT^H could be also an optimization variable but in the present case it will be a user defined adjustable parameters for each typology. Considering ΔT a variable could be used to suggest DSM measures to users such as informing the best set point definition for HVAC. A user could be available to change its thermal comfort zone limits if that would mean a lower electricity cost. At last there must be an upper limit for HVAC power consumption

$$p_{\omega,t}^H \leq p_{\omega,max}^H \quad (2.13)$$

The thermal model presented may be also used to model a refrigerator or a water heater. In Annex 6.4.2 the refrigerator model is presented. It is possible to study coordinated strategies between different thermal devices. For example electric heater operation may be coordinated with HVAC system or even different systems of HVAC or different units of fridges.

The total aggregated CBED load is the sum, at each timeslot, of the aggregated devices.

$$P_t^{Ecb} = \sum_{\omega \in E_k^{cb}} p_{\omega,t}^{Ecb} \quad (2.14)$$

2.4.1.2.6 Energy-Based Devices Energy-Based Elastic devices (EBED) $\omega \in E_k^{eb} \subseteq \Omega_k$ are characterized by a certain quantity of energy that, necessarily, must be consumed during a subset of timeslots. On this device category we find Plug-in-Electric Vehicles (PEV), an important subset of the model. Its major constraint is the following.

$$\mu^{kh} \sum_{t=t_{\omega,start}^{EV}}^{t_{\omega,end}^{EV}} p_{\omega,t}^{EVc} = \frac{E_\omega^{EV}}{\eta_\omega^{EVc}} \quad (2.15)$$

PEVs are characterized by two main parameters: E_ω^{EV} , its battery capacity and $P_{\omega,max}^{EV}$, the upper limit for charging power. η_ω^{EVc} is the charging efficiency of the PEV battery. The model must output the PEV battery charging power, $p_{\omega,t}^{EVc}$, at each timeslot. However, unlike shiftable loads, it is not imposed that power consumption should occur in consecutive timeslots. In this way the EBED model allows for pre-definition of different charging or discharging strategies like fast or slow charging setting higher or lower $P_{\omega,max}^{EV}$. Equations can be adapted not only to model some agent that needs a certain battery level at a specific time of the day but to model

different smart-charging strategies approaches when considered its V2G features. PEV can be set to charge or discharge their batteries whenever they want but they must have a full charged battery at a pre-defined specific ending timeslot t_{end}^{EV} . To model such behavior the binary variable $x_{\omega,t}^{EV}$ is used such that

$$x_{\omega,t}^{EV} = \begin{cases} 1 & \text{if PEV is charging} \\ 0 & \text{if PEV is discharging} \end{cases} \quad (2.16)$$

The full PEV model is then determined by the following constraints:

$$0 \leq p_{\omega,t}^{EVc} \leq P_{\omega,max}^{EVc} x_{\omega,t}^{EV} \quad (2.17)$$

$$0 \leq p_{\omega,t}^{EVd} \leq P_{\omega,max}^{EVd} (1 - x_{\omega,t}^{EV}) \quad (2.18)$$

$$SOC_{\omega,t}^{EV} = SOC_{\omega,t-1}^{EV} + \mu^{kh} (\eta_{\omega}^{EVc} p_{\omega,t-1}^{EVc} - \frac{p_{\omega,t-1}^{EVd}}{\eta_{\omega}^{EVd}}), \quad \forall t \in [t_{\omega,start}^{EV}, t_{\omega,end}^{EV}] \quad (2.19)$$

$$SOC_{\omega,t_{end}^{EV}}^{EV} = E_{\omega}^{EV} \quad (2.20)$$

Equation (2.15) guarantees that the quantity of energy charged to the PEV battery is no bigger than the battery capacity or the desired charging level. (2.17) and (2.18) constraints the charge/discharge strategy, guaranteeing that those two actions do not occur simultaneously. (2.19) models the State-of-Charge in time through a recursive expression and (2.20) states that at delivering timeslot t_{end}^{EV} SOC must be the battery capacity or the desired level. This approach allows typologies to have several PEV units, like for example, a household with more than one car. Extending that possibility, typologies can be thought as dedicated facilities for PEV charging where several charging and discharging strategies of several units is managed simultaneous through a PEV aggregator. However, PEV may operate only in G2V mode. In that case the binary variable is dropped and equations (2.18) and (2.19) become

$$p_{\omega,t}^{EVc} \leq P_{\omega,max}^{EVc} \quad (2.21)$$

$$SOC_{\omega,t}^{EV} = SOC_{\omega,t-1}^{EV} + \mu^{kh} (\eta_{\omega,c}^{EV} p_{\omega,t-1}^{EVc}), \quad \forall t \in [t_{\omega,start}^{EV}, t_{\omega,end}^{EV}] \quad (2.22)$$

Total Energy-Based load is the sum of all the EBED devices in a certain typology.

$$P_t^{E^{eb}} = \sum_{\omega \in E_k^{eb}} p_{\omega,t}^{EVc} \quad (2.23)$$

2.4.1.2.7 Total load

The common assumption in the present model is that all devices present in a typology fall into one of the aforementioned categories and load variety is reduced to the appliance classes shiftable, fixed or elastic. Total load profile is just the sum of all device's individual loads in a typology.

$$P_t^L = P_t^F + P_t^S + P_t^{E^{eb}} + P_t^{E^{cb}}, \quad \forall \omega \in \Omega_k, \quad \forall t \in H \quad (2.24)$$

Some of the above terms may be zero since not all categories may be present in a specific typology. Fixed load may be modeled as a group of devices and inputed as an aggregated base load.

2.4.1.2.8 Typology renewable energy production Let $g \in G_k$ be the set of all RES generators installed in a given typology. At each timeslot there is a produced power given by the sum of all generators

$$P_t^G = \sum_g P_t^g, t \in H \quad (2.25)$$

2.4.1.2.9 Production - Photovoltaics In order to determine power output from photovoltaic module, P_t^{PV} physical models will be used, namely the simplified method presented in [47] whose objective is to easily compute output power using solely photovoltaics data-sheets and irradiation data series. The set of equations are the following

$$I_t^{MP} = \frac{G_t}{G^r} I^{rMP} \quad (2.26)$$

$$V_t^{MP} = mV_t^T \log\left[\frac{\frac{G_t}{G^r(I^{rcc} - I^{rMP})}}{I_0\left(\frac{T_t^c}{T^r}\right)^3 e^{\left(\frac{N_s \varepsilon}{m} \left(\frac{1}{\sqrt{rT}} - \frac{1}{\sqrt{V_t^T}}\right)\right)}}\right] \quad (2.27)$$

$$V_t^T = \frac{K_B T_t^c}{q} \quad (2.28)$$

$$T_t^c = T_t^o + \frac{NOCT - 20}{800} G_t \quad (2.29)$$

$$P_t^{PV} = V_t^{MP} I_t^{MP} \quad (2.30)$$

For the photovoltaics LCOE it will be considered c^{PV} in €/kWh

Assuming that all modules have the same production, the total renewable production of a certain typology where only PV production exists, $P_{k,t}^G$ is given by

$$P_{k,t}^G = n_k^{PV} P_t^{PV} \quad (2.31)$$

Where n_k^{PV} is the number of PV modules for typology k .

2.4.1.2.10 Residential storage Residential storage through batteries is an important management device in future SmartGrid environment. Let $b \in B_k$ be a storage system present in a typology. \mathcal{M}_k must output a solution to the day-ahead charging-discharging profile of the storage system. Two main variables will be present, $r_{b,t}^c$ and $r_{b,t}^d$, namely the charge and discharge rates at each timeslot. In Annex 6.5 the storage full model can be found.

2.4.1.2.11 Exchanges with aggregator grid Typologies are inserted at the distribution side of the power system. SmartGrids assume the existence of bidirectional flows which means that they can act as *prosumers* with the possibility of several energy management actions such as selling or buying energy to or from the grid, charging or discharging batteries. However choosing a specific action will not be object of direct control but a solution from \mathcal{M}_k that outputs each \mathcal{A}_k strategy. Non-negative variables are considered in order to compute power balance. P_t^{imp}

and P_t^{inj} are defined as, respectively, imported and exported power at each timeslot and, x_t^{gr} , a binary variable to control interactions with the grid, is defined as follows

$$x_t^{gr} = \begin{cases} 1 & \text{if power is being exported at timeslot } t \\ 0 & \text{if power is being imported at timeslot } t \end{cases} \quad (2.32)$$

With the limits on the power variables values imposed by the following constraints.

$$0 \leq P_t^{imp} \leq P^{LimGrid}(1 - x_t^{gr}) \quad (2.33)$$

$$0 \leq P_t^{inj} \leq P_t^G x_t^{gr} \quad (2.34)$$

where $P^{LimGrid}$ specifies the upper power limit that typologies may import. The above constraints renders impossible to export more power than what was produced by distributed local generators such as photovoltaics modules or small wind turbines. x_t^{gr} guarantees that power is not simultaneously being injected and imported.

2.4.1.2.12 Power balance The power balance equation is given by the following equation.

$$P_t^{imp} + P_t^G + r_{b,t}^d + P_t^{EVd} = P_t^{inj} + r_{b,t}^c + P_t^L \quad (2.35)$$

Considering equation (2.24) and the fact that $P_t^{Eeb} = P_t^{EVc}$ it follows that

$$P_t^{imp} + P_t^G + r_{b,t}^d + P_t^{EVd} = P_t^{inj} + r_{b,t}^c + P_t^F + P_t^S + P_t^{EVc} + P_t^{Ecb} \quad (2.36)$$

Power balance equality constraint ensures that the typology's energy demand is always satisfied and it constitutes a major constraint on \mathcal{M}_k . Essentially, all variables are adjust to P_t^G and energy is imported from the grid only when local RES is insufficient. Typologies may not have all terms in (2.36) since they can be modeled with or without local generation, storage system or HVAC.

2.4.1.2.13 Objective function Before defining the typologies main objective function, some economic and market parameters must be defined. If energy is being bought, sold and stored there is an associated cost to all those exchanges and a marginal cost in €/kWh must be considered. The most important parameter is c_t^0 , the *dynamic marginal cost of electricity production* in the aggregator wich is a dynamic price that assumes different values for each timeslot and it is an input parameter for \mathcal{M}_k . However, a *dynamic electricity tariff* τ_t must be defined, since that is the actual price that typologies will pay for each kWh of electricity consumed. This tariff must consider not only production costs but grid operation costs in distribution or transmission sides. Therefore τ^{dist} , a general grid access tariff and τ_A^{com} , a commercialization tariff, both in €/kWh, must also be considered.

$$\tau_t = c_t^0 + \tau^{dist} + \tau_A^{com} \quad (2.37)$$

So the cost of electricity for each timeslot is given by

$$C_t = \mu^{kh}(c^{PV} P_t^G + \tau_t P_t^{imp} + c_{br}^d r_{b,t}^d - \pi_t P_t^{inj}) \quad (2.38)$$

Where, in this case, there is only photovoltaic renewable production. Each \mathcal{A}_k agent is paying τ_t for each kWh imported from the grid. This dynamic tariff or, more precisely, the shape of this dynamic tariff, is the decisive factor in \mathcal{M}_k solution. The price that \mathcal{A}_k agents are selling excess production through grid injection is π_t , also a dynamic price. This quantity doesn't necessarily equals the c^{PV} or τ_t , despite the fact that it can be modeled that way. There are a number of different remuneration mechanisms that can be considered like self-consumption, feed-in or net-metering tariffs. Hereby, only a general parameter that accounts for electricity trading business is considered and in Chapter 3 specific cases will be considered. \mathcal{M}_k objective is the minimization of the full day electricity cost given by

$$C_k = \tau^{fix} + \sum_{t=1}^H C_t \quad (2.39)$$

Where τ^{fix} is a daily fixed tariff accounting for contracted power in €. The full set of variables is the following where the hidden k index has been recovered

$$X_k = \{x_{\omega,k,t}^S, y_{\omega,k,t}^S, T_{k,t}^H, p_{\omega,k,t}^H, T_{k,t}^{Fr}, y_{\omega,k,t}^F, p_{\omega,k,t}^{EVc}, p_{\omega,k,t}^{EVd}, x_{\omega,k,t}^{EV}, x_{b,k,t}, r_{b,k,t}^c, r_{b,k,t}^d, x_{k,t}^{gr}, P_{k,t}^{imp}, P_{k,t}^{inj}\} \quad (2.40)$$

The full \mathcal{M}_k comes

$$\begin{aligned} & \underset{X_k}{\text{minimize}} && C_k(X_k) \\ & \text{subject to} && (2.5) - (2.39) \end{aligned} \quad (2.41)$$

\mathcal{M}_k is a *Mixed Integer Linear Problem* with the objective of minimizing typologies daily electricity cost subjected to the equations (2.5)-(2.39).

2.4.2 Detailed Model - \mathcal{M}_N

According to Table 2.1 \mathcal{A}_N represents a computational unit in connection with local transformers at the physical layers and, at the code layer, it represents a software module that run \mathcal{M}_N and computes aggregated load and production from \mathcal{A}_k . Furthermore, it is also responsible for communications, negotiation and mediation between \mathcal{A}_k and \mathcal{A}^0 . Unlike \mathcal{A}_k , it uses power grid information since a grid representation is needed to output data.

2.4.2.1 Matrix representation of Load and production aggregation process

\mathcal{M}_k outputs $P_{k,t}^{imp}$ and $P_{k,t}^{inj}$, the time series of imported and injected power, for every timeslot t and every \mathcal{A}_k . The K solutions can be structured in an array that constitutes the reference output solutions from where all the aggregated data will be produced. The imported and injected power superscripts (*imp* and *inj*) can be dropped for now since matrix operations are independent of the physical meaning of data. The reference solutions matrix is as follows

$$P_{t,k} = \begin{bmatrix} P_{1,1} & P_{1,2} & \dots & P_{1,K} \\ \vdots & \vdots & & \\ P_{H,1} & P_{H,2} & \dots & P_{H,K} \end{bmatrix}$$

where each column corresponds to one typology while each line corresponds to a timeslot. Next,

\mathcal{A}_N must have access to data on the distribution of typologies in the area served by the aggregator local grid. This data originates on smart-meter information but, for simulations purposes, it may be generated according to surveys on the composition of the load in specific areas. The next step is to consider the following matrix.

$$\mathbf{N}_{l,k} = \begin{bmatrix} n_{1,1} & n_{1,2} & \dots & n_{1,K} \\ \vdots & \vdots & & \\ n_{L,1} & n_{L,2} & \dots & n_{L,K} \end{bmatrix} \quad (2.42)$$

Where $n_{l,k}$ is the positive quantity elements of type k that exist in the low level aggregation load mix l , with $l = 1, \dots, L$. The method for simulating aggregated load and production is to create different typology mixes that will later be connected to different local nodes. On a more free interpretation, the lines in $\mathbf{N}_{l,k}$ are specific "recipes" or blends of typologies representing a zone like a neighborhood or building block that is served by a local transformer. The aggregated load has the following shape

$$(l = 1) \quad P_{t,k}^{mix} = \begin{bmatrix} n_{1,1}P_{1,1} & n_{1,2}P_{1,2} & \dots & n_{1,K}P_{1,K} \\ \vdots & \vdots & & \\ n_{1,1}P_{H,1} & n_{1,2}P_{H,2} & \dots & n_{1,K}P_{H,K} \end{bmatrix}$$

where the case of the $l = 1$ mix is considered. In $P_{t,k}^{mix}$ the load profile of each typology is multiplied by the quantity of dwellings that exist, on a certain mix l , from that typology. In practice the operation consists in considering each line of $\mathbf{N}_{l,k}$ and "scan" the H lines of $P_{t,k}$ computing point-by-point product. The result is a $L \times H \times K$ cubic matrix.

Finally the aggregated load profile for the L mixes are computed summing through the lines (for all k) of $P_{t,k}^{mix}$.

$$\begin{bmatrix} \sum_k n_{1,k}P_{1,k} \\ \vdots \\ \sum_k n_{1,k}P_{H,k} \end{bmatrix}_1 \quad \begin{bmatrix} \sum_k n_{2,k}P_{1,k} \\ \vdots \\ \sum_k n_{2,k}P_{H,k} \end{bmatrix}_2 \quad \dots \quad \begin{bmatrix} \sum_k n_{L,k}P_{1,k} \\ \vdots \\ \sum_k n_{L,k}P_{H,k} \end{bmatrix}_L$$

And we get L vectors with aggregated load for each mix.

$$\begin{bmatrix} P_{1,1} \\ \vdots \\ P_{H,1} \end{bmatrix}_1 \quad \begin{bmatrix} P_{1,2} \\ \vdots \\ P_{H,2} \end{bmatrix}_2 \quad \dots \quad \begin{bmatrix} P_{1,L} \\ \vdots \\ P_{H,L} \end{bmatrix}_L$$

Condensing into one matrix it follows that

$$P_{t,l}^T = \begin{bmatrix} P_{1,1} & P_{1,2} & \dots & P_{1,L} \\ \vdots & \vdots & & \\ P_{H,1} & P_{H,2} & \dots & P_{H,L} \end{bmatrix}$$

This data must have a format that fits load flow nodal analysis that considers the $i = 1, \dots, N$ nodes' set in a power network. For that it is considered that a certain typologies load mix l is

connected to grid node i and for that \mathcal{A}_N must have access to a *load connection matrix*

$$\mathbf{a}_{l,i}^{load} = \begin{bmatrix} a_{1,1}^{load} & a_{1,2}^{load} & \dots & a_{1,N}^{load} \\ a_{2,1}^{load} & a_{2,2}^{load} & \dots & a_{2,N}^{load} \\ \vdots & \vdots & \ddots & \vdots \\ a_{L,1}^{load} & a_{L,2}^{load} & \dots & a_{L,N}^{load} \end{bmatrix} \quad (2.43)$$

where the

$$a_{l,i}^{load} = \begin{cases} 1 & \text{if mix } l \text{ is connected to grid node } i \\ 0 & \text{else} \end{cases} \quad (2.44)$$

Having knowledge of $a_{l,i}^{load}$ and $P_{t,i}^T$ \mathcal{A}_N can compute $P_{t,i}^T$ and data able to feed a load flow model as a parameter can be generated. If another sum is performed along the i nodes we get the *total aggregated load*

$$P_t^T = \begin{bmatrix} \sum_i P_{1,i} \\ \vdots \\ \sum_i P_{H,i} \end{bmatrix} \quad (2.45)$$

The importance of \mathcal{A}_N is still to be fully understood since later on, communication between agents will be fully addressed. At that point additional equations will be added to \mathcal{M}_N and new functions to \mathcal{A}_N .

2.4.3 Detailed Model - \mathcal{M}^0

The main objective of \mathcal{A}^0 is to compute a solution for a *Power Flow* model in order to determine grid operation and compute local energy cost. For that it needs a physical and generic representation of the electrical grid, but also load data from \mathcal{A}_N along with the generators production data.

2.4.3.1 Aggregator renewable electricity production

For wind power production the model presented in Annex 6.6 is used to compute P_t^{WT} , the power output of one wind turbine. The power output for a WPP constituted by $n^{WT,0}$ wind generators is given by the product $n^{WT,0}P_t^{WT}$, i.e, the aggregated production of all turbines, not considering wake or other turbulence effects in wind power production. For solar PV the physical models defined in 2.4.1.2.9 are used. Considering P_t^{PV} as the output of one PV module the total output of a PV central constituted by $n^{PV,0}$ is given by the product $n^{PV,0}P_t^{PV}$

2.4.3.2 Power Flow

Grid model To solve a power flow model a specific grid model with defined lines and buses must be inputed as parameters. In Annex 6.7 a simple line model can be found. The grid is represented by its *adjacency matrix*

$$\mathbf{a}_{i,j} = \begin{bmatrix} a_{1,1} & a_{1,2} & \dots & a_{1,N} \\ a_{2,1} & a_{2,2} & \dots & a_{2,N} \\ \vdots & \vdots & \ddots & \vdots \\ a_{N,1} & a_{N,2} & \dots & a_{N,N} \end{bmatrix} \quad (2.46)$$

$$a_{i,j} = \begin{cases} 1 & \text{if node } i \text{ is connected to node } j \\ 0 & \text{else} \end{cases} \quad (2.47)$$

Where $i, j = 1, \dots, N$, are the total number of nodes in the grid.

Similar matrices are needed to define to which nodes renewable or conventional generators are connected and where transformers exist.

$$\mathbf{a}_{i,g}^g = \begin{bmatrix} a_{1,1}^g & a_{1,2}^g & \dots & a_{1,N_g}^g \\ a_{2,1}^g & a_{2,2}^g & \dots & a_{2,N_g}^g \\ \vdots & \vdots & \ddots & \vdots \\ a_{N,1}^g & a_{N,2}^g & \dots & a_{N,N_g}^g \end{bmatrix} \quad (2.48)$$

$$a_{i,g}^g = \begin{cases} 1 & \text{if node } i \text{ has generator } g \text{ connected to it} \\ 0 & \text{else} \end{cases} \quad (2.49)$$

Where $g = 1, \dots, N_g$ set may represent a thermal generator connected to a node but it may also represent a connection to a node of a external grid that represents a substation. In the present work it will be considered a substation external node from where energy is imported or exported from or to the higher level grid outside the aggregator.

For WPP and PVPP the following matrices must be considered

$$\mathbf{a}_{i,g^{wt}}^{wt} = \begin{bmatrix} a_{1,1}^{wt} & a_{1,2}^{wt} & \cdots & a_{1,N_g^{wt}}^{wt} \\ a_{2,1}^{wt} & a_{2,2}^{wt} & \cdots & a_{2,N_g^{wt}}^{wt} \\ \vdots & \vdots & \ddots & \vdots \\ a_{N,1}^{wt} & a_{N,2}^{wt} & \cdots & a_{N,N_g^{wt}}^{wt} \end{bmatrix} \quad (2.50)$$

$$a_{i,g^{wt}}^{wt} = \begin{cases} 1 & \text{if node } i \text{ has wind generator } g^{wt} \text{ connected to it} \\ 0 & \text{else} \end{cases} \quad (2.51)$$

Where $g^{wt} = 1, \dots, N_g^{wt}$ and $g^{pv} = 1, \dots, N_g^{pv}$. The matrix for the PV power plant is obtained considering the equivalent matrix $\mathbf{a}_{i,g^{pv}}^{pv}$.

DC Power Flow considering renewable production \mathcal{M}^0 will have a rather simple formulation adapted to the specific modeling interests of the present case but the modular nature of the framework allows any kind of OPF formulation to be considered as long as the output data may fit the communication process. The present formulation is adapted from the initialization model presented by Raquel Castanho in [48] with adaptations in order to make it a linear dynamic version based on the general OPF formulation presented in Annex 6.8. Therefore, the ideal Direct Current OPF is considered, a usual representation for the aerial tri-phase power transport and distribution version where only active power is considered [49].

The simplifications for this model are inexistent tension drops between nodes, $V_{t,i} = V_{t,j} = 1$ (p.u) but also inexistent limits, power losses in lines, and small ($R_{i,j} \sim 0$) phase differences between connected nodes, i.e, $\delta_{t,i,j} \sim 0$ leading to $\cos(\delta_{t,i,j}) \sim 1$ and $\sin(\delta_{t,i,j}) \sim \delta_{t,i,j}$.

Furthermore thermal generation is not considered but $x_{t,i,g}^{in}$ and $x_{t,i,g}^{out}$ will be considered. These two continuous variables model power imports and exports through node i where connection point g is connected. This will allow to model the aggregator's interactions with electricity wholesale market. The total generated power will be, in practice, the sum of the imported power and the local renewable generators. \mathcal{M}^0 model comprises the following equations:

The power transmission between nodes is given by

$$P_{t,i,j} = B_{i,j} \delta_{t,i,j} \quad (2.52)$$

Where $B_{i,j}$ and $\delta_{t,i,j}$ are, respectively, susceptance and phase difference between node i and j

According to equation (6.24), $B_{i,j}$ becomes

$$B_{i,j} = -\frac{1}{\chi_{i,j}} \quad (2.53)$$

The power balance at each node in (6.27) comes

$$\sum_g x_{t,i,g}^{in} + \sum_{g^{wt}} \frac{P_{t,i,g^{wt}}^{WT,0}}{S_b} + \sum_{g^{pv}} \frac{P_{t,i,g^{pv}}^{PV,0}}{S_b} + \sum_l \frac{P_{t,i,l}^{inj}}{S_b} - \sum_g x_{t,i,g}^{out} - \sum_l \frac{P_{t,i,l}^{imp}}{S_b} - \sum P_{t,i,j} - \sum P_{t,j,i} = 0 \quad (2.54)$$

Phase limits are imposed by:

$$-\frac{\delta_{i,j}^{max}}{\pi/180} \leq \delta_{t,i,j} \leq \frac{\delta_{i,j}^{max}}{\pi/180} \quad (2.55)$$

Total energy produced at the aggregator is given by the sum of imports from the power market, represented by the variable $x_{t,i,g}^{in}$, PVPP production, $P_{t,i,g^{pv}}^{PV,0}$, WPP production, $P_{t,i,g^{wt}}^{WT,0}$, and the typologies level power injections, $P_{t,l,i}^{inj}$, for all nodes. These three quantities are input parameters for the model. The produced energy is as follows

$$E_t^0 = \mu^h \left(\sum_i \sum_g x_{t,i,g}^{in} S_b + \sum_i \sum_{g^{wt}} P_{t,i,g^{wt}}^{WT,0} + \sum_i \sum_{g^{pv}} P_{t,i,g^{pv}}^{PV,0} + \sum_i \sum_l P_{t,i,l}^{inj} \right) \quad (2.56)$$

where μ^h is a conversion factor between power and energy. At each timeslot, the cost of producing E_t^0 must take in account the levelized costs of each type of production and the power grid tariffs. If available, \mathcal{A}^0 is obliged to buy $P_{t,l,i}^{inj}$ production at π_t in €/kWh. Only when production from $P_{t,i,g^{wt}}^{WT,0}$, $P_{t,i,g^{pv}}^{PV,0}$ and $P_{t,i,l}^{inj}$ are not enough to supply $P_{t,i,l}^{imp}$, power is imported. At timeslots where production exceeds $P_{t,i,l}^{imp}$ power is exported at the same imported price c_t^{mrk} . The production cost is as follows

$$C_t^0 = \mu^h \left((c_t^{mrk} + \tau_A^{HT}) \sum_i \sum_g x_{t,i,g}^{in} S_b + c^{WT} \sum_i \sum_{g^{wt}} P_{t,i,g^{wt}}^{WT,0} + c^{PV,0} \sum_i \sum_{g^{pv}} P_{t,i,g^{pv}}^{PV,0} + \pi_t \sum_i \sum_l P_{t,i,l}^{inj} \right) \quad (2.57)$$

where τ_A^{HT} is a High Tension tariff in €/kWh. The aggregator's *marginal electricity cost* is given by

$$c_t^0 = \frac{C_t^0}{E_t^0} \quad (2.58)$$

and can be interpreted as a *local electricity cost* in the aggregator.

$$Re_t^0 = \mu^h \left((c_t^{mrk} + \tau_A^{HT}) \sum_i \sum_g x_{t,i,g}^{out} S_b \right) + (c_t^0 + \tau_A^{com} + \tau^{dist}) \sum_i \sum_l P_{t,i,l}^{imp} \quad (2.59)$$

$$Pr_t^0 = Re_t^0 - C_t^0 \quad (2.60)$$

Equations (2.57), (2.56) and (2.59) consider aggregated quantities, i.e summed over all nodes and set elements of the considered grid. By defining

$$P_t^{Timp} = \sum_i \sum_l P_{t,i,l}^{imp} \quad (2.61)$$

$$P_t^{Tinj} = \sum_i \sum_l P_{t,i,l}^{inj} \quad (2.62)$$

$$x_t^{in} = \sum_i \sum_g x_{t,i,g}^{in} \quad (2.63)$$

$$x_t^{out} = \sum_i \sum_g x_{t,i,g}^{out} \quad (2.64)$$

$$P_t^{WT,0} = \sum_{g^{wt}} \sum_i P_{t,i,g^{wt}}^{WT,0} \quad (2.65)$$

$$P_t^{PV,0} = \sum_{g^{pv}} \sum_i P_{t,i,g^{pv}}^{PV,0} \quad (2.66)$$

Equations (2.56) and (2.57) become

$$E_t^0 = \mu^h (x_t^{in} S_b + P_t^{WT,0} + P_t^{PV,0} + P_t^{Tinj}) \quad (2.67)$$

$$C_t^0 = \mu^h ((c_t^{mrk} + \tau_A^{HT}) x_t^{in} S_b + c^{WT} P_t^{WT,0} + c^{PV,0} P_t^{PV,0} + \pi_t P_t^{Tinj}) \quad (2.68)$$

(2.68) is a linear equation that, for simplicity, does not contemplate thermal generators (normally with non-linear quadratic cost functions), large scale storage and production such as hydroelectric centrals. The intention is to model a situation that would allow for a simple understanding of the influence of hourly market electricity prices c_t^{mrk} , wind speeds v_t , irradiation G_t^0 and renewable generation LCOEs, c^{WT} and $c^{PV,0}$ in the production marginal cost c_t^0 .

Equation (2.59) becomes

$$Re_t^0 = \mu^h ((c_t^{mrk} + \tau_A^{HT}) x_t^{out} S_b + (c_t^0 + \tau_A^{com} + \tau^{dist}) P_t^{Timp}) \quad (2.69)$$

And the limits on exports and imports of electricity are also considered.

$$0 \leq x_t^{in} \leq P_t^{Timp} \quad (2.70)$$

$$0 \leq x_t^{out} \leq P_t^{WT,0} + P_t^{PV,0} + P_t^{Tinj} \quad (2.71)$$

Where it is imposed that, for each timeslot, the maximum imports must be less than the total aggregator demand and exports less than the production, in this case PV, WPP and typologies injection.

For the present model it is assumed that power is continuously available at all timeslots in the electricity pool and power can be imported or exported as much as needed through the node of interconnection. This external entity may be a regional electricity market, a market where other aggregator agents meet to exchange electricity or other players, e.g power plants, with whom \mathcal{A}^0 establish direct contracts or purchase agreements.

The objective function used by \mathcal{M}^0 is the variable C^0 defined by

$$C^0 = \sum_t C_t^0 + \tau^{HTpc} \quad (2.72)$$

where τ^{HTpc} is a daily tariff for the transformer contracted power at exchange node g in €/kW.day. The set of decision variables is

$$X^0 = \{x_{t,i,g}^{in}, x_{t,i,g}^{out}, c_t^0\} \quad (2.73)$$

where c_t^0 is not an independent variable but is still considered in the set because of its furthest importance for the whole framework. $x_{t,i,g}^{in}$ and $x_{t,i,g}^{out}$ are in p.u units but all other power quantities are in kW or MW.

The full \mathcal{M}^0 becomes

$$\begin{aligned} & \underset{X^0}{\text{minimize}} && C^0 \\ & \text{subject to} && (2.52) - (2.72) \end{aligned} \quad (2.74)$$

which is a linear model unless (2.58) is excluded which can be computed easily outside the OPF since is a fraction between variables belonging to X^0 . \mathcal{A}^0 objective is to minimize the production costs of delivering power supply to its load subjected to all the constraints in equations (2.52)-(2.72). It should be noted here that other perspectives leading to different objective functions may be considered instead.

The simple DC power flow model presented becomes very easy to solve since it has no binary variables nor considers the reactive terms. The main reason to consider such a simple model arises from the very low computational resources it needs for reasons that will be clear during solutions approach. However, more detailed and realistic versions of power flow models may be considered to compose \mathcal{M}^0 but, for the purpose of the present work, the subsequent improvement in the solution values does not worth the inevitable performance degradation.

\mathcal{A}^0 may be seen as a grid operator, an electricity retailer or some grid entity that assumes the role of setting and broadcasting prices and managing the grid. For those entities the cost of energy production is of utmost interest specially when tied to the obligation of supplying the consumers demand.

2.4.4 Tariffs and pricing

The cornerstones of the general framework are tariffs design and pricing, a task performed by \mathcal{A}^0 with huge impact in \mathcal{A}_k daily bills. Electricity pricing and tariff structure may be achieved through several different methods and value-chain concepts. In the present work the objective is to build a dynamic-tariff that has a daily hourly variation and serves as the base for a DR price signal to agents \mathcal{A}_k . In this case tariffs architecture must be driven by the real costs of electricity consumption, production and transport. In the Portuguese electricity system tariffs for consumers depend on price variables such as contracted power, peak average power, active and reactive energy and fixed tariffs that are related to the retail activity of the sector [50].

However, the aggregator model considered depends on imports from the electricity spot market and renewable generation from local generators to meet its demand. This two factors are a major

source of variability in electricity price since they depend on the time of the day, the year and the region where electricity is being bought and produced. Defining a tariff that reflects the costs of operation, distribution, retailing and production in a aggregator will result in a highly variable tariff for consumers. In order to consumers accept tariffs its structure must be perceptible and cost reductions in consumers bills must be a concrete result from load adaptation through DR programs [51]. It is expected that c_t^0 follows the c_t^{mrk} tendency except at the timeslots where $P_{t,i,g^{wt},0}^{WT}, P_{t,i,g^{pv},0}^{PV} > 0$ and when $c^{WT}, c^{PV,0} < c_t^{mrk}$, where it will be lower. The question that arises is in which timeslots will \mathcal{A}_k schedule their load.

2.4.5 Model's solution methods

2.4.5.1 Model as a bi-level model

As seen in 1.5.5.1, BLP and Stackelberg games were used on multiple works to solve DR and tariff design models. The present proposal for a framework that solves the load optimization problem will also approach its solution from the context of BLP. However its beyond the scope of the present work to present formal proofs and demonstrations for the existence (or not) of the bi-level model's solutions. Our compromise is solely on proposing a heuristic method that fits the wanted load optimization solutions. Nonetheless the formal formulation of the bi-level general model is a starting point and from there move into a solution approach. As seen previously, models output solutions, which are optimal values for the objective function and the output values for the variables it depends on. Namely, \mathcal{M}_k outputs $s_k = X_k$ and C_k , and \mathcal{M}^0 outputs $s^0 = X^0$ and C^0 .

Recalling the bi-level problem definitions in section 1.5.2.1 the present general framework's model can be formulated as

$$\begin{aligned}
 & \min_{P_{k,t}^{imp} \in X_k, c_t^0 \in X^0} && C^0(c_t^0, P_{k,t}^{imp}) \\
 & \text{subjected to} && \begin{cases} (2.52) - (2.72) \\ P_{k,t}^{imp} \in \underset{P_{k,t}^{imp} \in X_k}{\operatorname{argmin}} \{C_k(c_t^0, P_{k,t}^{imp}) : s.t (2.5) - (2.39)\} \end{cases}
 \end{aligned} \tag{2.75}$$

and can be interpreted as the problem of finding the marginal cost price vector c_t^0 that minimizes the production cost C^0 such that the requested power imports vector $P_{k,t}^{imp}$ minimizes the daily electrical bill $C_{k,t}$. So the general output solution for the general model are the pairs

$$\mathbf{S} = (C_k, C^0) \tag{2.76}$$

$$\mathbf{s} = (s_k, s^0) \tag{2.77}$$

The *upper level* model (*leader*) is \mathcal{M}^0 and the *lower-level* (*followers*) are \mathcal{M}_k . The leader computes the price vector c_t^0 that is used to induce changes in the followers load scheduling solutions s_k , modeling in this way, the relation between a price setting entity in the form of an aggregator and the consumers reactions to prices. Upper-level \mathcal{M}^0 wishes to minimize its daily cost of producing electricity while lower-level \mathcal{M}_k 's all wish to minimize their daily electrical

bill. However, to interpret the general model as a BLP model some further remarks must be done. The first is that, in reality, the multi-level nature of the proposed framework makes it a trilevel model since \mathcal{M}_N acts as an intermediary between \mathcal{M}_k and \mathcal{M}^0 . Adding to this, the lower level models are, in fact, K models what would derive in a multi-follower model. To reduce the problem it must be taken in consideration that upper-level objective, C^0 do not explicitly represent $P_{k,t}^{imp}$ but only represents $x_{t,i,g}^{in}$. However, constraint (2.54) states the dependency of $x_{t,i,g}^{in}$ relative to $P_{t,l,i}^{imp}$. The market imports are made, essentially, to meet the load demands from typologies level consumers. The focus of our problem is the pair $(c_t^0, P_{k,t}^{imp})$ so the BLP needs to be formulated using these variables. The equivalence between local variables in different models is established having in mind that they are interdependent between them although a model's specific variable is inserted in another model as a parameter. Concerning the aggregated quantities, it must be noticed that $P_{t,l,i}^{imp}$ parameter in \mathcal{M}^0 is obtained from \mathcal{M}_k 's variable output $P_{k,t}^{imp}$ through the aggregation process in \mathcal{M}_N . The \mathcal{M}_k 's are solved independently of one another, simultaneously or asynchronously, and their influence in one another is through their influence in c_t^0 but they interact with aggregator in an aggregated way hiding their individual solutions. These observations strongly suggest that in reality the 1-leader- K followers problem may be solved as a 1-leader-1-follower since, like in [36], what \mathcal{A}^0 observes is the aggregated power imports in each of its power flow nodes, not having knowledge of the K individual solutions nor the typologies mixes in each node.

Several BLP models were solved transforming it into a single-level problem using KKT conditions to represent lower-level problem as upper level constraints. However, reducing to single level is not possible or desirable for several reasons. First, the lower-level problems are discrete due to the presence of binary variables in X_k what makes it impossible to use the KKT reduction approach. But the framework is a general one and is easily adaptable to a situation where \mathcal{M}_k is linear, continuous and convex allowing KKT conditions to be used. Then two questions would arise. First, the conversion into a single-level problem would reveal lower-level models and parameters to the upper-level model violating the privacy preserving principle. Second, the number of constraints and equations in the single-level model would be too big and the solving process would become time-prohibitive when applied to a real situation where huge numbers of lower-level models needs to be solved [37]. On top of that the resulting BLP is much more complex to solve than the individual problems not being able to be solved in acceptable polynomial time [21].

Because of that the process of finding a solution to the bi-level model must be thought as a game encoded in an algorithm which, in turn, displaces the attention into modeling the interactions between level agents considering the decoupled models \mathcal{M}_k and \mathcal{M}^0 . Consequently, one can only expect to obtain a *feasible solution*.

2.4.5.2 Interaction and communication between agents

In order to consider communication between agents it must be noticed that model's output solutions will become other model's input parameters. This dynamic property of interaction constitutes the fundamental mechanism in which the communication between agents is based upon. One must refer to *signals* when considering the transmission of messages whose content are output solutions. Solutions constitute *strategies*, considered as one agent's decision about which variable values place in messages. If an agent outputs a solution, it then declares its

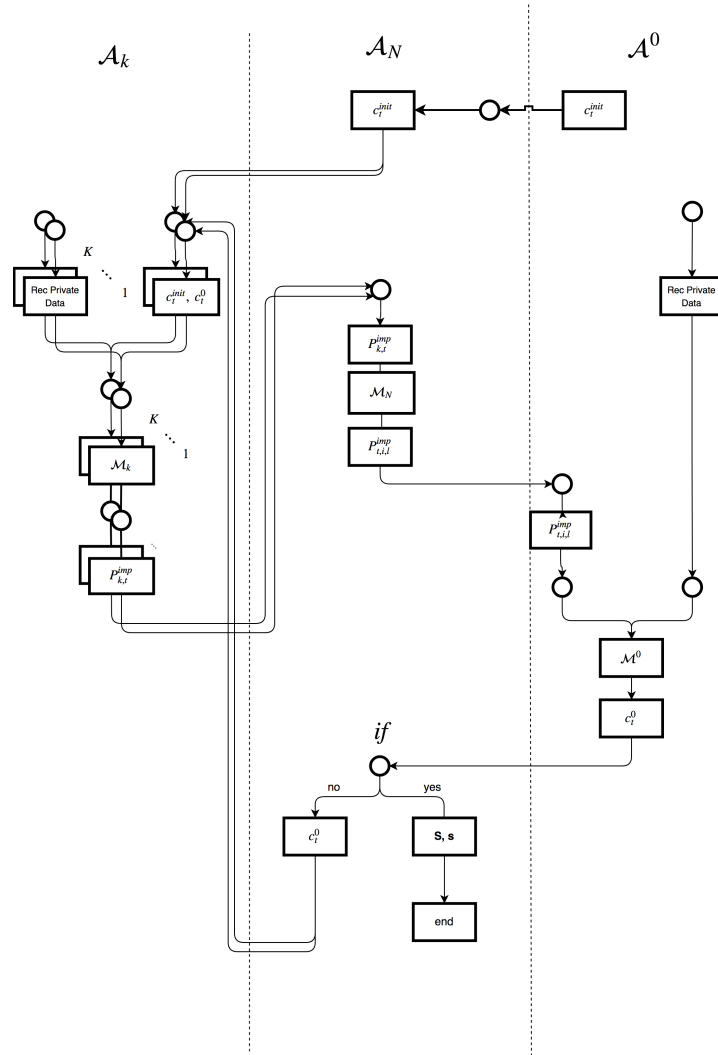


Figure 2.8: Petri Net depicting communication between agents

strategy by transmitting that solution through a message encoded in a signal on to other agent. The dynamic operation for determining \mathbf{s} and \mathbf{S} consists in programming an algorithm for the exchange of signals between agents where content is composed of $P_{k,t}^{imp}$ and $P_{k,t}^{inj}$ when \mathcal{A}_k are senders and c_t^0 when \mathcal{A}^0 is the sender. Changes in s_k will influence s^0 and \mathbf{S} , and vice-versa. This communication between agents through the information signals (P_k^{inj} , P_k^{imp} , c_t^0) will be the basis of an iterative process that may be interpreted as a game between agents. For that, an *iteration index* γ must be defined. What is expected is a signal exchange along iterations in a process through which agents adapt their solutions and that, eventually, will converge to a final general solution $\mathbf{S}_\gamma = (C_{\gamma,k}, C_\gamma^0)$ and $\mathbf{s}_\gamma = (s_{\gamma,k}, s_\gamma^0)$. The dynamic communication process may be viewed through the FMC petri-net diagram in Figure 2.8 that describes the communication channel between \mathcal{A}_k , \mathcal{A}_N and \mathcal{A}^0 .

The *if* query in the diagram represents the convergence criteria evaluation. The communication process ends if neither \mathcal{A}_k or \mathcal{A}^0 reviews its strategy (or the changes are very small) and if the *mean local electricity production cost*, $c_\gamma^0 = \overline{c_{\gamma,t}^0}$, stabilizes i.e.,

$$\mathbf{S}_\gamma = \mathbf{S}_{\gamma-1} \quad (2.78)$$

$$\mathbf{s}_\gamma = \mathbf{s}_{\gamma-1} \quad (2.79)$$

$$c_\gamma^0 = c_{\gamma-1}^0 \quad (2.80)$$

Just like in [35] it will be considered an algorithm to encode the iterative game between agents depicted in Figure 2.8

Algorithm 1: Simple Algorithm

```

1 while  $\gamma \leq \gamma^{max}$  do
2    $\mathcal{A}^0$  sets  $c_{\gamma,t}^0 = c_t^{init}$  ▷ Aggregator agent initializes price vector
3    $\mathcal{A}^0$  sends  $c_{\gamma,t}^0$  to  $\mathcal{A}_N$ 
4    $\mathcal{A}_N$  receives  $c_{\gamma,t}^0$ 
5    $\mathcal{A}_N$  sends  $c_{\gamma,t}^0$  to all  $\mathcal{A}_k$  ▷ Consumers agents receive price vector
6    $\mathcal{A}_k$  runs  $\mathcal{M}_k$  and compute  $s_k$ 
7    $\mathcal{A}_k$  send  $P_{k,t}^{imp}$  to  $\mathcal{A}_N$  ▷ Consumers agents communicate Power imports
8    $\mathcal{A}_N$  receive  $P_{k,t}^{imp}$ 
9    $\mathcal{A}_N$  run  $\mathcal{M}_N$  and compute  $P_{t,i,l}^{imp}$ 
10   $\mathcal{A}_N$  send  $P_{t,i,l}^{imp}$  to  $\mathcal{A}^0$ 
11   $\mathcal{A}^0$  run  $\mathcal{M}^0$  and compute  $c_{\gamma,t}^0$  ▷ Price vector is computed
12  if  $\mathbf{S}_\gamma = \mathbf{S}_{\gamma-1} \wedge \mathbf{s}_\gamma = \mathbf{s}_{\gamma-1} \wedge c_\gamma^0 = c_{\gamma-1}^0$  then
13    print  $\mathbf{S}_\gamma, \mathbf{s}_\gamma$  and  $c_\gamma^0$  [(2.78)] ▷ If no agent reviews its strategy the process is over
14    else if then
15       $\gamma = \gamma + 1$ 
16      go to 3
    
```

Algorithm 1 is rather simple. There's no coordination or cooperation between the \mathcal{A}_k agents and a natural convergence to a solution is expected. That solution must be a good solution for \mathcal{A}_k (consumers) but not necessarily a good one for \mathcal{A}^0 (grid entity). Under the idea underlying bi-level games a natural adaptation will take place and rendering $\mathbf{S}_\gamma, \mathbf{s}_\gamma$ beneficial for all agents. However, the communication based nature of the process does not guarantee any pre-determined adaptation since the model cannot be formulated as a single-model like referred in 2.4.5.1. Thus the different models do not compute solutions for other model's variables and instead consider them as input parameters. What is expected is that after initialization, encoding c_t^0 strategy in a signal and sending it to \mathcal{A}_k will produce an outcome from \mathcal{M}_k consisting in scheduling the load at lower prices timeslots. After that, $P_{t,i,l}^{imp}$ will produce the expected outcome from \mathcal{M}^0 that generates a new c_t^0 that corresponds to the real cost of supplying power. The problem is that this "ping-pong" game of solutions does not account for negotiation or coordination between \mathcal{A}^0 and \mathcal{A}_k . That is why it must be considered as the scaffold of a more complex process that takes coordination or negotiation into consideration.

2.4.5.3 Demand Response mechanism

DSM is the determination of s_k which is the product of the day-ahead load scheduling and planing for a time period, i.e a strategy. DR is a mechanism that imposes an adaptation in s_k and, specifically, an adaptation in the shape of the imported power load diagram for each typology $P_{k,t}^{imp}$. This is implemented by using c_t^0 as the fundamental part of the DR signal. From \mathcal{M}_k objective (equation (2.38)) one can expect each typology to schedule its load at timeslots where c_t^0 is lower, i.e where the production cost is lower.

But as seen in 2.4.3.2 the most probable timeslots for scheduling do not match periods of low P_t^{Timp} values allowing load to be be scheduled in high peaks. Therefore a DR signal must be capable of avoiding high peak effect and a way to do so is to consider *Load Factor* as a part of DR mechanism and tariff design. Load factor is a instantaneous measure of the variability of P_t^{Timp} relative to load peak P_{max}^{Timp} during time horizon H and it is defined as

$$L_t^f = \frac{P_t^{Timp}}{P_{max}^{Timp}} \quad (2.81)$$

Ideally, load factor should be close to one meaning that load imports follows a stable and constant curve during horizon H . However this is hardly the case in any power system.

Considering the instant load factor mean for the H horizon $\overline{L_t^f} = \frac{\sum_t L_t^f}{H}$ a *Mean Normalized Load Factor* (MNLF) can be built as

$$L_t^{ff} = \frac{L_t^f}{\overline{L_t^f}} \quad (2.82)$$

which is an instant factor that translates the deviation of the load factor from the mean factor for every timeslot. The actual price vector that is used in the DR signal is then

$$c_t^f = L_t^{ff} c_t^0 \quad (2.83)$$

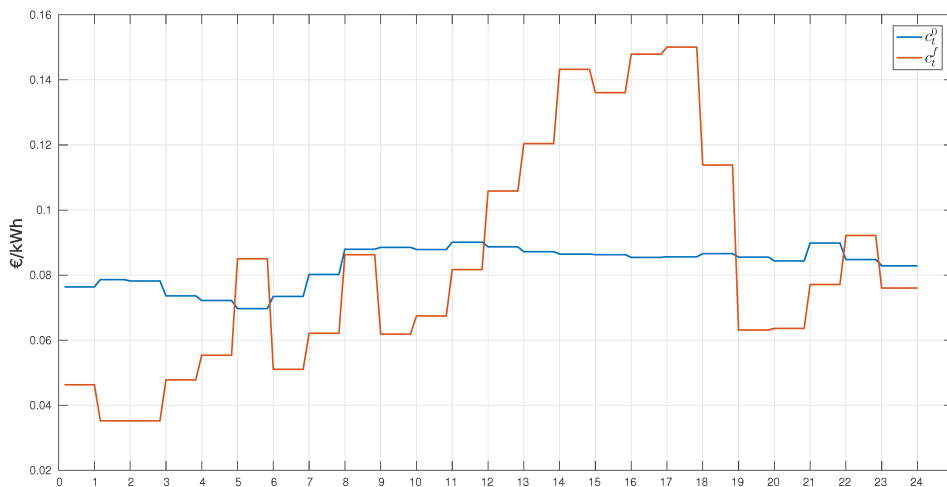


Figure 2.9: Mean normalized price vector and production cost example

\mathcal{M}_k tariff τ_t in (2.37) becomes

$$\tau_t^f = c_t^f + \tau^{dist} + \tau_A^{com} \quad (2.84)$$

MNLF was designed so that the DR tariff gets indexed to load peak, therefore following its shape. As can be seen in Figure 2.9 it can be greater or smaller than c_t^0 . The objective of the DR signal is to schedule load at low LMNF timeslots raising in that way the daily mean load factor of the system. Aggregator revenue losses that may occur from selling electricity at prices below the production cost at low LMNF timeslots are compensated by selling above production cost at high LMNF timeslots. One should not forget that there will always be a part of consumers load that is fixed so if prices are raised on certain timeslots, \mathcal{A}_k will still be buying electricity.

2.4.5.4 An heuristic *ad hoc* iterative algorithm for Demand Response

When considering K typologies the MNLF factor, by itself, may not be sufficient to avoid high peaks since the same c_t^f signal will be sent to all \mathcal{A}_k and is expected that \mathcal{M}_k 's load will be scheduled at low peaks since C_k is the same for all agents. This will degenerate in a situation of peak shifting through a phenomenon called *herding effect*. It results in overcrowded timeslots which will create new high load peaks in different timeslots. Authors in [52] clearly identify this problem and propose a DR mechanism and a pricing mechanism that, although having some similarities with LMNF, it is quite different. LMNF, by itself, aims at solving the problem of scheduling at high load timeslots but do not avoid the herding problem. For that reason some degree of *coordination* between \mathcal{A}_k needs to be imposed so that some diversity on the s_k solutions may exist. This coordination will be managed by \mathcal{A}_N and consists in using $c_{\gamma,t}^f = L_{\gamma,t}^{ff} c_{\gamma,t}^0$, a value that will be updated between iterations, as a DR signal to \mathcal{A}_k . The agent \mathcal{A}_N will arbitrary order each \mathcal{A}_k in a queue and make it output its $s_{\gamma,k}$. Defining $l_k = [\mathcal{A}_1 \cdots \mathcal{A}_K]$ as the line vector containing the ordered queue of agents, the order in which each \mathcal{A}_k will receive its $c_{\gamma,t}^f$ is the result of a sequential selection from a random queue given by

$$q_m = \sigma(l_k) \quad (2.85)$$

where σ is a permutation of the elements (agents) of l_k . From each iteration a new $c_{\gamma,t}^f$ is computed and sent to the next agent in the queue q_m . In this way, when computing $s_{\gamma,k}$ each agent do so accordingly to the state of the previous iteration aggregated load factor through the $L_{\gamma,t}^{ff}$ resulting in a asynchronous coordinated DR mechanism. When an agent receives its iteration LMNF, it sticks to it avoiding re-scheduling after defining its strategy. However not all \mathcal{A}_k will participate in this game since agents may represent a typology that is not composed by any device or appliance allowing for DSM. As we will see in Chapter 3 those agents will be slaves to price variations produced by the agents that participate in the DR game since the only way that agents influence each other is by influencing the c_t^0 . The demand response mechanism will be encoded in the following algorithm for agent communication management. It should be noticed that (2.81), (2.82), (2.83), (2.85) are equations that must be added to \mathcal{M}_N and (2.84) to the \mathcal{M}_k .

Algorithm 2: Demand Response Coordination Algorithm

```

1 while  $\gamma \leq \gamma^{max}$  do
2    $\mathcal{A}^0$  sets  $c_{\gamma,t}^0 = c_t^{init}$  ▷ Aggregator agent initializes price vector
3    $\mathcal{A}^0$  sends  $c_t^{init}$  to  $\mathcal{A}_N$ 
4    $\mathcal{A}_N$  receives  $c_t^{init}$ 

5   Loop 1
6      $\mathcal{A}_N$  sends  $c_{\gamma,t}^0$  to all  $\mathcal{A}_k$  ▷ Consumers agents receive initial price vector
7      $\mathcal{A}_k$  receives  $c_{\gamma,t}^0$ 
8     if  $\gamma = 1 \vee \gamma > K + 1$  then
9        $\mathcal{A}_k$  runs  $\mathcal{M}_k$  and compute  $s_k$ 
10      else if  $1 < \gamma \leq K + 1 \wedge A_{q_m}$  is registered for DR mechanism then
11         $A_{q_m}$  Receives  $L_t^{ff}$  and fixes-it as his permanent LMNF
12         $A_{q_m}$  runs  $\mathcal{M}_{q_m}$  and computes  $s_{q_m}$ 
13         $\mathcal{A}_k \setminus A_{q_m}$  run  $\mathcal{M}_k$  and compute  $s_k$  ▷ The  $s_k$  solution also includes the  $s_{q_m}$ 
14       $\mathcal{A}_k$  send  $P_{k,t}^{imp}$  to  $\mathcal{A}_N$  ▷ Consumers agents communicate their strategy on power imports
15       $\mathcal{A}_N$  receive  $P_{k,t}^{imp}$ 
16       $\mathcal{A}_N$  run  $\mathcal{M}_N$  and compute  $P_{t,i,l}^{imp}$  and  $P_t^{Timp}$ 
17       $\mathcal{A}_N$  compute  $L_t^{ff}$ 
18       $\mathcal{A}_N$  send  $P_{t,i,l}^{imp}$  to  $\mathcal{A}^0$ 
19       $\mathcal{A}^0$  run  $\mathcal{M}^0$  and compute  $c_{\gamma,t}^0$  ▷ Price vector is computed
20       $\mathcal{A}^0$  send  $c_{i,t}^0$  to  $\mathcal{A}_N$ 
21       $\mathcal{A}_N$  receives  $c_{\gamma,t}^0$ 
22      if  $\gamma = 1$  then
23         $\gamma = \gamma + 1$ 
24        exit Loop 1
25      else if  $1 < \gamma \leq 1 + K$  then
26         $\gamma = \gamma + 1$ 
27        go to Start Loop 2 (line 36)
28      else if  $\gamma > K + 2$  then
29        if  $\mathbf{S}_\gamma = \mathbf{S}_{\gamma-1} \wedge \mathbf{s}_\gamma = \mathbf{s}_{\gamma-1} \wedge c_\gamma^0 = c_{\gamma-1}^0$  then
30          print  $\mathbf{S}_\gamma, \mathbf{s}_\gamma$  and  $c_\gamma^0$  [(2.78)]
31          ▷ If no agent reviews its strategy process is over
32        else if then
33           $\gamma = \gamma + 1$ 
34          go to Start Loop 1 (line 5) ▷ The process keeps on going
35       $\mathcal{A}_N$  generates  $q_m = [q_1 \cdots q_K]$  ▷ The queue line is generated
36      Loop 2
37         $\mathcal{A}_N$  finds next  $\mathcal{A}_{q_m}$  registered for DR
38         $\mathcal{A}_N$  send  $L_t^{ff}$  to  $\mathcal{A}_{q_m}$ 
39        go to Start Loop 1 (line 5)
    
```

Algorithm 2 is an adaptation of Algorithm 1 in which the DR mechanism for raising the load factor was inserted through a centralized coordination mechanism. A first observation is that the convergence criteria only starts to be evaluated after $K + 1$ iterations since first iteration is a initialization iteration and after that ($1 < \gamma < K + 1$, step 8) the \mathcal{A}_k must coordinate. The DR mechanism is centralized because \mathcal{A}_k are not communicating with each other but \mathcal{A}_N is imposing the coordination thus performing the role of a mediator. However, the process is easily adaptable into a fully decentralized coordination mechanism between the \mathcal{A}_k . On one hand the mechanism acts on behalf of \mathcal{A}^0 interests by lowering load factor, but on the other it lets \mathcal{A}_k define their strategies and lower their costs. The centralized coordination process is an attempt to go around the effect that was, euphemistically called the "ping-pong effect" since it accounts for the influence of \mathcal{M}^0 (the leader) on s_k , the variables of the followers. This process will take place until all registered agents adapt their load and when convergence criteria (2.78) is met. If there's not a convergence the process will exit when a maximum number of iterations is reached.

2.5 Final considerations on methodology

Even though the formulation of the general model have been stated as a formal bi-level model and the solution approached through the GT point of view, it is beyond the scope of the present work to prove known GT results like the Nash and Stackelberg equilibrium or the convergence of the proposed algorithms to an optimal solution. The same goes to prove the existence of an optimal solution of the formal bi-level model. The heuristic hereby proposed as a solution method cannot guarantee that the solutions found are optimal. In further chapters numerical results and computational implementation of the proposed model will be presented and from them the effectiveness and quality of the solutions can be evaluated. The creation of a DR mechanism that, in practice, differentiates tariffs to consumers may raise equity issues because of the fact that different consumers are subjected to different prices although they may be in the same aggregator. The extent of this issues must be analyzed through the impact in \mathcal{A}_k daily bills.

Chapter 3

Numerical implementation

To implement an instance of the general model and solve through the algorithms presented in previous chapters two major elements must be considered. First one must choose software and computational tools and second, datasets must be available or, like in the present case, gathered and assembled.

3.1 Software and computational Tools

GAMS optimization *General Algebraic Modeling System* [53] is a proprietary high-level algebraic modeling language for solving mathematical programming models. It represents the problems in a declarative, rather than an imperative way, i.e, it focus on *what is the problem* rather than *how the problem is solved* [54, pag. 6]. In GAMS problems can be written almost the same way as their mathematical representation. There is a clear separation between the model's formulation, the solving process and the data used. Therefore it uses external, state of the art, *solvers* for computing model's solutions. [55]

GAMS and MATLAB integration MATLAB is a proprietary numerical environment that can treat and process data through matrix manipulations. It is also a very powerful tool for scripting and implementing dynamical and physical models as well as running simulations. The concept map in Figure 2.2 clearly relates *data*, *models* and *software*. The optimization agent model is comprised by mathematical models that produce data to feed back the agent model. This loop structure is the basis of the DR mechanism encoded in the Algorithms 1 and 2 and the bi-Level solution approach. The software implementation of this system uses the synergies between GAMS and Matlab. MATLAB implements physical models, process data-series and parameters and assembles data. Temperatures and irradiation data series, physical parameters, wind turbine, PV and \mathcal{M}_N models are implemented in MATLAB. Optimization Models, \mathcal{M}_k and \mathcal{M}^0 , are implemented and solved in GAMS. The dynamic process between data input and output and visualization is controlled in MATLAB as a loop. In Annex 6.9.1 are presented the details of the software implementations and the workflow algorithm.

All code was implemented and results obtained in a *Intel(R) Core(TM) i5-3320M CPU @ 2.60GHz* CPU with *4GB* RAM, *SSD* disk using *LinuxMint 18.1 Serena*

3.2 Data

3.2.1 Simulation configurations

For the time discretization of the model simulation we're going to consider a timestep $\Delta t = 10$ minutes what, for a 24 hours day, corresponds to a time horizon of $\mathcal{T} = 24 \times 60 \times \Delta t = 1440$ minutes and a timestep horizon of $H = \frac{\mathcal{T}}{\Delta t} = 144$ timesteps.

3.2.2 Convergence criteria

The convergence criteria in equations (2.78) account for the situation in which no agent reviews its strategy, i.e its solution at a specific iteration is the same as the immediately iteration before. When implementing the algorithms and models numerically this analytical, ideal situation is never verified so a convergence factor $0 \leq \epsilon \leq 1$ must be considered such that the convergence criteria actually implemented is the following

$$\frac{\mathbf{S}_\gamma - \mathbf{S}_{\gamma-1}}{\mathbf{S}_\gamma} \leq \epsilon \quad (3.1)$$

$$\frac{\mathbf{s}_\gamma - \mathbf{s}_{\gamma-1}}{\mathbf{s}_\gamma} \leq \epsilon \quad (3.2)$$

$$\frac{c_\gamma^0 - c_{\gamma-1}^0}{c_\gamma^0} \leq \epsilon \quad (3.3)$$

$$(3.4)$$

The value used is $\epsilon = 0.01$ or $\epsilon = 0.05$, whenever the solution consumes larger time resources.

3.2.3 \mathcal{M}_k data

Meteorological data

A general hot day was chosen to implement the framework. The temperature and irradiance profiles can be seen in Figure 6.4 in Annex 6.9.3

3.2.3.1 Photovoltaic system

Typologies PV system will be composed of a general commercial PV module with the characteristics and parameters in Table 6.4 in Annex 6.9.2. Using the physical model in 2.4.1.2.9 we obtain the profile in Figure 6.3.

3.2.3.2 Machine and devices characteristics

Shiftable Loads 6 different general shiftable devices will be considered

Table 3.1: Shiftable devices parameters

ω	ω_5	ω_6	ω_7	ω_2	ω_3	ω_4
D_ω^S	12	6	4	3	5	9
l_ω^S	1000	600	100	750	400	500

The methodology will consist in assigning machines to typologies and the models in 2.4.1.2.2 output the following exemplifying load profiles

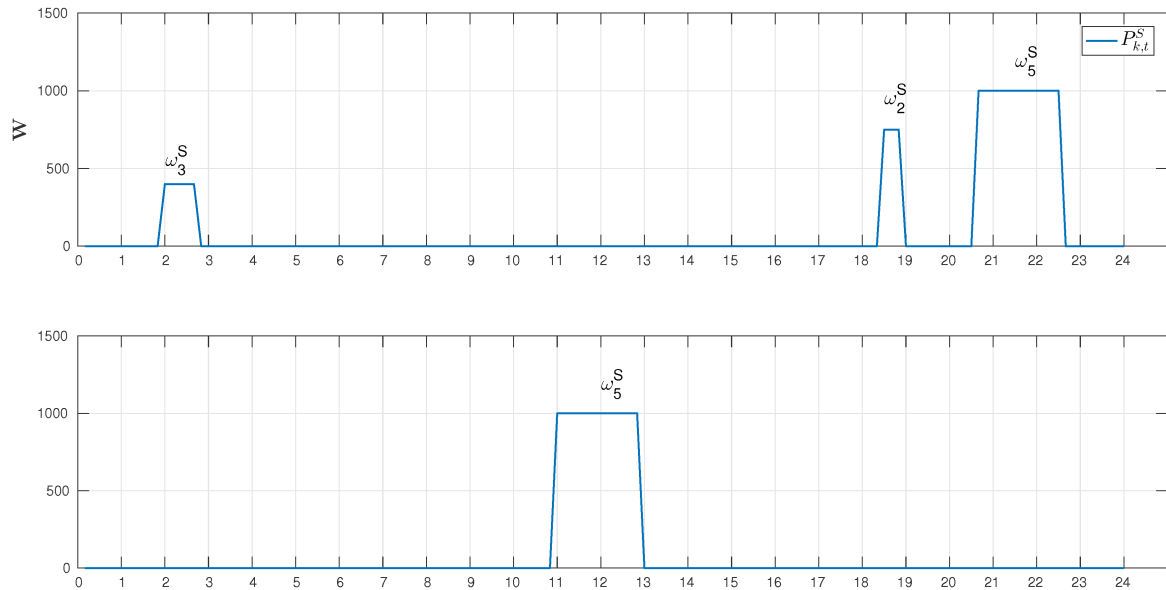


Figure 3.1: Shiftable devices output solution

The figure represents shiftable appliances load for two different typologies where the top one has 3 appliances assigned and the down one only one. The task of \mathcal{M}_k is to "decide" where to schedule these loads.

Electric Vehicles Two models of Electric Vehicles will be considered, both having near average battery sizes [56, p. 93].

Table 3.2: Electric Vehicles characteristics

ω^{EV}	Type	E_{ω}^{EV} (kWh)	$P_{\omega,max}^{EVc}$ (kW)	V_{ω}^{EV} (V)	I_{ω}^{EV} (A)	η_{ω}^{EVc}
ω_1^{EV}	PHEV	13	2.8	220	16	0.9
ω_2^{EV}	PEV	24	3.5	220	16	0.9

The typical outputs are as follows where we can see $P_{\omega,k,t}^{EVc}$ on the left y axis and $SOC_{k,t}^{EV}$ on the right y axis

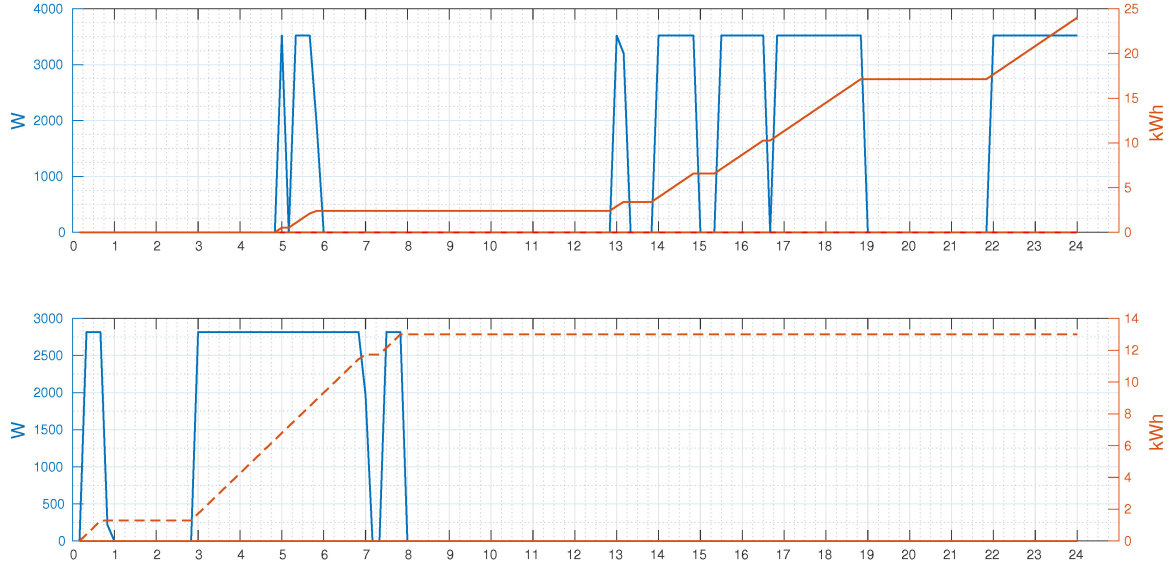


Figure 3.2: On top: type $k = 6$ with ω_1^{EV} . Down: type $k = 5$ with ω_2^{EV}

According to [56] charging strategies for EVs can be considered *dumb* when these charge only during day-time or night-time. Unlike the referred work, V2G capabilities will not be considered but an hybrid charging approach that consists in allowing \mathcal{M}_k to manage the charge profile for each typology, during $t_{k,\omega,start}^{EV} \leq t \leq t_{k,\omega,end}^{EV}$. As shown in the plots EVs do not charge continuously like the shiftable devices and the shape of the charge profile are entirely an output from the optimization solver. Logically, the output becomes unfeasible if $t_{k,\omega,end}^{EV} - t_{k,\omega,start}^{EV} < \frac{E_{\omega}^{EV}}{P_{\omega,max}^{EV}}$, what translates the situation in which there is no time to charge the vehicle with the maximum power. Imposing a smaller delivering charge is the only possibility to go around this problem. In any case \mathcal{M}_k always outputs values of $P_{\omega,k,t}^{EVc}$ that are close to $P_{\omega,max}^{EV}$ using all the available power.

HVAC The HVAC system considered has the characteristics in Table 6.4.1 in Annex 6.4.1 but before plotting its output typologies physical characteristics data must be presented

Typologies Data Typologies are reference sets of parameters for simulating load. In the present implementation 6 typologies will be considered and detailed, thus reducing all residential and commercial elements to these 6 archetypes. This choice may be acceptable for a small sized area, but extending this methodology to bigger areas like entire regions or cities would imply a careful study of statistical distribution of physical parameters, based on surveys such as [57]–[59], to assess the number and the adequate composition of typologies needed. Table 6.6 in Annex 6.9 presents the relevant parameter values of the typologies used. The greater part of typologies total load is fixed therefore not being subjected to DR and DSM procedures. $P_{k,t}^F$ accounts for the fixed part of the total load in equation (2.24) and will be, from here on, referred as *base load*. It will be modeled from reference profiles published by ERSE [60] and using only their general shape. Base load should make around 70% of total load and, since average daily dwelling consumption in Portugal is 11.8 kWh [61], we get the values presented in Table 6.6 for

E_k^F . As an example, if the EDP simple tariff in the year 2017 of 0.16 €/kWh [62] is used as a reference value for electricity price, the daily average electricity bill in Portugal would be around 1.9 €/day.

Concerning typologies overall heat transfer coefficients U and conductance K^{th} one must notice that each one of the different construction elements in a dwelling (roof, floor, door and window) has its own value. However in equation (2.10) a single value is used for $\beta = \frac{1}{K^{th}}$ as an input for each typology. That value corresponds to the mean of all construction elements and is arranged in the following vector

$$\mathbf{K}_k^{thH} = [K_1^{thH} \quad K_2^{thH} \quad K_3^{thH} \quad K_4^{thH} \quad K_5^{thH} \quad K_6^{thH}]^T$$

The operation to determine these values can be found in Annex 6.9.6. The methodology results in the following profile for HVAC

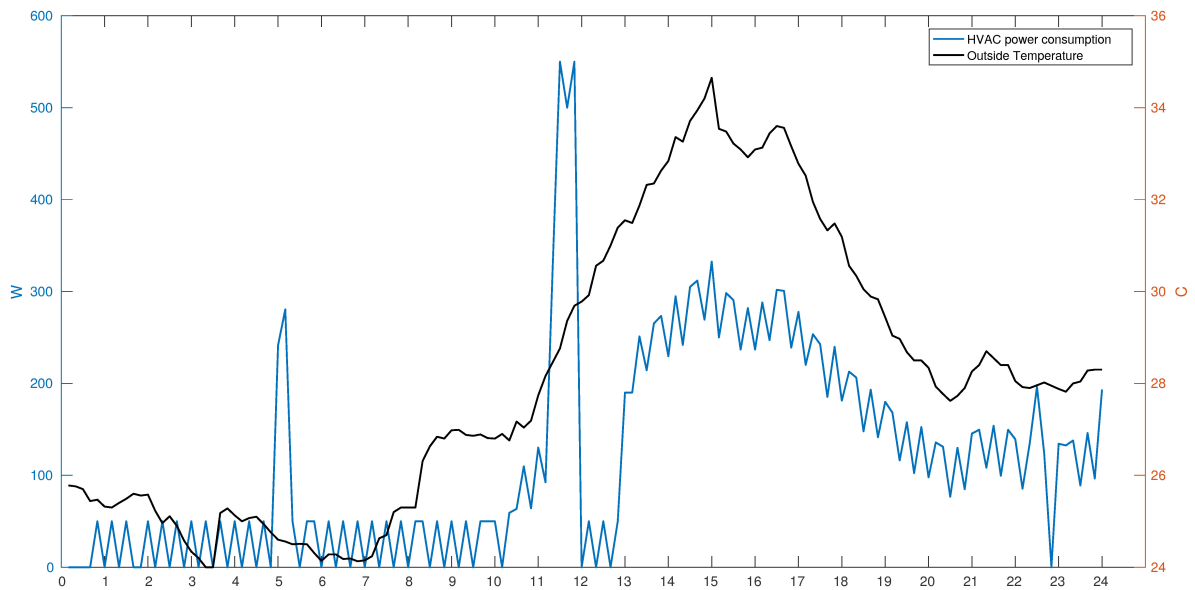


Figure 3.3: HVAC load profile for Typology $k = 6$

The plot shows the cyclic functioning of HVAC and also that $P_{k,t}^H$ is controlled by the outside temperature. The method used assumes that the fixed part of load also includes the thermal component for the typologies that have HVAC devices assigned. The reason for this has to do with the decision to reduce the model's complexity by reducing the number of output variables without loss of generality. A simulation of thermal appliances has been made and summed with base load resulting in the following load profiles:

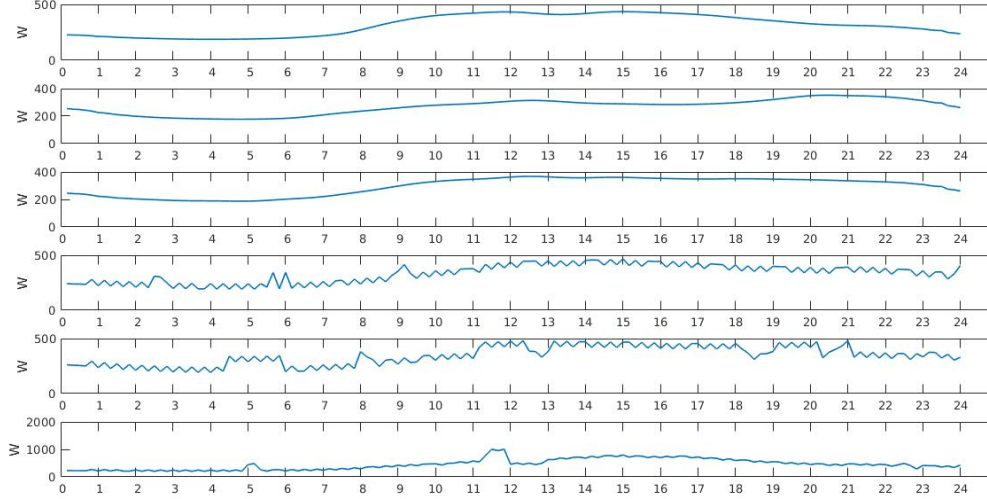


Figure 3.4: Base Loads for all 6 typologies

The 6 typologies are based in 4 referenced works where parameters were consulted (see Table 6.6 in Annex 6.9.5). Type $k = 4, 5$ are the same in terms of construction and thermal properties but they are assigned with different appliances and different base load. Typologies identified by $k = 1, 2, 3$ do not have HVAC system so their base load diagram assumes a more regular shape. Type $k = 6$ is the same as $k = 2$ in terms of construction and thermal properties but it has a bigger fixed load and a HVAC system with a bigger $p_{\omega, max}^H$ than the others. This typology stands for a commercial archetype such as a small business and its fixed load increases during the daytime.

3.2.3.3 Modeling approach

The modeling approach consists in outputting variable load diagrams from shiftable devices and EV's "on top" of the base load in order to evaluate its impact on each typology aggregated load diagram and objective C_k . Types $k = 1, 2$ will be assigned with no shiftable or EV and they will stand for the fixed part of the total aggregator fixed base load. The remaining 4 typologies, having shiftable and EV loads, but also their own fixed part, will make for the variable part.

3.2.3.4 Load vs Imported power

The communication between agents is based on $P_{k,t}^{imp}$, the typologies imported power from upper levels, rather than the total load, $P_{k,t}^L$. This means that the agents communication acts are imported power requests. From (2.35) it can be seen that $P_{k,t}^L = P_{k,t}^{imp}$ only if typology have no storage system assigned ($r_{b,k,t}^c = r_{b,k,t}^d = 0$), no V2G mode for PEV ($P_{k,t}^{EVd} = 0$) and, above all, no installed PV capacity ($P_{k,t}^G = P_{k,t}^{inj} = 0$).

The two following plots exemplify two of the many possible output solutions for $P_{k,t}^{imp}$. Namely when there is not enough RES local production to inject in the grid and when there is.

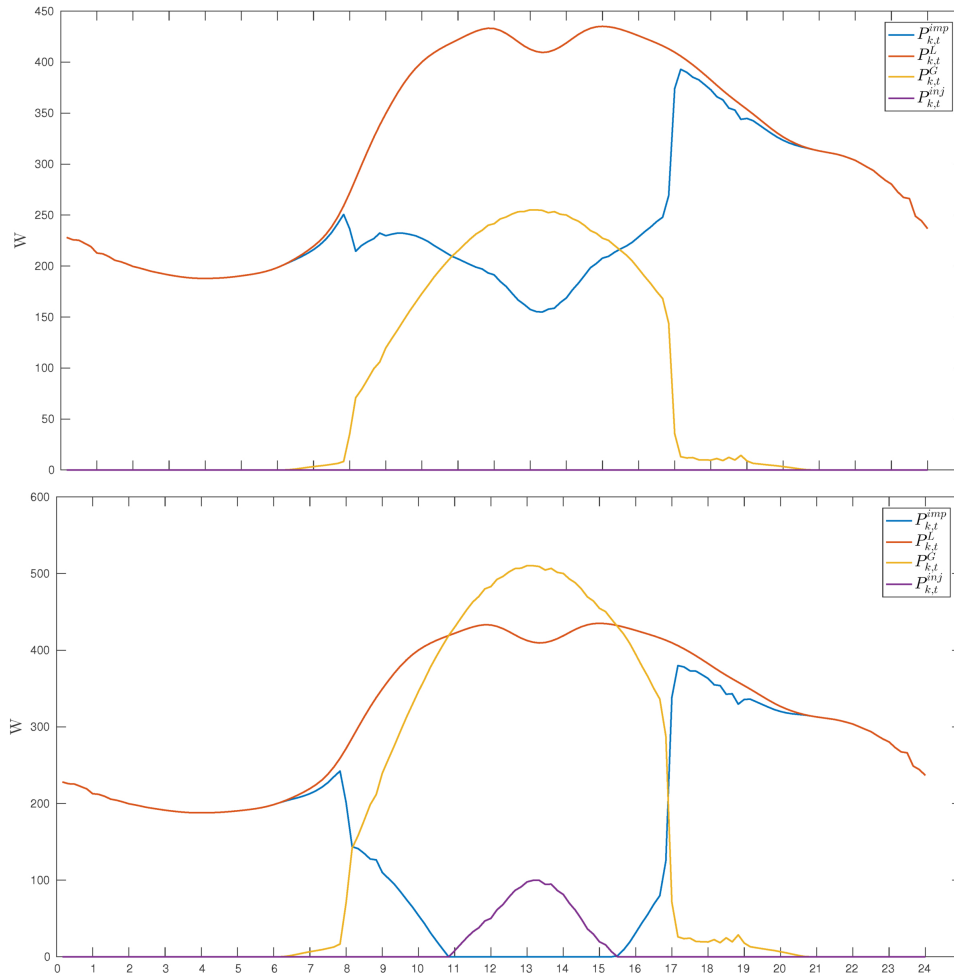


Figure 3.5: Generic typology power balance with and without excess PV production

As shown in the plots, $P_{k,t}^{imp} = P_{k,t}^L$ when $P_{k,t}^G = 0$ and $P_{k,t}^{imp} = 0$ when $P_{k,t}^{inj} \neq 0$. In this example typologies import all the production from the grid except when there is PV production. In the bottom plot, the same configuration is represented but with twice the PV capacity installed which results in excess production that is injected in the grid.

Concerning the contracted power $P^{LimGrid} = 4.6$ kVA will be considered for each element in typologies. Other typical values, such as 3.45 or 6.9 kVA, may be considered. However 4.6 KVA is an intermediate value that allows for EV charging in typologies, on one side, and avoids huge peaks, on the other, since maximum allowed power consumption at each typology is constrained by that value.

3.2.4 \mathcal{M}_N data

Within local node level a size for the aggregator must be defined in term of number of elements (residential dwellings, commercial shops, etc) of each typology. A total number of elements $N_T^{mix} = 4510$ will be considered. This corresponds to 1 Km^2 of an urban area with a population density around 9000 persons per Km^2 if a 2 persons per dwelling mean [63, p. 47] is considered. For Portugal these numbers may represent several known areas in the most populated urban areas. The specific power grid topology is given in the following picture

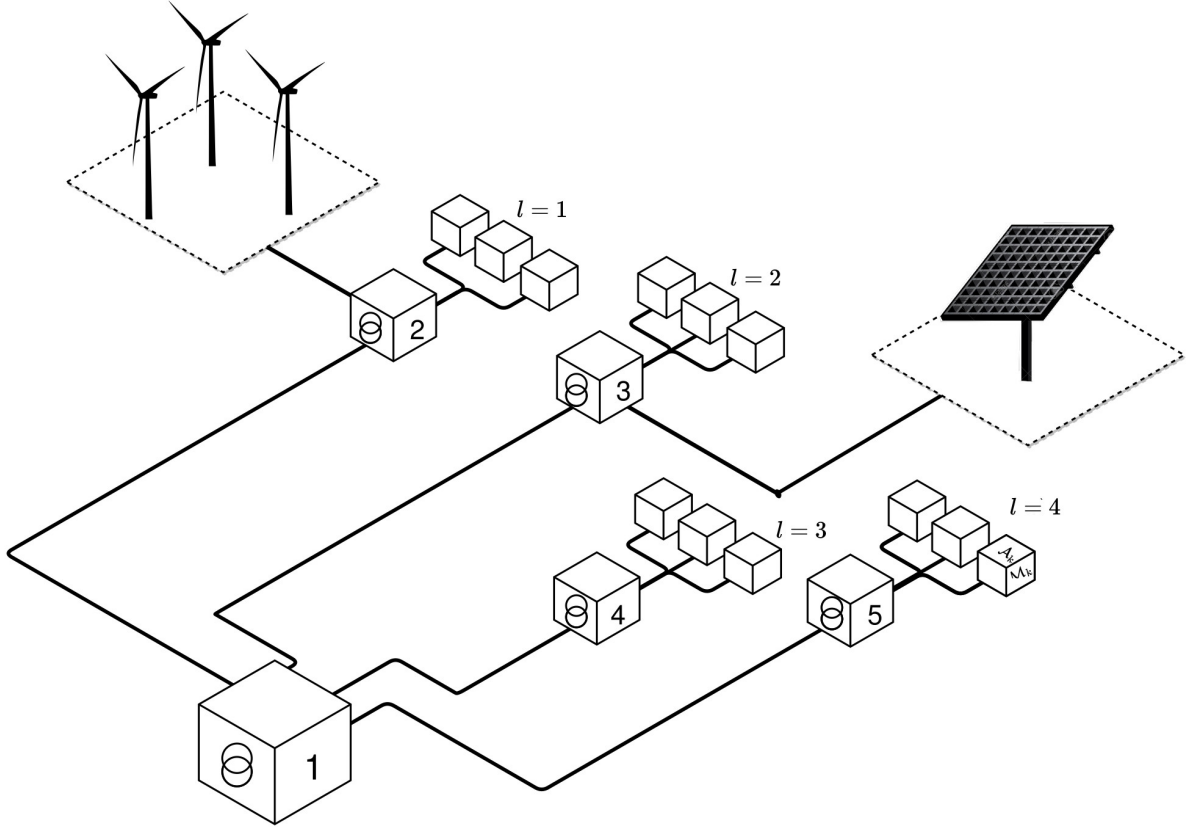


Figure 3.6: General star topology for the aggregator power grid

which is a 5 bus general network in a star configuration. The figure shows that there are 4 buses requesting or injecting power from/to 4 local aggregation buses. In Annex 6.9.7 the adjacency and connection matrices for this grid are presented. Figure 6.6 in Annex 6.9.8 shows an example of the load profile at the 4 aggregation buses. In the example, MT-LT 2000 kVA transformers were considered. Matrix $\mathbf{N}_{l,k}$ in equation (2.42) gives the dimension of the load at the aggregator and can be used to define different scenarios. If typologies have different characteristics and output different load diagrams, then different "blends" will allow to test the effects arising from the inclusion of specific typologies. The most basic of these blends is the one in which types $k = 1, 2$ make up for the majority of elements in the matrix accounting for a fixed load in the aggregator. From here, scenarios can be built by changing the relations between elements leading to the generation of different $\mathbf{N}_{l,k}$.

The scenarios considered are the ones depicted in the bar diagram in Figure 6.7 of Annex 6.9.9. Annex 6.9.9.1 presents the full $\mathbf{N}_{l,k}$ matrices for them. The followed approach will consider that the total number of elements in the aggregator is fixed and its just given by

$$N_T^{mix} = \sum_l \sum_k \mathbf{N}_{l,k} \quad (3.5)$$

3.2.5 \mathcal{M}^0 data

Grid Topology

There is a great tendency to view the aggregators at the distribution system, as energy management entities or as new players at local energy markets as seen in introduction chapter. Referring to Figure 3.6 one can observe that HT-MT substation at bus 1 establishes the border of the aggregator and it is where \mathcal{A}^0 acts as manager of power imports and exports. Beyond this border other entities exist that can supply the aggregator needs for instant power or buy the excess production. The remaining nodes stand for MT-LT feeders in which the aggregated load from typologies is connected. Again, different and much complex topologies may be considered to represent real power networks. The small size of the present network is related to the fact that only 6 typologies are considered and the diversity of consumer types is reduced to that number. An aggregator representing a wider area would, most certainly imply a greater number of typologies. The present aggregator allows to present a suitable general framework to simulate an island, a city or a region if the needed parametrization data sets are available.

Parameters for a simple DC power flow linear model for \mathcal{M}^0 are summarized in the following table:

Table 3.3: \mathcal{M}^0 power flow parameters

Substation installed capacity (MVA)	P^{SE}	10
Lines length (Km)	$L_{i,j}$	1
Line Reactances (Ω / Km)	$\chi_{i,j}$	0.09
Base Power (MVA)	S_b	10
Maximum phase difference variation (degrees)	$\delta_{i,j}^{max}$	20

Wind Power Plant

It will be considered only one WPP ($N_{gwt} = 1$) connected to node $i = 2$ as can be seen in Figure 3.6. To model the aggregator local renewable production a WPP constituted by twenty ($n^{wt} = 20$) 100 kW rated power wind generators is used and power curve and characteristics are depicted in Figure 6.2 and Table 6.3 in Annex 6.6.1. Figure 6.5 in Annex 6.9.4 shows the hub height corrected values for high and low wind speed scenarios. The power output of the WPP is plotted in Figure 3.7.

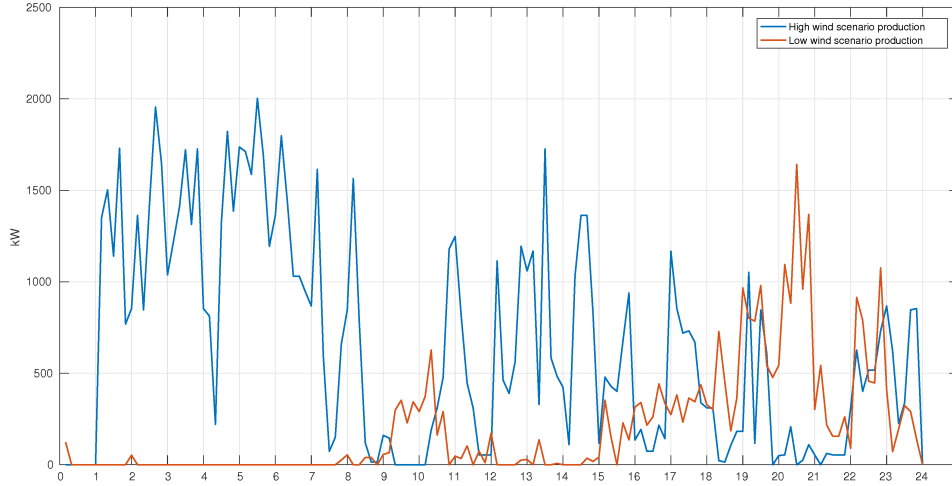


Figure 3.7: Power output for WPP with $n^{WT} = 20$ for high and low wind scenarios

Wind Power LCOE

LCOE for WPP will be considered as $c^{WT} = 0.0454$, the average value for Onshore WPP in 2016 [64], but other values can be considered such as the ones in Table 3.2.5 (see Tables)

Table 3.4: LCOE for Wind power in 2016 (€/kWh)

Minimum	Average	Maximum
0.0194	0.0454	0.114

PV power plant

A 3MW PV power plant will be considered with $n^{PV,0} = 11321$ modules ($N_{g^{pv}} = 1$) connected to node $i = 3$ as can be seen in Figure 3.6. The chosen modules are the same as in 3.2.3.1. Considering the solar resource in Figure 6.4 and the models in 2.4.1.2.9 the PV production profile is depicted in Figure 3.8.

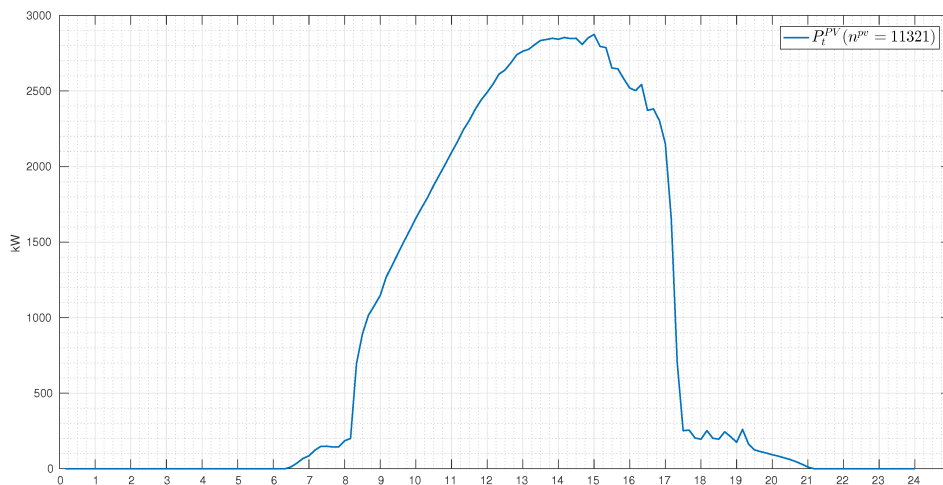


Figure 3.8: PV Power Plant output

All adjacency and connection matrices can be consulted in Annex 6.9.7

PV PCOE

A value of $c^{PV,0} = 0.0435$ was chosen, the minimum value for PV in 2016 [64]

Grid Tariffs

According to equations (2.37) and (2.39), tariffs at typologies level are constructed considering grid access tariffs, fixed daily tariffs and commercialization tariffs. According to (2.57) the tariffs applied to aggregator refer to power imports and exports from the external grid and a daily cost related to transformer installed capacity. It will be assumed that tariffs are the same whether power is imported or exported. The values used at both levels are the reference values for Portugal as published by the regulator ERSE [65] and can be consulted in Annex 6.9.10

Electricity market price vector

The vector c_t^{mrk} plays a major role in the model because it has a big influence on the electricity production cost c_t^0 . The input price vector must be an information data set that \mathcal{A}^0 has previous access through a market agent or another aggregator agent that broadcasts it or negotiates with it. Being beyond the scope of the present work to model those interactions the available dynamic hourly price vectors from the MIBEL [66], depicted in Figure 3.9, will be used.

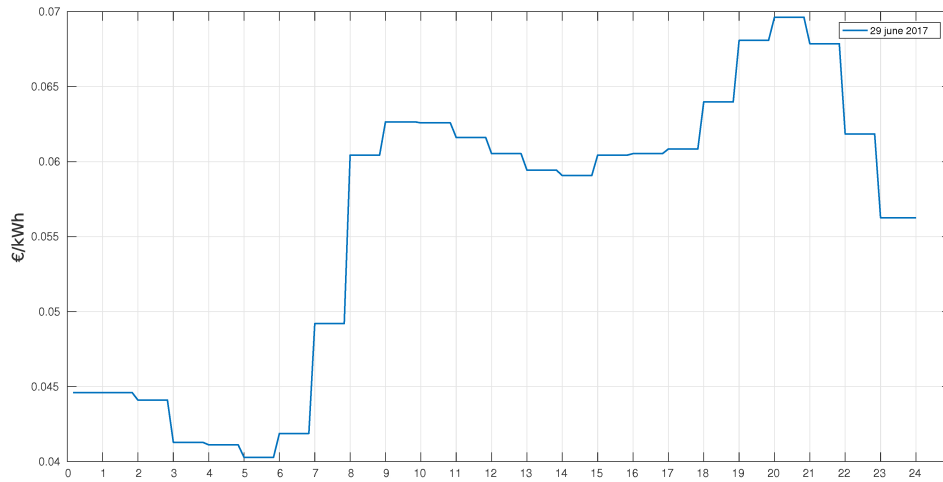


Figure 3.9: MIBEL prices in 29th June 2017

Chapter 4

Case Studies

4.1 Simple case

The simple base case study will consider the central scenario, $N_{l,k}^{central}$, given in Annex 6.9.9.1 and the appliances and devices distribution among typologies presented in Table 4.1 (see Tables 3.2 and 3.1)

Table 4.1: Base case devices assignment

k (Typology)	1	2	3	4	5	6
Electric Vehicles	-	-	ω_1^{EV}	ω_2^{EV}	ω_2^{EV}	ω_1^{EV}
Shiftable devices	-	-	ω_5^S, ω_3^S	ω_5^S	ω_2^S	ω_5^S
Storage system	-	-	-	-	-	-
P_k^{Wp} (W)	0	0	0	0	0	0

Aggregator Load balance Figure 4.1 presents one example of an output solution from \mathcal{A}^0 for the aggregated load balance quantities defined in equations (2.61) - (2.66)

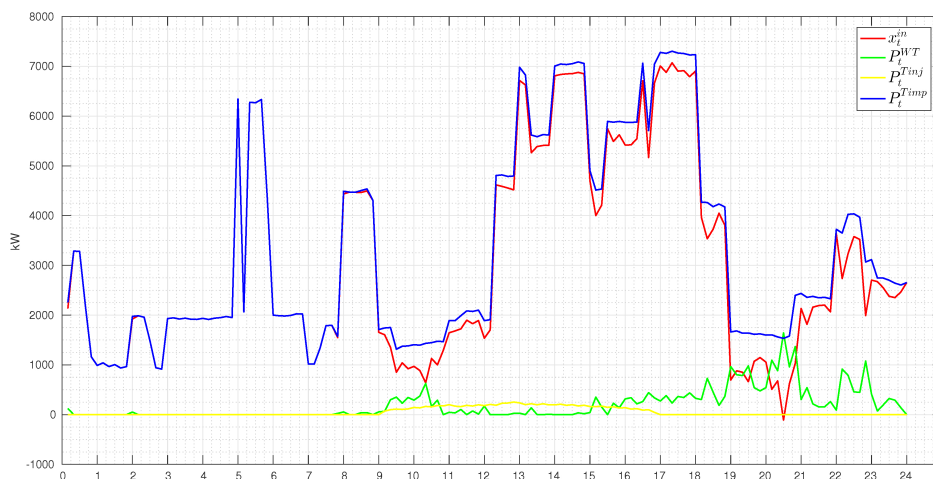


Figure 4.1: Power balance at the aggregator

As shown, power is only imported when $P_t^{WT,0}$ and P_t^{Tinj} do not meet the supply demand P_t^{Timp} . Concerning P_t^{Tinj} , the excess production from the typologies level, it is assumed that

power balance is maintained at aggregated level and the power flow on the low tensions side of the local level transformers is not computed since no lower level grid topology or characteristics exist. This means that the excess production in one typology element is consumed by a different element from a different typology since elements of the same typology use the same variables. Between 20h and 21h there is a moment in which the aggregator is actually exporting ($x_t^{in} < 0$) power to the grid and we see that this is due to a surplus of wind power production.

Aggregator marginal production cost Considering equations (2.57), (2.56) and (2.58) one may look at an example output for c_t^0 for an entire day.

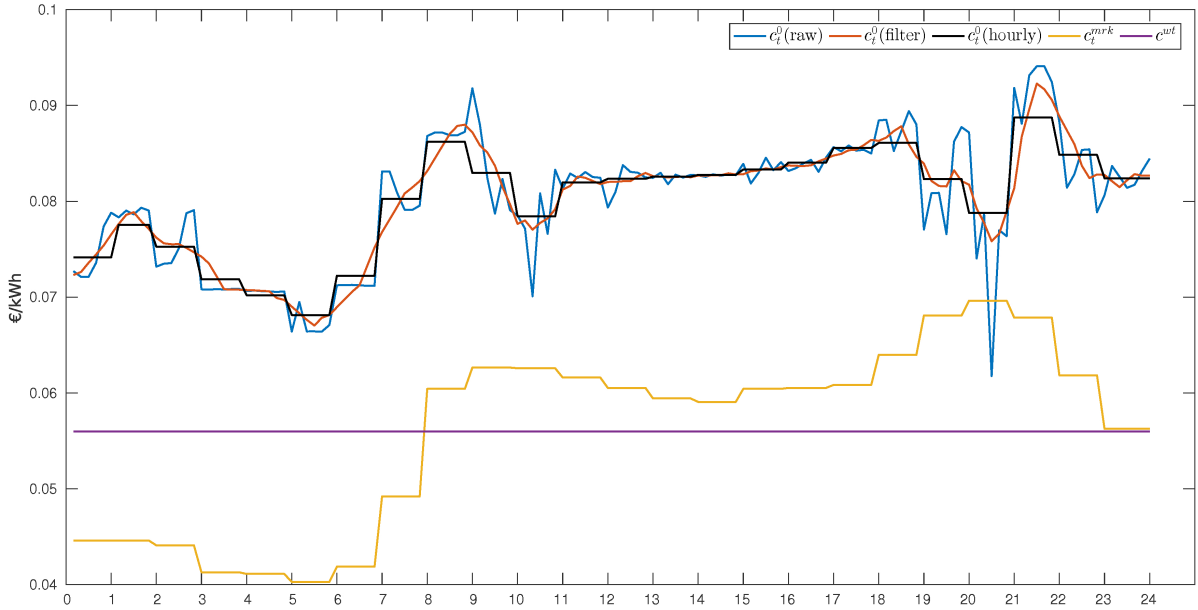


Figure 4.2: Original, filtered and hourly aggregator electricity production marginal cost plotted against market price vector and WPP LCOE

The real output solution for c_t^0 is in fact extremely variable, which is expectable since power flow is computed with a timestep of $\Delta t = 10$ minutes and variability follows this time scale. But vector price used as signal in communication between agents must be smoother and hourly which implies filtering the real output c_t^0 with a central moving average of length 6 thus computing hourly mean values from the filtered price series. This is so because \mathcal{M}_k may be very sensitive to price vector with solutions changing very abruptly with slight changes in price signals. A more stable price signal is important if \mathcal{A}_k reactions to DR signals are to be anticipated. The plot also depicts the MIBEL hourly electricity market prices and a relation between c_t^0 and c_t^{mrk} is noticeable. An obvious conclusion is that as long as the the majority of electricity supplied to consumers originates from market imports, c_t^0 will be indexed to c_t^{mrk} . However, this is not the case for timeslots between 10h and 11h and between 20h and 21h where the marginal cost lowers considerably reaching values below the market marginal cost. From Figure 4.1 it can be noticed that these timeslots correspond to the moments when WPP production reaches a maximum and a part of the power consumption in the aggregator is supplied by the WPP. Therefore c_t^0 becomes indexed to wind power LCOE, c_t^{WT} . Coincidentally, in these timeslots it also holds that

$c_t^{mrk} > c^{WT}$, fact that contributes to lowering c^0 which benefits consumers.

Output solutions and results The number of output variables and input parameters present in the whole model is considerably high and a criteria for choosing among the former is needed. The interest is to look at variable subsets that allows to look at the BLP model solutions when using the Algorithms 1 and 2. Given the difficulty to analyze the evolution of some time-dependent quantities along the iterative process a mean value for selected output variables may be considered instead, as in the case of c_t^0 . It is possible to look at γ plots of t values each and analyze the evolution of the shape of the marginal cost but looking at mean marginal cost in each iteration delivers more information about the adaptation that this quantity is suffering. Following the same logic, one should look at $L_\gamma^f = L_t^f$ to evaluate the evolution of the aggregator mean load factor. Concerning typologies it is not practical to look at the K solutions that \mathcal{M}_k 's are delivering for daily electricity bill since consumers are considered an aggregated entity. Obviously a specific typology evolution can be followed but an evaluation of the consumers evolution as a group is given by a mean daily typologies bill $C_\gamma = \frac{\sum_k C_{\gamma,k}}{K}$. Choosing \mathcal{M}_k variables, s_k , will depend on the specific case study considered. The following plots display variables subset $(c_\gamma^0, C_\gamma^0, C_\gamma)$

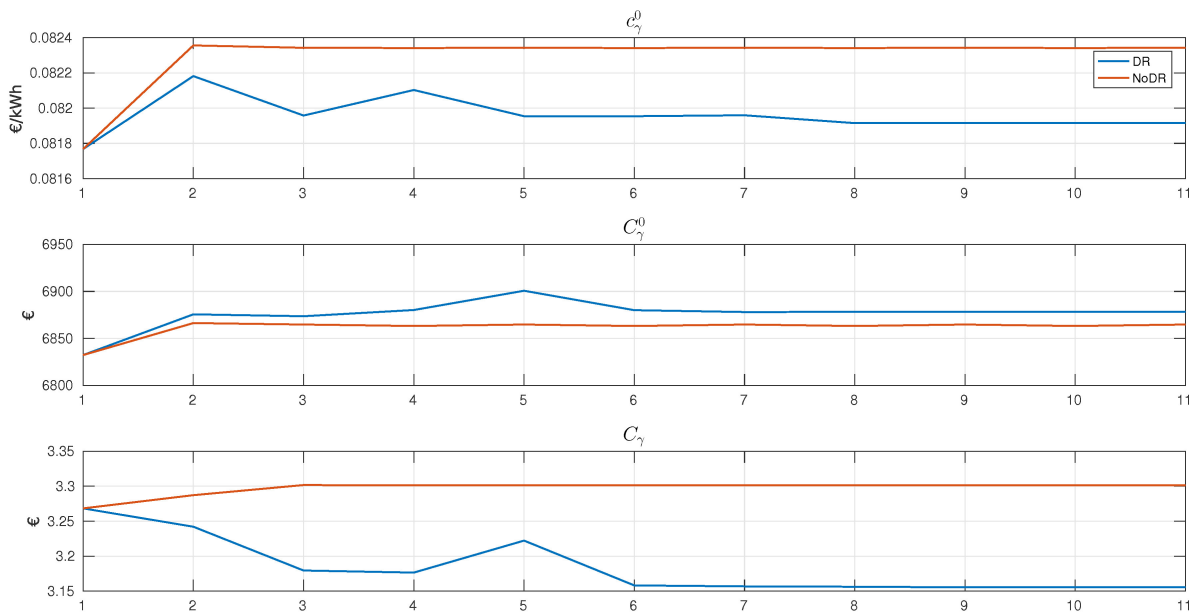


Figure 4.3: Bi-level variables and solutions for \mathcal{M}_k and \mathcal{M}^0 with and without DR mechanism

Figure 4.3 depicts the solution to which both algorithms converged after 11 iterations. As can be seen, the top two plots present slightly different outputs when considering both algorithms although they depart from the same solution at $\gamma = 1$. The DR algorithm converged into a lower value for c_γ^0 and the shape of the curve reveals the adaptation of the solution towards the convergence. The simple algorithm converges much faster and the regular flat shape highlights the inexistent adaptation process. In the case of C_γ^0 the same pattern can be observed but the DR algorithm converges to a worst solution for the aggregator. These two plots illustrate one possible output in which DR mechanism is beneficial to consumers but prejudicial to the

aggregator that gets its revenues from selling power to the former. C^0 and C_k are not necessarily cooperative and a deeper look into the nature of output solutions will be addressed in next case studies. The third plot reveals the extent of this benefit and it is clear that typologies C_γ decreases and these were able to lower their mean electricity bill.

Nonetheless, all plots show a small variation interval what poses the question of the real need for a DR mechanism. However the last plot shows a variation of around 0.15 € between both algorithms final solution. To understand what such a variation can mean to typologies it is important to look at the following plot depicting each typology $C_{\gamma,k}$.

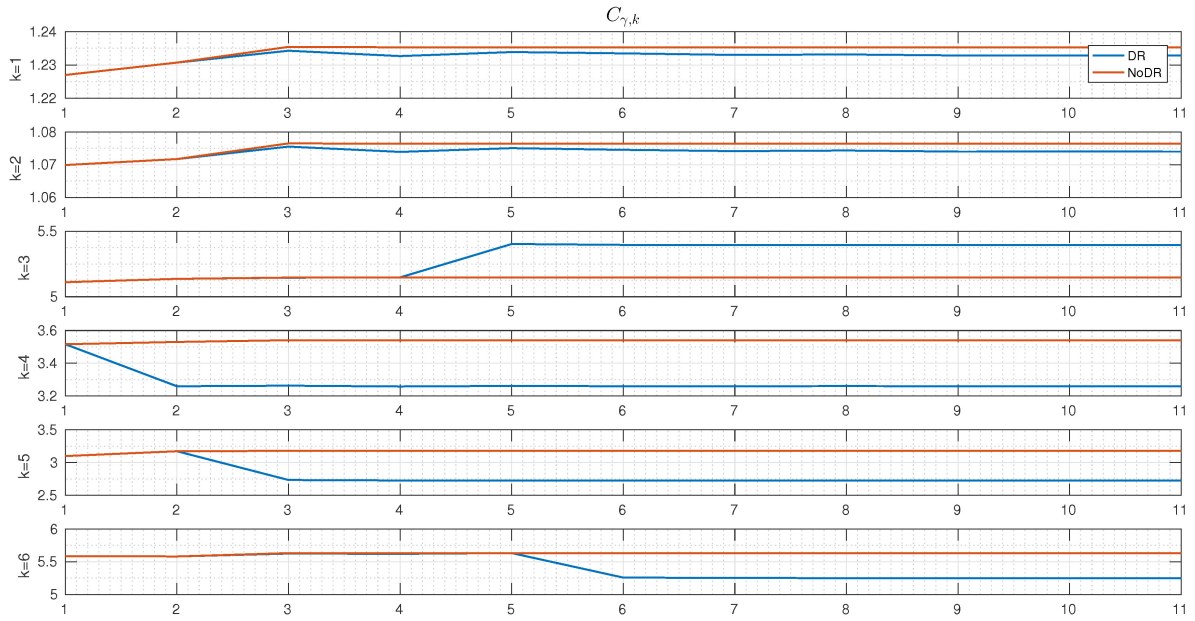


Figure 4.4: Solutions for \mathcal{M}_k with and without DR mechanism

The first observation is that for this specific run the random queue generated was

$$q_m = [4 \ 5 \ 2 \ 3 \ 6 \ 1]$$

and the plot shows the order in which each typology is allowed to schedule its load. For $\gamma = 2$, type $k = 4$ makes its move and the game go on until $\gamma = 6$, when type $k = 6$ makes its move. All typologies, except $k = 3$, were able to lower its daily cost and at this scale the variation its not despicable since changes can go as further as 0.37 € between the first and last iteration costs. In a monthly basis may amount to more than 11 € in the electricity bill. Recall that types $k = 1$ and $k = 2$ do not have variable loads assigned therefore do not have the possibility of playing the DR game. Nonetheless these types were beneficiaries from the decrease in c_γ^0 along iteration. This result is expected because a decrease in the marginal cost of production means a decrease in typologies daily bills. P_t^{Timp} should be compared between the two cases with the following figure:

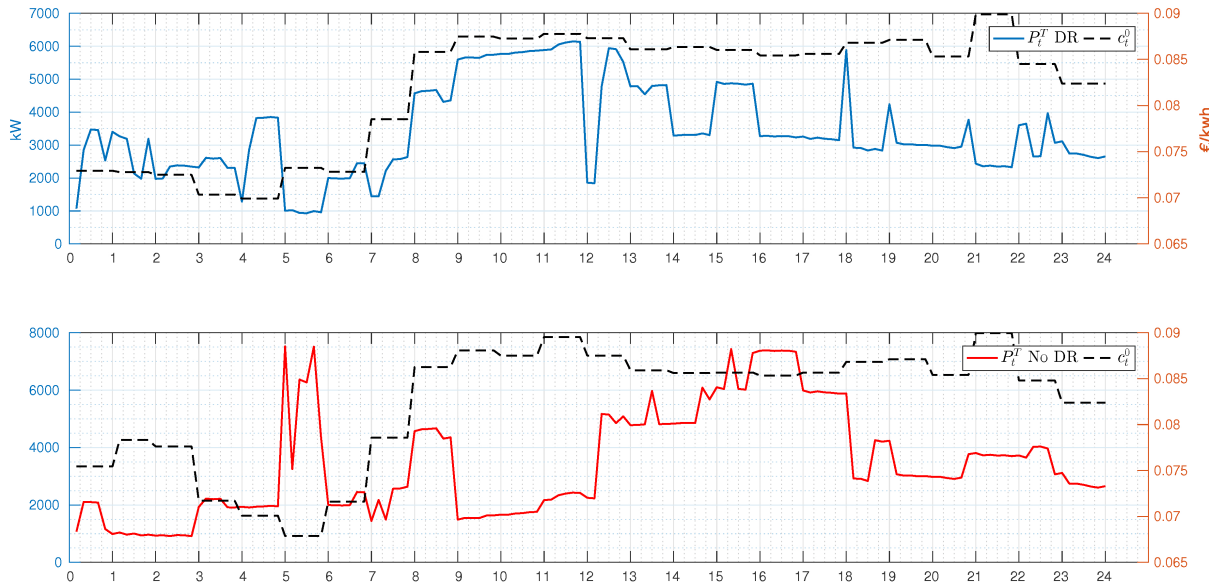


Figure 4.5: Aggregated load with and without DR mechanism

At bottom plot it can be seen, in the positive side, that load is scheduled at low c_t^0 timeslots but, in the negative side, the herding effect is evident with huge spikes in low price timeslots. On the top plot the DR mechanism clearly produces a slightly more regular aggregated load diagram although is far from an ideally flat load. However the DR mechanism was able to eliminate some spikes and the ones that it produces are less intense than the ones seen on the bottom plot. Some of the load was displaced to late morning periods since these periods were exactly the ones where load valleys show in bottom plot. This is a consequence of a load factor based DR mechanism that spreads load along the time horizon. The trade off between the two algorithms is that the total load, P_t^T , ends up following the shape of c_t^0 what is unintuitive since the objective is to schedule load at low price timeslots. In the example, the intuitive solution would be to place all variable load at morning timeslots since c_t^0 is lower. However, the DR mechanism is based on the combined effect of production cost and load factor, through c_t^f , which benefits consumers bill like can be seen in Figure 4.4. In any way c_t^f is indexed to c_t^0 in a sense that the values of the former will always be in the order of magnitude of the latter.

More information for evaluating the two cases may be taken from the evolution of the daily mean load factor, L_t^f , along iterations in the following plot

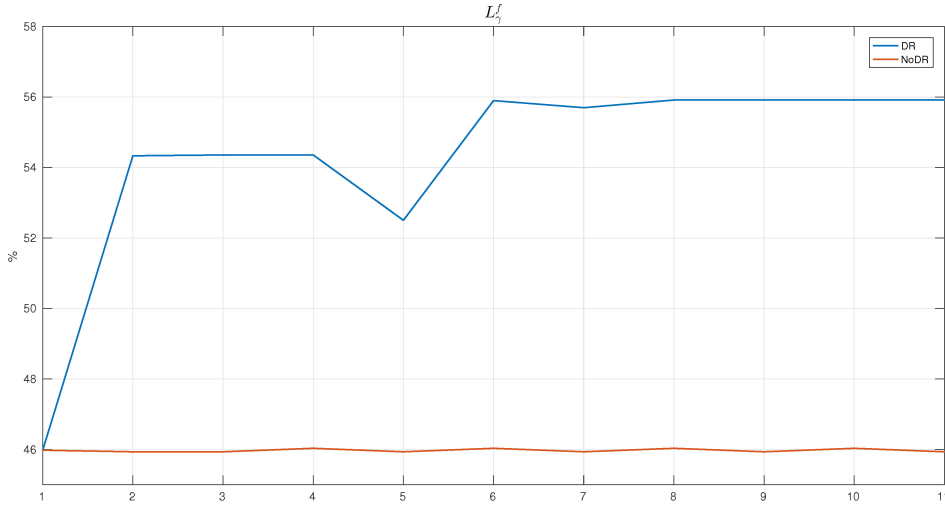
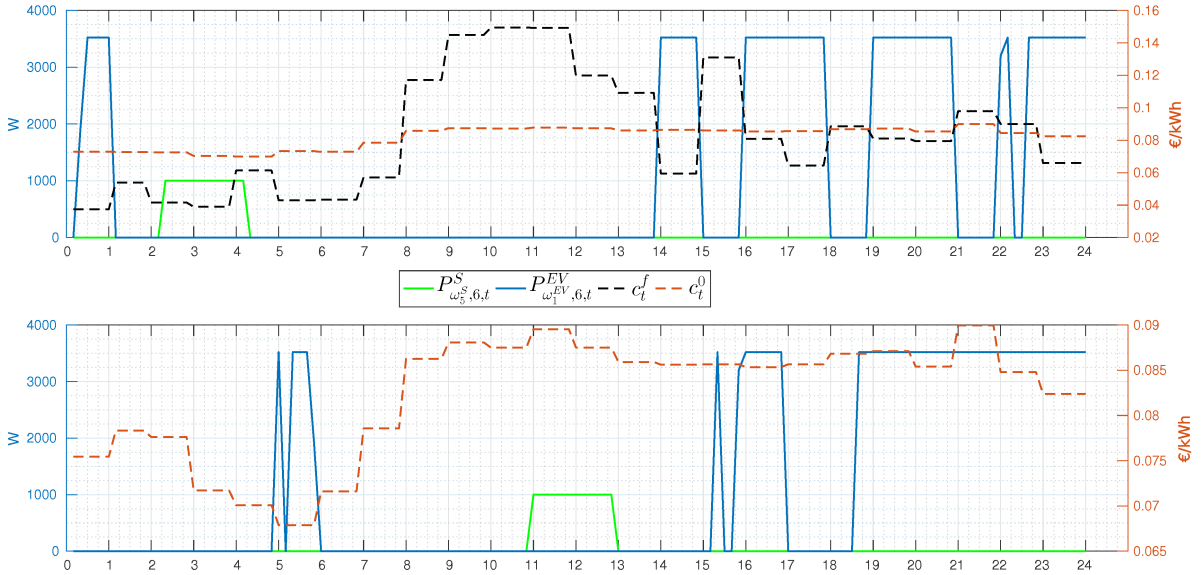


Figure 4.6: Daily mean load factor along iterations

The plot shows that the mechanism produced a 10 % increase in load factor with a slight increase in aggregator cost (middle plot in Figure 4.3). This result was theoretically expected since the essential idea of the DR mechanism is to schedule load at low load factor timeslots.

4.1.1 An individual solution

To see what is happening at low level scales one may look at a specific output from an individual typology, $k = 6$, in order to demonstrate the functionality of the DR mechanism.


 Figure 4.7: Type $k = 6$ example solution for EVs with and without DR mechanism

In Figure 4.7 the two final iteration output solutions are shown for this typology depicting price vectors, shiftable and Evs outputs. Looking at non DR bottom plot it is noticeable that \mathcal{A}_6

strategy is to schedule a part of ω_1^{EV} load at lower price timeslots during the morning period, but the same cannot be said for ω_5^S that is scheduled to functioning at 12h during peak price. This device could not be scheduled between 5 and 6 am because it would superpose with the load from ω_1^{EV} , therefore summing up to a greater load than $P_6^{LimGrid}$. But it could have been scheduled immediately before because $c_{4h}^0 < c_{12h}^0$. A possible explanation for such a solution derives from the fact that c_t^0 has a maximum variation of 0.02 € between its higher and lower prices and the sensibility of \mathcal{M}_k may not be as big as expected, therefore perceiving the price vector as flat. A different situation emerges when the top plot is considered. Clearly the solution is highly influenced by c_t^f vector that has a greater variation oscillating more that 0.1 € during the day producing easily avoidable price peaks and highly attractive price valleys. This plot depicts a perfect output for DR, although we have no guarantees that this behavior will be verified for all \mathcal{A}_k . Not only \mathcal{A}_6 schedules both ω_5^S and ω_1^{EV} at the lowest price timeslot but also its strategy is to adapt $P_{\omega_1^{EV},6,t}^{EV}$ in order to fit the small fringes of low price timeslots during the afternoon. This behavior is the result of using MNLF as a basis for DR.

Costs and revenues The DR mechanism can be seen as an artificial reshape of the price vector towards influence of typologies solution. Inevitably there will be differences in the daily revenue Re^0 between the two algorithms. What consumers are actually paying to aggregator is given by each type's objective multiplied by the number of that type elements in all grid nodes with connected loads $N_k^{mix} = \sum_l N_{l,k}$

$$Re_\gamma^0 = \sum_k (N_k^{mix} \circ C_{\gamma,k}) \quad (4.1)$$

For the base case that have been considered one should look at the following table with the results from the last iteration in Figure 4.3

Table 4.2: Costs, Revenues and Profits for $\mathcal{A}^0(\text{€})$

	Re^0	C^0	Pr^0
DR	11904	6878.2	5015.8
No DR	12139	6864.8	5274.2

The table shows that there is a greater revenue and profit for the NO-DR case relative to the DR case with similar costs. The difference is about 2% for revenues and 5% for profits. **In practice, the Demand Response mechanism is a sequence of rebates and increases in dynamic electricity tariffs for \mathcal{A}_k agents applied to specific timeslots with positive or negative impacts in \mathcal{A}^0 revenues and profits. The objective is to produce the combined effect of increasing the system load factor and decreasing the consumer's daily electricity bill.**

4.2 Production System Scenarios

In order to model a possible future day-ahead decision problem an aggregator with 3 different production configuration will be considered. Namely, **a)** only electricity market imports (scenario **SM**), **b)** market plus WPP (scenario **SMW**) and **c)** market plus WPP and a PVPP (scenario **SMWP**). The production profiles for the WPP and PVPP are the high wind resource scenario

and the 3 MW PVPP presented in 3.2.5. The combined production profile is presented in Figure 4.8

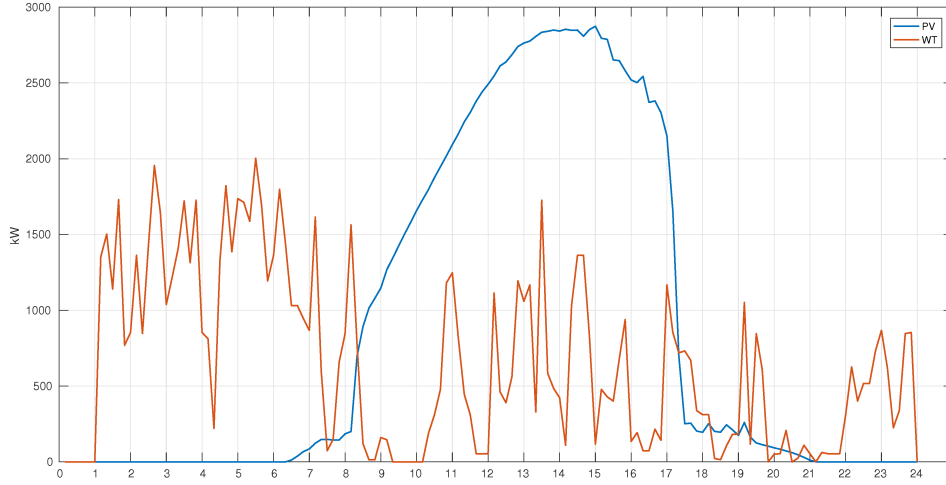


Figure 4.8: PVPP and WPP production

Values for LCOE are the ones in Table 4.3

Table 4.3: LCOE in €/kWh Source: [64]

c^{WT}	$c^{PV,0}$
0.0454	0.0435

A future central scenario of 61 % EV penetration is chosen from Figure 6.7 in Annex 6.9.9 and the assignment distribution of EVs in Table 4.1. The scenario typology mix is given by $N_{l,k}^{central}$ matrix in Annex 6.9.9.1. The following table must also be considered

Table 4.4: Data PEV (source: [56])

cars in 2015 ($\frac{cars}{1000 \text{ inhabitants}}$)	406
Total number of typologies elements (N_T^{mix})	4510
Number of persons per house (N_p^H)	2
Total number of cars at the aggregator in 2015 (N_{cars}^{2015})	(aprox) $406 \times N_T^{mix} N_p^H \approx 3662$
Very low penetration rate (% of total cars / Number of EVs)	10% (≈ 330)
Low penetration rate (% of total cars / Number of EVs)	26% (≈ 864)
Central penetration rate (% of total cars / Number of EVs)	61 % (≈ 2020)

where it is assumed that 10% of EVs are always driving at a given time, thus decreasing the number of simultaneously charging vehicles. Next table defines the allowed charging timeslots for each typology

Table 4.5: Electric vehicle schedule distribution

k (Typology)	1	2	3	4	5	6
$t_{\omega,k,start}^{EV}$ (h)	-	-	0	0	0	0
$t_{\omega,k,end}^{EV}$ (h)	-	-	24	8	8	24

The idea behind this time distributions is that type $k = 4, 5$ represent users that impose their smart-charging devices to deliver the full charged EV at 8 o'clock in the morning while the remaining two EV-assigned typologies may use the full time horizon, H . This permits the evaluation of the possible pathways of load adaptation but also increase the solution search space. This kind of modeling assumes that consumers are charging their EV's in their own dwelling or at commercial type own electrical installation since EVs are regarded as appliances. Inevitably, groups of EVs within the same typology will be charged simultaneously since the solutions are the same for each typology. Values of $P_{\omega, max}^{EVc}$ in Table 3.2 are acceptable for home or small workshop electrical installation and compatible with typical contracted power values assuming a slow charging mode. According to Algorithm 2, q_m will be re-generated each time the model's solution process is initiated. To avoid that extra source of variability it have been assumed, for all scenarios in the present chapter, $q_m = [6, 4, 5, 1, 3, 2]$.

The results are the following

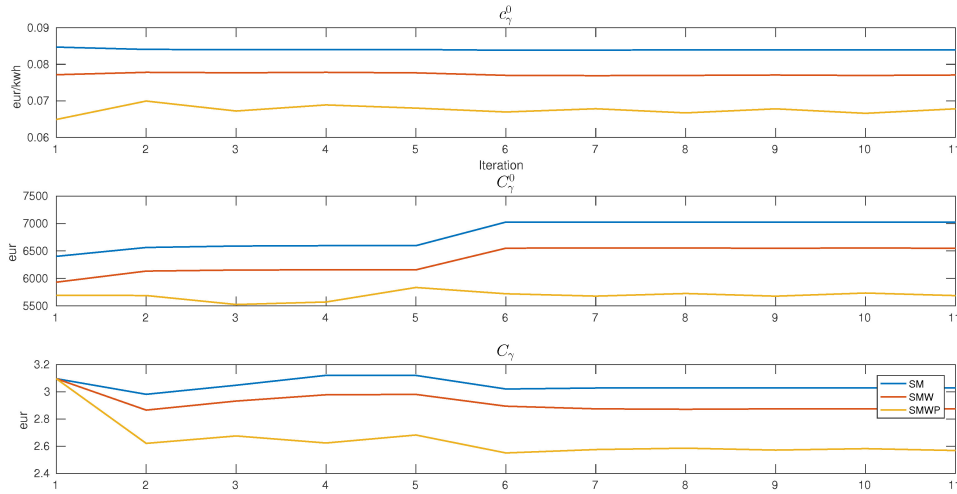


Figure 4.9: Bi-level variables and solutions for \mathcal{M}_k and \mathcal{M}^0 for SM, SMW and SMWP scenarios

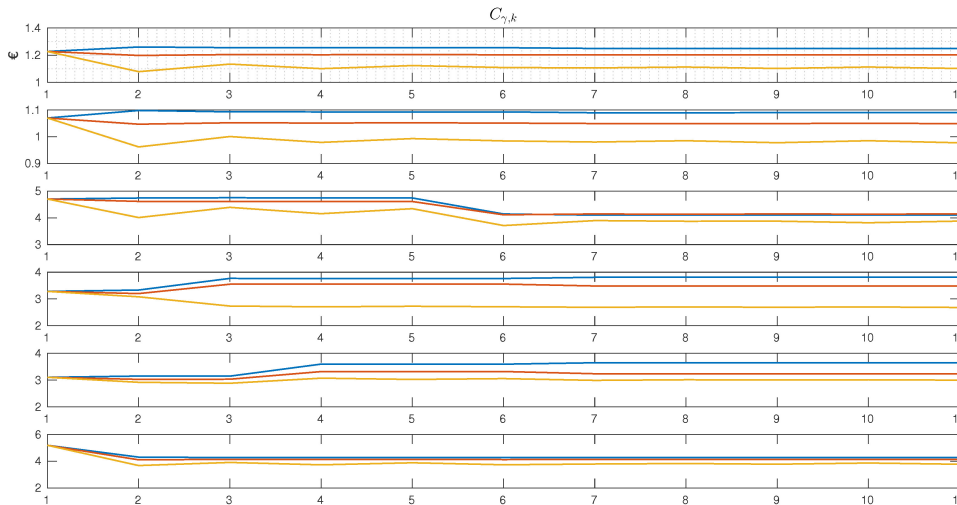


Figure 4.10: Solutions for \mathcal{M}_k for SM, SMW and SMWP scenarios

In Table 4.6 and 4.7 the first 3 columns present the percentage variation between initial and final values, respectively, from the first and last iteration, for the bi-level variables for the three scenarios relative to first iteration. The last column presents the variation on the values, for the same variables, between **SM** and **SMWP** relative to **SM** final values.

Table 4.6: Percentage variations along iterations for C_γ^0 and c_γ^0

Variable	SM	SMW	SMWP	SM → SMWP
C_γ^0	9.8	10.4	-0.08	-19.1
c_γ^0	-0.9	-0.1	4.5	-19.2

Table 4.7: Percentage variations along iterations for $C_{\gamma,k}$

-	SM	SMW	SMWP	SM → SMWP
1	1.8	-2.1	-10.2	-11.9
2	1.9	-1.9	-8.7	-10.3
3	-12.8	-11.9	-17.6	-5.5
4	16.1	6.2	-18.3	-29.6
5	17.5	4.3	-3.4	-17.8
6	-17.8	-20.5	-27.3	-11.6

Figure 4.9 and Table 4.6 present a small variation, always under 5%, in c_γ^0 along the iterations for all scenarios. When looking at C_γ^0 , the actual \mathcal{M}^0 's objective, there is a considerable positive variations except for **SMWP** that shows a negative variation along iterations of 0.08 %. This means that the adaptive process increases the cost of producing energy in all scenarios except in **SMWP** when RES penetration increases. Therefore the 19 % negative variation for the variables when comparing scenarios is expected given the injection of high rates of electric power with low LCOE in the aggregator's power system. The solutions of \mathcal{M}_k for the different scenarios can be seen in the plot in Figure 4.10 and Table 4.7. For **SM**, all types except \mathcal{A}_6 and \mathcal{A}_3 , increase their bills along iterations. Recalling that these two agents are the only ones with the full time horizon H available for scheduling it is only natural to assume that this particular configuration makes it possible to find better solution when compared with other time-constrained agents. This leads to an asymmetric game configuration that raises equity issues. When comparing the increase for the same scenario, \mathcal{A}_4 and \mathcal{A}_5 have the biggest increase even if compared to \mathcal{A}_1 and \mathcal{A}_2 that don't play the game. This occurs because they have constrained schedules and on top of that they have a big EV battery to be charged during those timeslots which leaves them no scheduling options.

In **SMW** all agents can lower their objectives except, once again, \mathcal{A}_4 and \mathcal{A}_5 . However the increase in $C_{\gamma,k}$, from first to last iteration, is lower because theres a general lower c_γ^0 between **SM** and **SMW** scenarios. Again \mathcal{A}_6 and \mathcal{A}_3 are the winners. In **SMWP** finally the two constrained agents are able to lower their cost between iterations. Again, the introduction of PV production proves to be a great benefit, as is the high wind production during the morning timeslots. The last column in Table 4.7 translates the variation between convergence values for **SM** scenario to the convergence ones for **SMWP** scenario. In this case the two constrained agents are the ones that benefit the most from the game and \mathcal{A}_6 and \mathcal{A}_3 are the ones that benefit less. This reinforces the idea that unconstrained agents are able to always search for a better

solution being less vulnerable to RES introduction (or subtraction) and constrained agents are "slaves" to price variation, namely the variations imposed by the other agents
 The following plot shows the \mathcal{M}_6 individual solution

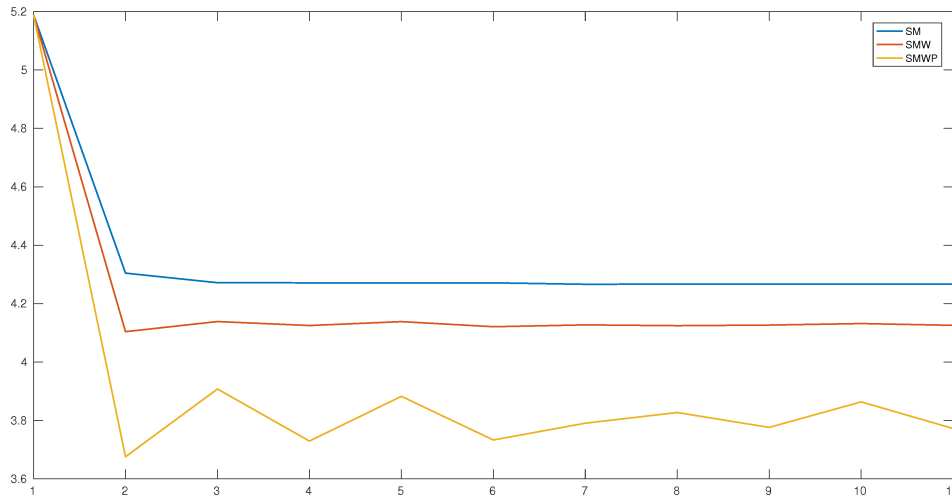


Figure 4.11: \mathcal{M}_6 daily electricity bill, $C_{\gamma,6}$, along iterations

As can be seen, the penetration of RES introduces variability in the \mathcal{M}_6 solutions as noticed by the oscillatory behavior for **SMWP**. Depending on the order of magnitude of the solution they all show this effect to some extent. However, this effect is reduced along iterations mainly because of the influence of other \mathcal{M}_k 's solutions in the whole DR mechanism. The process is a centralized cooperative adaptation one and the mechanism is intended to achieve a final stable solution for all agents involved. But has been seen it does not guarantee the optimality of the solutions found neither the possibility that other, better solutions, could have been achieved through the present DR mechanism. For now it suffices to create a DR mechanism that, for a wide range of situations, converges to a more stable feasible solution.

The following plot shows the evolution of \mathcal{A}_6 specific EV strategy for ω_1^{EV} along scenarios.

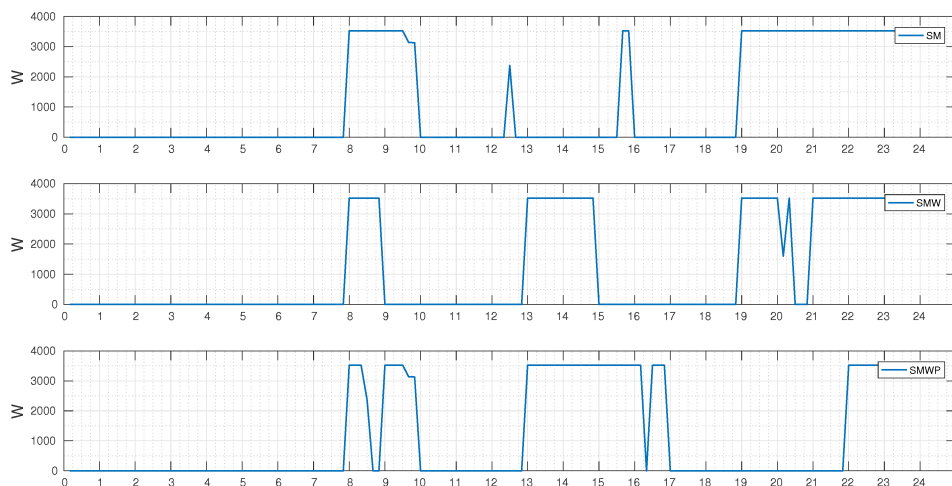


Figure 4.12: \mathcal{M}_6 Electric vehicle profile $P_{\omega,6,t}^{EVc}$ for SM, SMW, SMWP scenarios

The plot clearly shows that \mathcal{A}_6 adapts the EV solution to the RES penetration and it gradually schedules EV at midday. For **SMW** this occurs because there is a peak in wind production between 13h and 14h as shown in Figure 4.8. However, EV is not scheduled at the periods of higher peaks during the morning timeslots because the DR mechanism avoided these timeslots because of the constraint imposition to \mathcal{A}_4 and \mathcal{A}_5 , that raised c_t^f at those periods. In **SMWP** the PV peak production explains the charging strategy found. This opens possibilities to exploit the synergies between EV charging strategies and solar PV production profiles but, obviously, only if \mathcal{M}_k is allowed to search the midday timeslots where the PV production peaks.

Nonetheless, these behaviors only take place if LCOES for PV and WPP, c^{PV} and c^{WT} , are low enough when compared to hourly market prices, c_t^{mrk} , and much more evident if RES production is high enough and can distance c_t^0 from c_t^{mrk} influence. This is what happens during midday timeslots in **SMWP** and morning period in **SMW** and that is precisely what the following plot shows

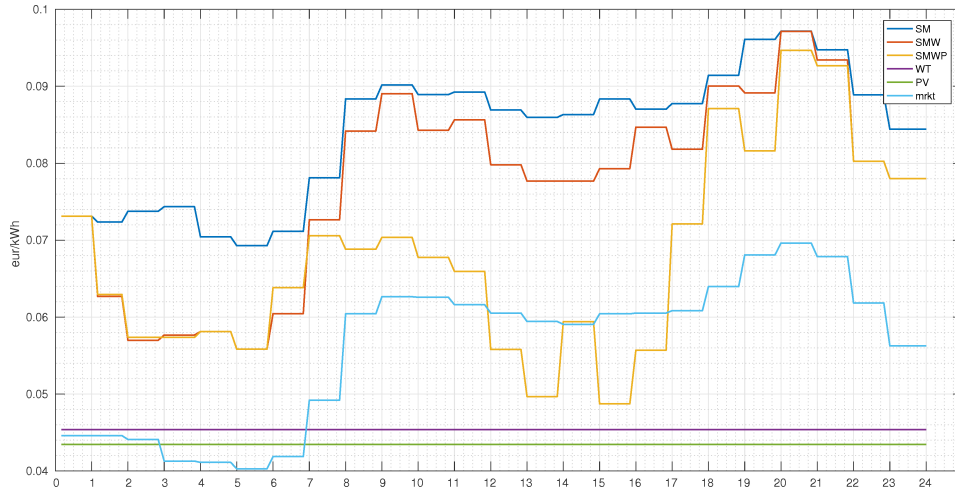


Figure 4.13: Marginal cost of electricity production final solution, c_t^0 , for SM, SMW and SMWP scenarios

The DR mechanism is designed so that c_t^f signal can control the strategies obtained. But the joint influence of low LCOEs for RES and high production profiles for PV and WPP rises the variability of c_t^0 . Therefore, after the definition of a fixed L_t^{ff} for a specific agent in a specific iteration, c_t^0 may have a bigger influence in c_t^f than L_t^{ff} attracting the solutions to low cost timeslots. A conclusion is that DR mechanism is more effective when c_t^0 is more stable since the price signal c_t^f still depends on it and the fixed L_t^{ff} may have less influence on the \mathcal{M}_k behavior

The following plot shows the evolution of load factor.

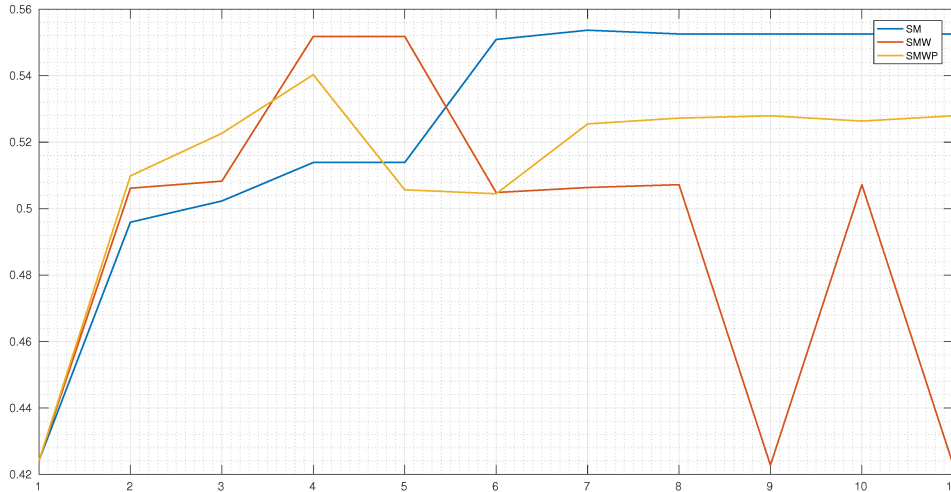


Figure 4.14: Daily mean Load factor L_γ^f final solution for SM, SMW and SMWP scenarios

In terms of mean load factor the best solution is obtained for **SM** with 55%. **SMW** reached 42% and **SMWP** 52%. As expected there is, in general, a rise in L_γ^f along iterations except for **SMW**. There is a clear oscillatory behavior with the introduction of WPP. This oscillation may be due to the fact that some \mathcal{A}_k strategy oscillates due to the variability introduced by RES in the output solutions. This forces the conclusion that the DR mechanism reduces the oscillation but it is not 100% effective and further sensitivity analysis must be made. The best solution was obtained for the scenario in which there is no RES of any kind. This points also to the need of using any possible form of energy storage, associated to the RES production, in order to cope with the referred variability.

4.3 Electric vehicle Schedules

The strategies of \mathcal{A}_k for EVs are mainly defined by $t_{\omega,k,start}^{EV}$ and $t_{\omega,k,end}^{EV}$. To further analyze the impact of time distribution in the solutions obtained two opposed scenarios were defined in Table 4.8.

Table 4.8: Electric vehicle scheduling distribution for Free and Constrained scenario

Scenario	Free (F)						Constrained (C)					
Typology k	1	2	3	4	5	6	1	2	3	4	5	6
$t_{\omega,k,start}^{EV}$ (h)	-	-	0	0	0	0	-	-	0	1	0	8
$t_{\omega,k,end}^{EV}$ (h)	-	-	22	24	24	22	-	-	9	11	8	18

Scenario **F** accounts for an unconstrained time distribution in which all \mathcal{A}_k have the whole day for scheduling. **C** scenario accounts for a constrained situation in which the majority of agents are constrained to charge EVs during the morning time. Agent \mathcal{A}_6 is scheduled during work hours since it is a commercial type. The following plots show the outputs of the 2 scenarios and Table 4.9 shows the variations along iterations and the variation between scenarios

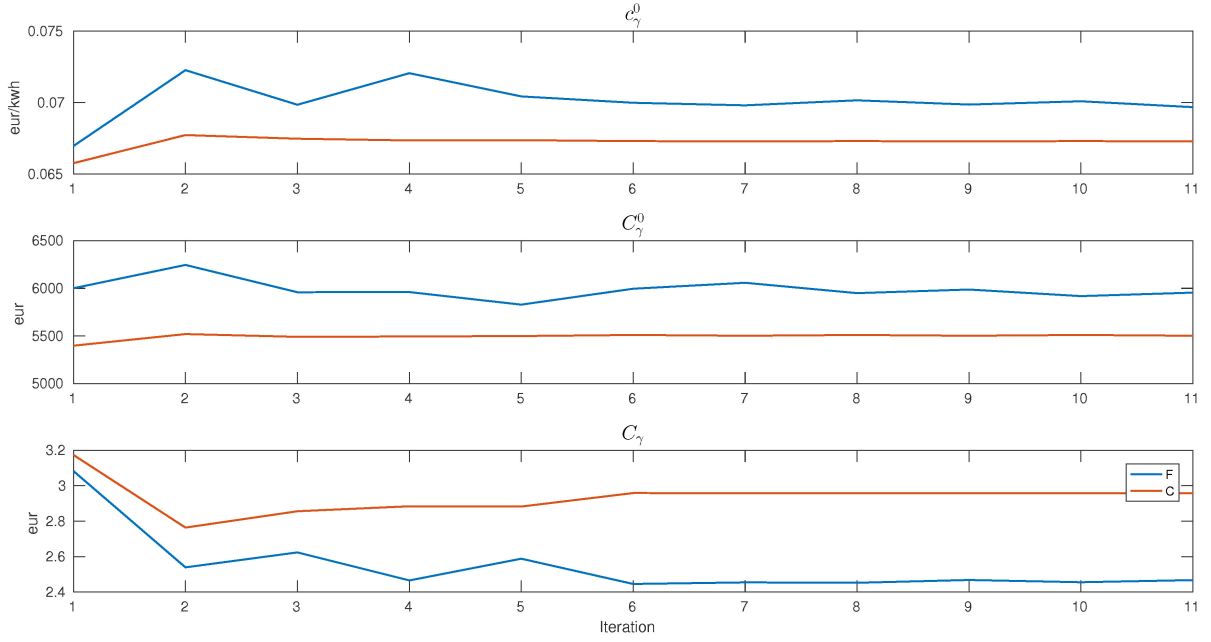

 Figure 4.15: Bi-level variables and solutions for \mathcal{M}_k and \mathcal{M}^0 for **F** and **C** scenarios

 Table 4.9: Percentage variations along iterations for C_γ^0 and c_γ^0

Variable	F	C	F \rightarrow C
C_γ^0	4.1	2.3	3.6
c_γ^0	-0.8	1.9	8.2

Scenario **C** not only converges to a lower c_γ^0 than **F** but it does so in a more steady manner, converging as soon as $\gamma = 2$. The difference between solutions is 8.2 %. The same pattern is observed for C_γ^0 but with a smaller difference of 3.6 % between scenarios. **F** actually can lower its cost by a residual percentage of 0.8 %. Last plot shows that $C_{\gamma,k}$ for **F** decreases along the iteration process while **C** converges to a worst final solution with a difference of 16 % between scenarios. As in the previous case study, the explanation for the stable convergent behavior in scenario **C** steams from the search space for EVs being smaller making it easier to find a final solution. However, for **F** the \mathcal{A}_k agents have the possibility, through the DR mechanism, to search for a lower mean daily cost. Table 4.10 and plot in Figure 4.16 allows us to analyze individual solutions

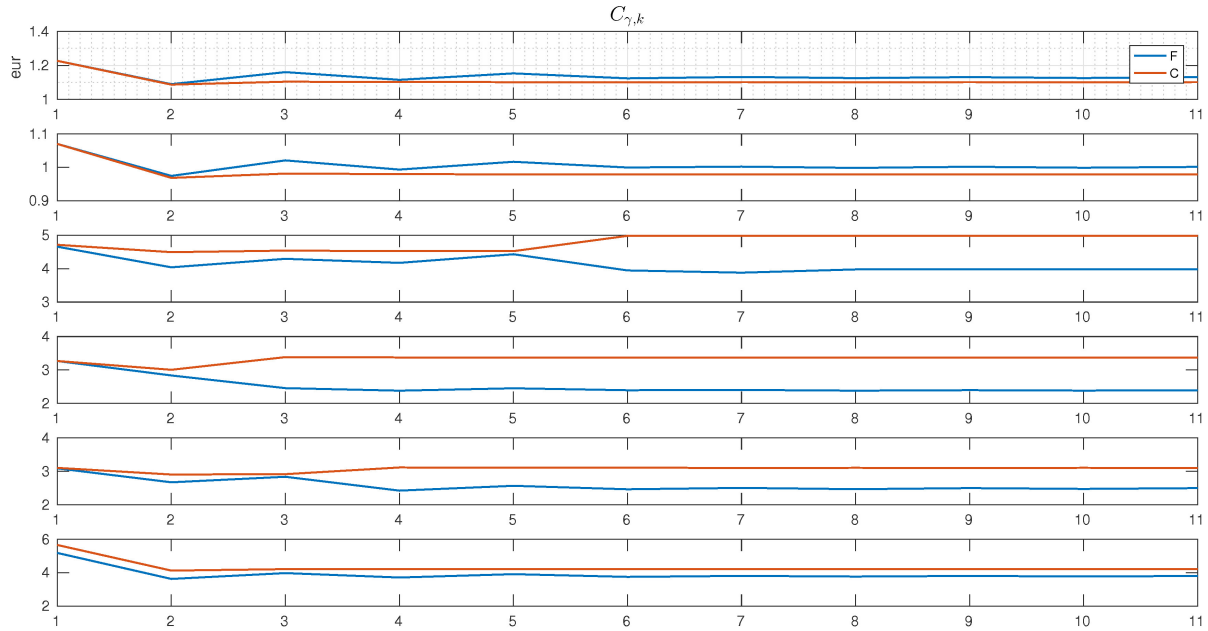

 Figure 4.16: Solutions for \mathcal{M}_k for **F** and **C** scenarios

 Table 4.10: Percentage variations along iterations for $C_{\gamma,k}$

-	F	C	F \rightarrow C
1	-7.9	-10.2	2.6
2	-6.4	-8.5	2.3
3	-14.6	5.7	-20.2
4	-26.7	3.3	-29.0
5	-19.2	-0.1	-19.4
6	-26.6	-25.6	-9.6

Table 4.10 shows that for **F** all agents are able to lower their bills. For **C**, non participating agents have a bigger decrease in $C_{\gamma,k}$ while two out of the three morning constrained agents ($\mathcal{A}_3, \mathcal{A}_4$ and \mathcal{A}_5) increase their bills along iterations while $C_{\gamma,k}$ do decrease by a residual 0.1 % which is the lowest absolute value registered. Again, \mathcal{A}_6 is highly favored by midday periods and it performs the greatest reduction from all agents. What happens is that with such a scheduling distribution all EV load is concentrated in the morning rising c_t^f for those timeslots and lowering it for the afternoon exactly where \mathcal{A}_6 will schedule its load. Concerning the differences between scenarios it must be noticed the fact that differences are computed relative to **C**. It is shown that \mathcal{A}_1 and \mathcal{A}_2 increase their costs and all the remaining agents have reductions. The conclusion is that **C** is more beneficial for non DR participants while **F** is much more beneficial for participant agents. Again, questions of equity may rise from this observation since not all agents have the same search space.

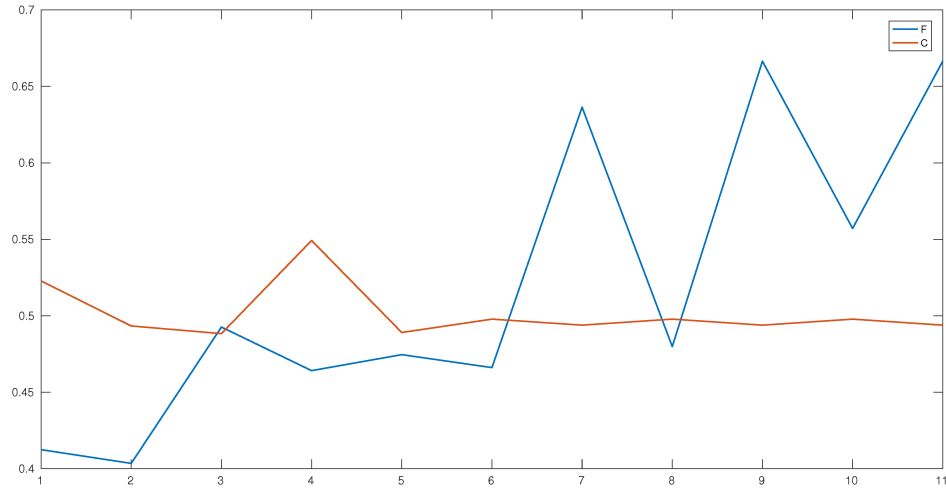


Figure 4.17: Daily mean Load factor L_{γ}^f final solution for **F** and **C** scenarios

Looking at plot in Figure 4.17, the influence of EV schedules distribution in load factor is clear. There is a 61 % increase for **F** and a 5 % decrease in **C**. Between the scenarios, the difference in convergence is 41 %. The DR mechanism is effective in rising the load factor but only for scheduling distributions that actually allow the mechanism to function and distribute the load. The EV load profile final strategy at convergence is showed in the two following plots.

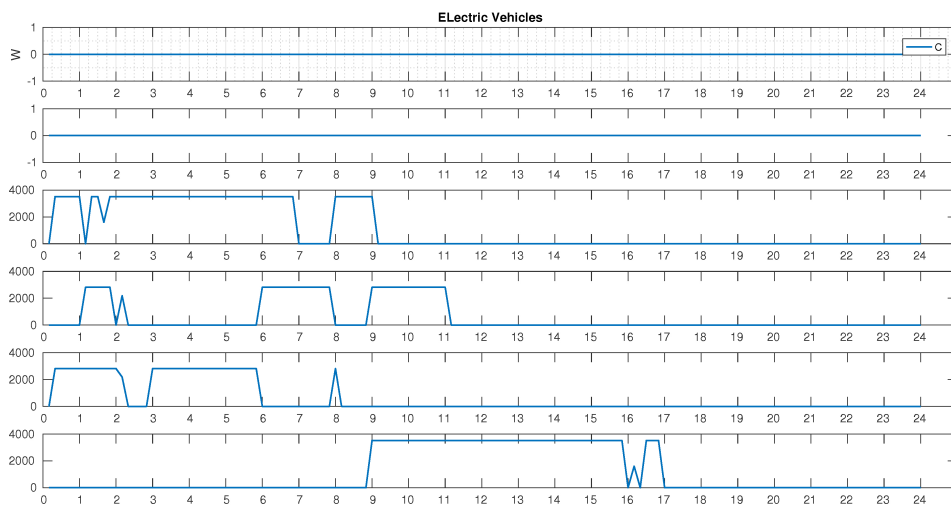


Figure 4.18: All typologies EVs final load profile $P_{\omega,k,t}^{EVc}$ for **C** scenario

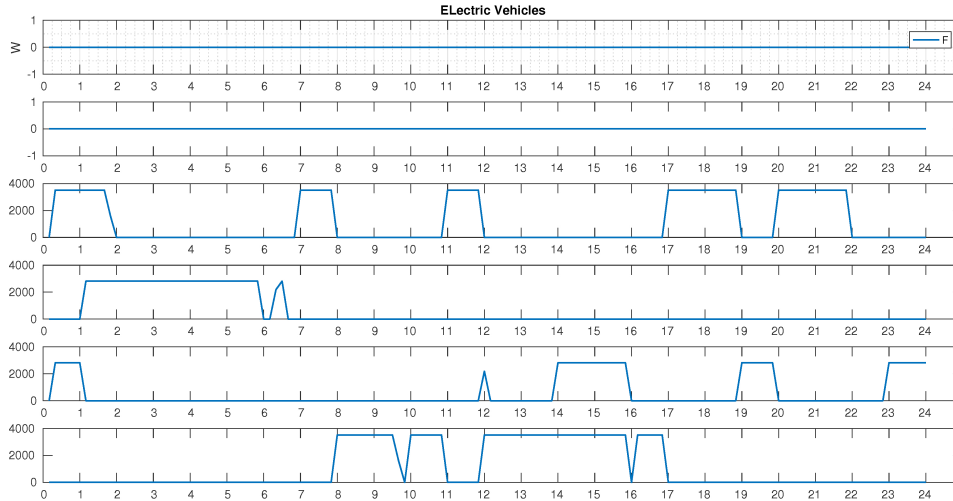


Figure 4.19: All typologies EVs final load profile $P_{\omega,k,t}^{EVc}$ for **F** scenario

The pre-definition of $t_{\omega,start}^{EV}$ and $t_{\omega,end}^{EV}$ can be interpreted as a centralized coordination strategy since \mathcal{A}^0 may impose it to users in order to force \mathcal{M}^0 's objectives and coordination. Case **C** is an example of such a scenario and as can be see from the plot in Figure 4.17 the DR mechanism is not effective in that case. On the contrary, for **F**, $t_{\omega,start}^{EV}$ and $t_{\omega,end}^{EV}$ are not defined since all \mathcal{A}_k have the whole day available. This accounts for a totally decentralized scenario where only the DR mechanism may act to impose coordination. Comparing the two Case Studies one must recall that in Case Study 4.2 what was varying was the renewable generator present while in Case Study 4.3 different scheduling distributions were tested. It can be observed that \mathcal{A}^0 is more sensitive to system configuration than to the scheduling distributions. Considering the linear shape of C^0 and the absence of an explicit capacity charge this is an obvious conclusion. Similarly, the \mathcal{A}_k are extremely sensitive in both case studies. However it can be observed that agents that do not play the game are more affected by system configuration while flexible, or free, ones are always able to perform better than the others.

4.4 DR vs No DR for highly renewable system configuration

A third case study will be considered to further highlight the functionality of the DR mechanism. Considering scenario **F** from the previous case it will now be considered the situation when DR mechanism is disabled. It is in fact an extreme, totally unconstrained scenario that assumes no EV scheduling distribution and does not implement the DR mechanism. The outputs are the following plots

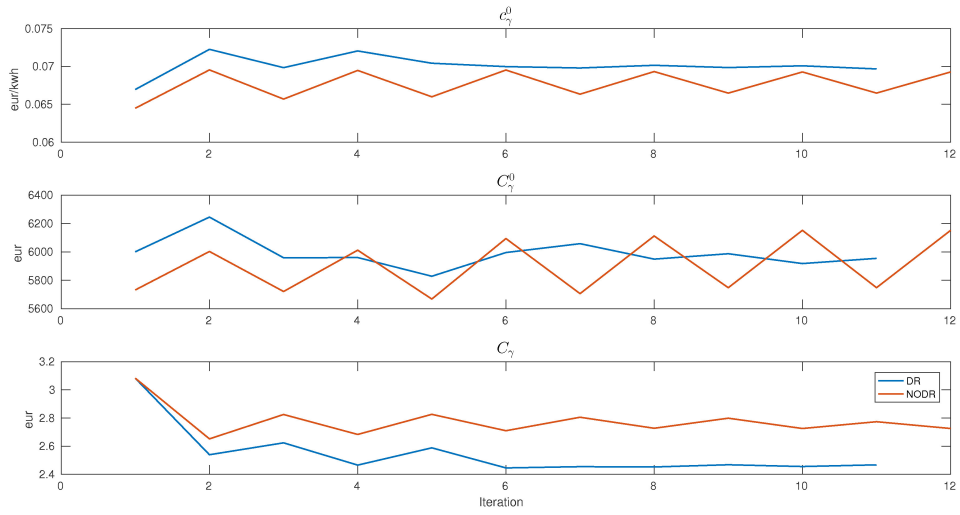


Figure 4.20: Bi-level variables and solutions for \mathcal{M}_k and \mathcal{M}^0 for **F** scenario with and without DR mechanism

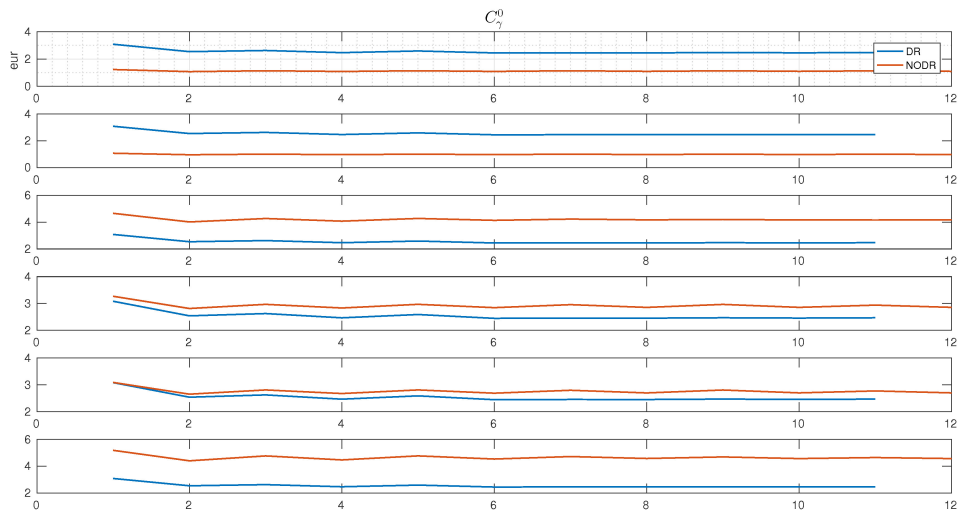


Figure 4.21: Solutions for \mathcal{M}_k for **F** scenario with and without DR mechanisms

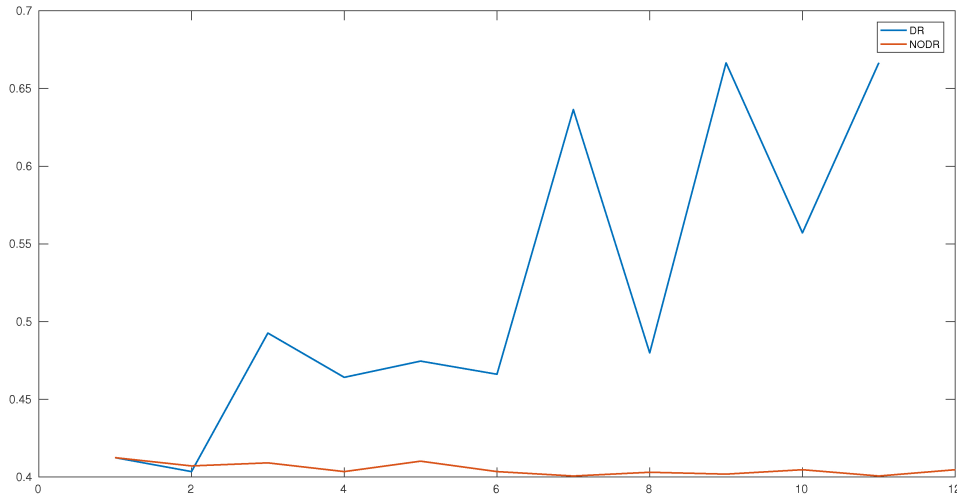


Figure 4.22: Daily mean Load factor L_{γ}^f final solution for **F** scenario with and without DR mechanisms

From Figure 4.20 it is evident that **NODR** is trapped in what have been called the "ping-pong" effect, permanently oscillating between two values for all bi-level variables and not even converging. When looking at the \mathcal{M}_k solutions in the plot in Figure 4.21 it can be seen that the aggregated oscillating behavior in the plot in Figure 4.20 rise from the lower level oscillating behaviors. One of the great features of the DR mechanism is to avoid such a kind of behavior. In particular, the DR mechanism is very beneficial for \mathcal{A}_k agents by lowering their objectives. However, this benefit is not the same for all agents, since the ones that participate in DR game are able to lower their bill but, tragically, there is a great increase in daily bill for non-participating agents that considerably increase their bills even if along iterations it partially decreases. Concerning load factor in Figure 4.22 it is shown that without DR mechanism, typical values are very low and again the DR mechanism proves to be effective in increasing it. The following plots depicts the two final EV load profile strategy for all \mathcal{A}_k

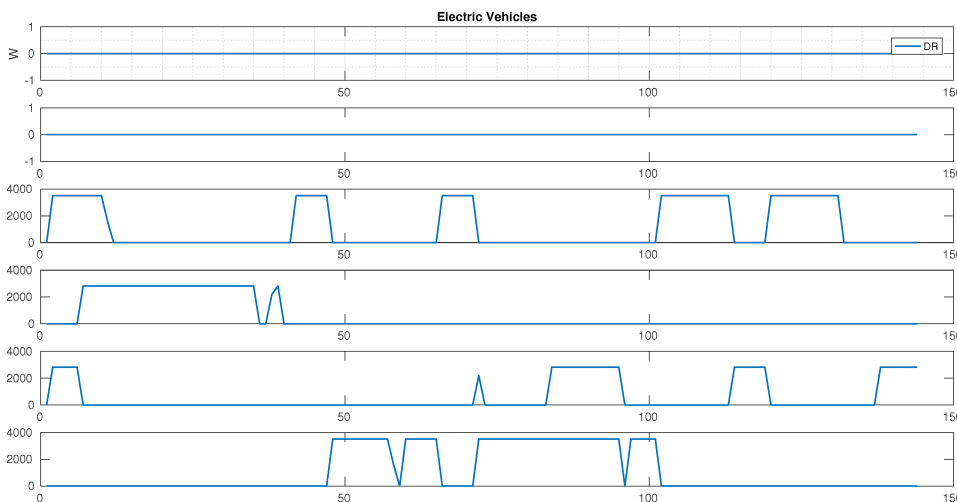


Figure 4.23: All typologies EVs final load profile $P_{\omega,k,t}^{EVc}$ for scenario **F** with DR mechanism

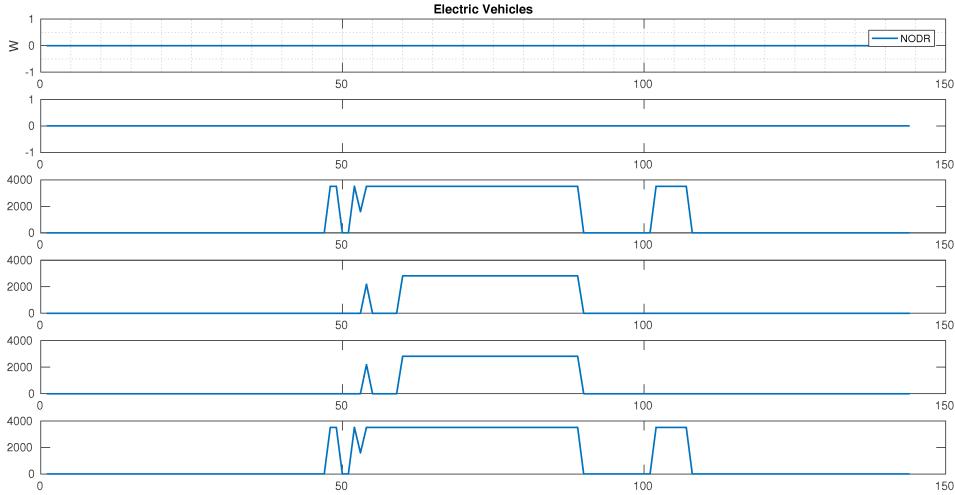


Figure 4.24: All typologies EVs final load profile $P_{\omega,k,t}^{EVc}$ for scenario **F** without DR mechanism

Again it is shown that the DR mechanism forces coordination. The **NODR** solution leads to a situation in which, given an aggregator with a high PV penetration with low LCOE, all \mathcal{A}_k agents will schedule their EVs at the middle of the day thus presenting a perfect illustration of the herding effect as can be seen in Figure 4.24. The DR plot in Figure 4.23 shows exactly the opposite situation in which agents coordinate among them to reach a common strategy that benefits all agents the most, exception made to the ones that do not play the game.

4.5 Results discussion

The present case studies were designed to show the functionalities of the agent-based DR mechanism when applied to real day-ahead load optimization decision problems. The results highlight the potentialities of the model and point out needed refinements.

Tariffs

A deep understanding of the dynamic tariffs structure is essential to implement DR mechanisms since \mathcal{A}_k may be induced do adapt to market prices variations, to local RES production or load factor. depending on the marginal costs c_t^{mkt} , c^{PV} , c^{WT} and LMNF factor L_t^{ff} . The mechanism used is sufficiently versatile to model the tariffs by tweaking its influencing factors in order to model the influence of the competing factors.

Models

The linear and integer optimization models used for appliances in \mathcal{M}_k have shown to respond quite well to the shape of the price signal resulting in the expected scheduling solutions and behaviors. Also the DC power flow, in \mathcal{M}^0 at aggregator level, has proven to be a good choice for modeling and optimization. All used models are simple and easy to compute thus allowing to create a working framework for commercial laptop computers. However the implications of this simplifications at the aggregator level tends to be more problematic since the OPF model, if considered on a complex real situation, would have to consider the full AC power flow

model leading to a non-linear problem which would increase its computational complexity. In a real world implementation of such models one can expect OPF to be solved in grid entities mainframes and appliances models to be solved in home or business smart-meters thus adapting the problem's complexity to the computational resource capacity they need. However future implementations of the framework should focus in better, improved and more realistic models at all system levels but also fully distributed OPF solving methods to lower the computational resources.

Equity

As have been seen, the individual \mathcal{A}_k solutions differ depending on the imposed scheduling time constraints and some agents conditions. Agents that were unconstrained were able to search for better solutions and become less vulnerable to price variations but also the participation in the DR game was determinant to obtain a good solution which raises equity issues with non participating agents being impaired. Flexible agents have a greater possibility to lower its costs but it is simply not fair that the ones that don't own EVs are subjected to the same c_t^0 as the other. This may suggest the introduction of a fair market fixed price for those particular cases, namely by using the initial aggregator price. For this specific point, the presented framework is an excellent starting point since it identifies these questions. Further problems may arise from the fact that q_m is random since theres no criteria or metric to guide the definition of q_m and the sequence order in which agents determine their strategy. This is a source of indetermination since different q_m produce different solutions and we can expect the quality of one solution to be dependent on randomness. The coordination mechanism and algorithms do not specifically address and solve all these equity issues and future efforts must be put in designing equity preserving DR mechanisms.

Demand Response mechanism

DR mechanism proved to be effective in increasing load factor and to induce agents coordination but also to always search for a more stable feasible solution even in the presence of variable RES production and unstable c_t^0 . In any way stability in prices is a greater guarantee for the DR mechanism to work. The proposed approach is the result of the specific framework architecture and thats why it was labeled as *ad-hoc*. The fact that the DR mechanism stands on the communication of different price signals to different consumer agents types may be problematic since there must be a clear understanding of the implications of such differentiation. The power grid has a network structure and the power flow model is composed of nodal equations that would originate a nodal price $c_{i,j}^0$ defined by line reactances $\chi_{i,j}$ and its specific costs. This would place the tone of the coordination algorithm not on consumers \mathcal{A}_k agents but on grid nodes.

Algorithm

Algorithm 2 only evaluates the convergence criteria (2.78) after all typologies are coordinated, i.e, for iteration $\gamma > K + 1$. For $K = 6$ this is a very short time since models are simple and distributed, therefore demanding low computational resources. However if the number of typologies increases, the minimum number of iterations for a convergence may become extremely

high. This is an algorithm's bottleneck that can be solved by aggregating several types or by a nodal demand response mechanism. However the most promising way to solve this problem is to make use of a fully distributed mechanism using P2P distributed consensus mechanism between all consumers or, in the case of a nodal analysis, between nodes in the network.

Chapter 5

Conclusion and future work

In the present work the general structure for an agent-based framework has been defined in order to solve the load optimization problem. The framework was applied to case studies aggregating residential and commercial consumers in power markets with solar and wind local production. Furthermore it is proposed a Demand Response mechanism based on a dynamic tariff in order to force coordination among the \mathcal{A}_k with the intent of increasing the load factor. The framework stands on a mixed approach between the domains of agent-based systems, optimization and game theory applied to power systems specific problems. Although never aiming at advancing the knowledge of the diverse domains used it constitutes a starting point in developing an agent-based general methodology that can be implemented in software and a design tool to address load optimization problems from a SmartGrid point of view in the context of a changing and adapting complex power system where communication capabilities among agents exists. Next paragraphs present final conclusions and future work.

Simulation vs real implementation

The present work presents simulation results for electricity consumption profiles in residential and commercial consumers but also a system architecture to solve a DR model. However, if a real situation of hundreds or thousands of \mathcal{A}_k , acting on behalf of dwelling smart-meters, interact with \mathcal{A}_N and \mathcal{A}^0 , several new problems arise that range from data storage to the need of new real-time, complex aggregation processes and algorithms. In fact, considering only 6 \mathcal{A}_k imposes limits on evaluating the robustness of the proposed methodology under real conditions but it suffices to demonstrate the fundamental functionality of load adaptation through Demand Response. In general, the mechanisms proposed are functional and effective.

Future Work

The future work can be set in two different work pathways. On one hand, to move from abstract and general architectures to real cases. However, the task of finding real data with which new ideas and mechanisms may be tested is not a simple one and it is expected that the present framework, or similar architectures, may begin by being implemented as demonstration projects, in specific laboratory-like implementations on urban or rural zones where all the mechanisms can assertively be tested. On another hand, it is essential that mathematical models and algorithms continue to be studied and researched since there is a number of open questions and problems. Next paragraphs point-out specific possible future work

Aggregator configurations Power production in the aggregator has its origin only in market imports and RES sources. In case studies we have seen that the RES variability induced oscillatory behavior in \mathcal{A}_k solutions that could have been avoided with the introduction of storage systems such as hydroelectric, community storage or EV bulk storage in order to balance the system. This would also allow to test other different day-ahead strategies for market interactions. Testing new aggregator configurations such as regional power systems, microgrids or renewable energy cooperatives is also an area for extensive future research.

Nodal analysis As seen in conclusions, nodal analysis may be considered as the base for the DR mechanism in future researches. One possible solution is a hybrid approach in which there is a nodal-based tariff but also a typology-based tariff. Mixed approaches for this specific question may be an extra guarantee of a smoother aggregated power demand profile.

Tariff design Other design mechanism should be considered, namely EV's specific tariffs to avoid non-Ev owner agents to be dependent on the marginal cost changes induced by EV's.

Diversity To further improve the simulation possibilities and the evaluation of the present framework in real situations, data surveys must be analyzed in order to get a clear characterization of the physical parameters distribution representative of specific regions. However this question exists only for simulation purposes since the privacy protection is a design characteristic of any system. Using statistical distribution of certain parameters may be a viable option towards this end.

Lower level archetypes EV aggregators such as community owned charging stations are viable if higher charging powers and lower charging times are expected to promote EV adoption. In this way specific simulations for such an archetype may be modeled with the present framework where coordination is established between several distributed charging stations agents.

Lower level generation Auto-consumption regimes for PV and small wind turbines may have major influence in the DR solutions found with the present framework. Therefore it is important that future studies focus on this specific context.

Holonic multi-agent system architectures One important potential of the present framework is that \mathcal{A}^0 can be interpreted as a basic unit towards the construction of an holonic multi-agent system. Research can be driven by the idea that \mathcal{A}^0 is a general agent-based architecture comprising a self-contained system with a variable internal configuration in time. Eventually, this configuration can be designed through specific optimization models. Conceiving local energy markets from this perspective may also be a fruitful research direction. Holonic multi-agent energy systems are explored and reviewed in [1] and one possible holonic architecture in the context of the present framework is illustrated in Figure 5

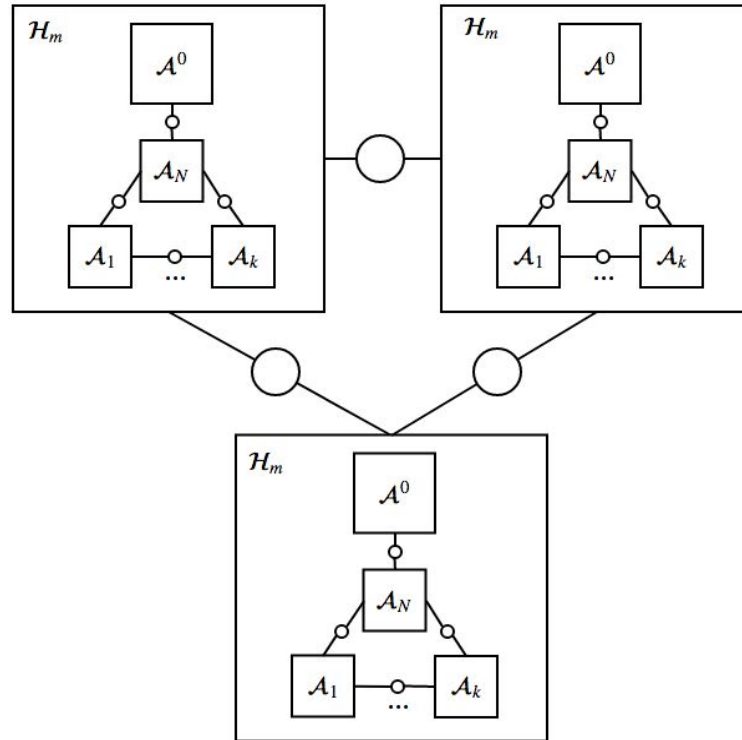


Figure 5.1: Holonic agent-based local electricity market where different \mathcal{A}^0 can exchange power and information between them and coordinate through negotiation by exploring cooperative or non cooperative strategies

Agent negotiation Modeling the relations among agents in MAS pose several future paths for which the present framework can be a contribution. Namely internal negotiations between \mathcal{A}^0 and \mathcal{A}_k towards DR. But, also relations among \mathcal{A}^0 in local market environment or relations among \mathcal{A}_k towards distributed consensus presented in the previous paragraph. The extensive work about GT and negotiation for MAS in [18] and [19] are an important source towards this end.

Distributed optimization models Agent-based distributed optimization is especially interesting for solving BLP. Within this intersection there are innumerable model formulations, innumerable exact methods and evolutionary methods or heuristics yet to be tested for the specific problem of DR and DSM. In the same line of thought, technologies such as *blockchain* and *smart-contracts* are a fruitful research path towards implementing distributed optimization mechanisms.

Software The software used in the present implementation was *MATLAB* and *GAMS*. However future studies with the present framework need to be implemented in MAS specific software such as *JADE* or *SPADE* or ABM specific software such as JAVA based *Repast Symphony* [67] or PYTHON based *MESA* [68]. However, our application is focused in studying the optimization models that constitutes a part of the agents internal reasoning process, on one side, and thinking the load optimization problem from an agent-based architecture point-of-view, on the other. For the present work, it was given priority to modeling

interactions and mathematical modeling rather than to the communication process issues or the practical implementations in computer networks. However, using specific MAS software would allow to use real load data and a specific focus on information exchange might be placed. Nonetheless, MATLAB and GAMS are proprietary software that can pose problems in model distribution for community and academic development. Towards this end open source languages such as PYTHON may be a viable solution in future framework's implementations not only for MAS modeling but for physical models and even for optimization. This conclusion may not be that straightforward for optimization if models become very large. In that case GAMS is a specially fit tool when models become complex. But, in a distributed optimization approach the fundamental idea is that big problems could be decomposed in many small problems.

Bibliography

- [1] S. Howell, Y. Rezgui, J.-L. Hippolyte, B. Jayan, and H. Li, “Towards the next generation of smart grids: Semantic and holonic multi-agent management of distributed energy resources,” *Renewable and Sustainable Energy Reviews*, vol. 77, pp. 193–214, Sep. 2017. DOI: [10 . 1016 / j . rser . 2017 . 03 . 107](https://doi.org/10.1016/j.rser.2017.03.107). [Online]. Available: <https://doi.org/10.1016/j.rser.2017.03.107> (Go back).
- [2] C. Giotitsas, A. Pazaitis, and V. Kostakis, “A peer-to-peer approach to energy production,” *Technology in Society*, vol. 42, pp. 28–38, Aug. 2015. DOI: [10.1016/j.techsoc.2015.02.002](https://doi.org/10.1016/j.techsoc.2015.02.002). [Online]. Available: <https://doi.org/10.1016/j.techsoc.2015.02.002> (Go back).
- [3] A. Barbato and A. Capone, “Optimization models and methods for demand-side management of residential users: A survey,” *Energies*, vol. 7, no. 9, pp. 5787–5824, Sep. 2014. DOI: [10.3390/en7095787](https://doi.org/10.3390/en7095787). [Online]. Available: <https://doi.org/10.3390/en7095787> (Go back).
- [4] A. Soares, A. Gomes, and C. H. Antunes, “Categorization of residential electricity consumption as a basis for the assessment of the impacts of demand response actions,” *Renewable and Sustainable Energy Reviews*, vol. 30, pp. 490–503, Feb. 2014. DOI: [10 . 1016 / j . rser . 2013 . 10 . 019](https://doi.org/10.1016/j.rser.2013.10.019). [Online]. Available: <https://doi.org/10.1016/j.rser.2013.10.019> (Go back).
- [5] J. Garcia-Villalobos, I. Zamora, J. S. Martin, F. Asensio, and V. Aperribay, “Plug-in electric vehicles in electric distribution networks: A review of smart charging approaches,” *Renewable and Sustainable Energy Reviews*, vol. 38, pp. 717–731, Oct. 2014. DOI: [10.1016/j.rser.2014.07.040](https://doi.org/10.1016/j.rser.2014.07.040). [Online]. Available: <https://doi.org/10.1016/j.rser.2014.07.040> (Go back).
- [6] KLENERGY, “Whitepaper for the pylon token sale,” 2017 (Go back).
- [7] E. Munsing, J. Mather, and S. Moura, “Blockchains for decentralized optimization of energy resources in microgrid networks,” in *2017 IEEE Conference on Control Technology and Applications (CCTA)*, IEEE, Aug. 2017. DOI: [10.1109/ccta.2017.8062773](https://doi.org/10.1109/ccta.2017.8062773). [Online]. Available: <https://doi.org/10.1109/ccta.2017.8062773> (Go back).
- [8] S. Hall and K. Roelich, “Business model innovation in electricity supply markets: The role of complex value in the united kingdom,” *Energy Policy*, vol. 92, pp. 286–298, May 2016 (Go back).
- [9] C. Eid, L. A. Bollinger, B. Koirala, D. Scholten, E. Facchinetti, J. Lilliestam, and R. Hakvoort, “Market integration of local energy systems: Is local energy management compatible with european regulation for retail competition?” *Energy*, vol. 114,

- pp. 913–922, Nov. 2016. DOI: [10.1016/j.energy.2016.08.072](https://doi.org/10.1016/j.energy.2016.08.072). [Online]. Available: <https://doi.org/10.1016/j.energy.2016.08.072> (Go back).
- [10] J. Rodriguez-Molina, M. Martinez, J.-F. Martinez, and W. Perez-Aguiar, “Business models in the smart grid: Challenges, opportunities and proposals for prosumer profitability,” *Energies*, vol. 7, no. 9, pp. 6142–6171, Sep. 2014. DOI: [10.3390/en7096142](https://doi.org/10.3390/en7096142). [Online]. Available: <https://doi.org/10.3390/en7096142> (Go back).
- [11] R. V. Moura, “Energy self-consumption policy, the future of distributed renewable generation?” Dissertação de Mestrado, Faculdade de Ciências da Universidade de Lisboa, 2016 (Go back).
- [12] E. A. Kremers, *Modelling and Simulation of Electrical Energy Systems through a Complex Systems Approach using Agent-Based Models*. KIT Scientific Publishing, 2013, ISBN: 3866449461 (Go back).
- [13] X. Yu and Y. Xue, “Smart grids: A cyber–physical systems perspective,” *Proceedings of the IEEE*, vol. 104, pp. 1058–1070, 2016 (Go back).
- [14] M. Wooldridge, *An Introduction to MultiAgent Systems*. Wiley, 2009 (Go back).
- [15] H. Coelho, *Teoria da Agência: Arquitetura e Cenografia*. FCUL, 2008 (Go back).
- [16] P. J. Ireneusz Czarnowski, *Agent-Based Optimization*, ser. Studies in Computational Intelligence 456. Springer-Verlag Berlin Heidelberg, 2013 (Go back).
- [17] K. Leyton-Brown, *Essentials of Game Theory: A Concise, Multidisciplinary Introduction*, ser. Synthesis Lectures on Artificial Intelligence and Machine Learning. Morgan and Claypool Publishers, 2008 (Go back).
- [18] K. L.-B. Yoav Shoham, *Multiagent systems: Algorithmic, game-theoretic, and logical foundations*. Cambridge University Press, 2009, ISBN: 9780521899437 (Go back).
- [19] H. Coelho and F. Lopes, *Negotiation and argumentation in multi-agent systems : Fundamentals, theories, systems and applications*. Bentham Science Publishers Ltd., 2014 (Go back).
- [20] X.-S. Yang, *Engineering Optimization*. John Wiley & Sons, Inc., 2014 (Go back).
- [21] E.-G. Talbi, *Metaheuristics for Bi-level Optimization (Studies in Computational Intelligence)*. Springer, 2013, ISBN: 3642378374 (Go back).
- [22] A. Sinha, P. Malo, and K. Deb, “A review on bilevel optimization: From classical to evolutionary approaches and applications,” *IEEE Transactions on Evolutionary Computation*, vol. 22, no. 2, pp. 276–295, Apr. 2018. DOI: [10.1109/tevc.2017.2712906](https://doi.org/10.1109/tevc.2017.2712906). [Online]. Available: <https://doi.org/10.1109/tevc.2017.2712906> (Go back).
- [23] L. N. Vicente and P. H. Calamai, “Bilevel and multilevel programming: A bibliography review,” *Journal of Global Optimization*, vol. 5, no. 3, pp. 291–306, Oct. 1994. DOI: [10.1007/bf01096458](https://doi.org/10.1007/bf01096458). [Online]. Available: <https://doi.org/10.1007/bf01096458> (Go back).
- [24] M. Barbati, G. Bruno, and A. Genovese, “Applications of agent-based models for optimization problems: A literature review,” *Expert Systems with Applications*, vol. 39, no. 5, pp. 6020–6028, Apr. 2012. DOI: [10.1016/j.eswa.2011.12.015](https://doi.org/10.1016/j.eswa.2011.12.015). [Online]. Available: <https://doi.org/10.1016/j.eswa.2011.12.015> (Go back).

- [25] S. D. J. McArthur, E. M. Davidson, V. M. Catterson, A. L. Dimeas, N. D. Hatziargyriou, F. Ponci, and T. Funabashi, “Multi-agent systems for power engineering applications—part i: Concepts, approaches, and technical challenges,” *IEEE Transactions on Power Systems*, vol. 22, no. 4, pp. 1743–1752, Nov. 2007. DOI: [10.1109/tpwrs.2007.908471](https://doi.org/10.1109/tpwrs.2007.908471). [Online]. Available: <https://doi.org/10.1109/tpwrs.2007.908471> (Go back).
- [26] F. Lopes and H. Algarvio, “Customer load strategies for demand response in bilateral contracting of electricity,” in *E-Commerce and Web Technologies*, Cham: Springer International Publishing, 2014, pp. 153–164, ISBN: 978-3-319-10491-1 (Go back).
- [27] S. Ramchurn, P. Vytelingum, A. Rogers, and N. Jennings, “Agent-based control for decentralised demand side management in the smart grid,” in *10th Int. Conf. on Autonomous Agents and Multiagent Systems – Innovative Applications Track (AA- MAS 2011)*, Tumer, Yolum, Sonenberg and Stone (eds.), May, 2–6, 2011, Taipei, Taiwan, vol. 1, May 2011, pp. 5–12 (Go back).
- [28] B. Ramachandran and A. Ramanathan, “Decentralized demand side management and control of PEVs connected to a smart grid,” in *2015 Clemson University Power Systems Conference (PSC)*, IEEE, Mar. 2015. DOI: [10.1109/psc.2015.7101679](https://doi.org/10.1109/psc.2015.7101679). [Online]. Available: <https://doi.org/10.1109/psc.2015.7101679> (Go back).
- [29] A.-H. Mohsenian-Rad, V. W. S. Wong, J. Jatskevich, R. Schober, and A. Leon-Garcia, “Autonomous demand-side management based on game-theoretic energy consumption scheduling for the future smart grid,” *IEEE Transactions on Smart Grid*, vol. 1, no. 3, pp. 320–331, Dec. 2010. DOI: [10.1109/tsg.2010.2089069](https://doi.org/10.1109/tsg.2010.2089069). [Online]. Available: <https://doi.org/10.1109/tsg.2010.2089069> (Go back).
- [30] S. Abras, S. Pesty, S. Ploix, and M. Jacomino, “Advantages of mas for the resolution of a power management problem in smart homes,” in *Advances in Practical Applications of Agents and Multiagent Systems*, Berlin, Heidelberg: Springer Berlin Heidelberg, 2010, pp. 269–278, ISBN: 978-3-642-12384-9 (Go back).
- [31] F. Ren, M. Zhang, and D. Soetanto, “Agent-based demand management in a power distribution network by considering distributed generations,” in *Agent Based Simulation for a Sustainable Society and Multi-agent Smart Computing*, Springer Berlin Heidelberg, 2012, pp. 109–124. DOI: [10.1007/978-3-642-35612-4_8](https://doi.org/10.1007/978-3-642-35612-4_8). [Online]. Available: https://doi.org/10.1007/978-3-642-35612-4_8 (Go back).
- [32] H. S. V. S. K. Nunna and S. Doolla, “Energy management in microgrids using demand response and distributed storage—a multiagent approach,” *IEEE Transactions on Power Delivery*, vol. 28, no. 2, pp. 939–947, Apr. 2013. DOI: [10.1109/tpwrd.2013.2239665](https://doi.org/10.1109/tpwrd.2013.2239665). [Online]. Available: <https://doi.org/10.1109/tpwrd.2013.2239665> (Go back).
- [33] J. Monteiro, J. Eduardo, P. J. S. Cardoso, and J. Semiao, “A distributed load scheduling mechanism for micro grids,” in *2014 IEEE International Conference on Smart Grid Communications (SmartGridComm)*, IEEE, Nov. 2014. DOI: [10.1109/smartgridcomm.2014.7007659](https://doi.org/10.1109/smartgridcomm.2014.7007659). [Online]. Available: <https://doi.org/10.1109/smartgridcomm.2014.7007659> (Go back).
- [34] P. N. N. Laboratory, “Gridlab-d, a unique tool to design the smart grid,” 2018. [Online]. Available: https://www.gridlabd.org/brochures/20180212_gridlabd_brochure.pdf (Go back).

- [35] M. Yu and S. H. Hong, "Supply–demand balancing for power management in smart grid: A stackelberg game approach," *Applied Energy*, vol. 164, pp. 702–710, Feb. 2016. DOI: [10.1016/j.apenergy.2015.12.039](https://doi.org/10.1016/j.apenergy.2015.12.039). [Online]. Available: <https://doi.org/10.1016/j.apenergy.2015.12.039> (Go back).
- [36] Z. Zhang, R. Deng, T. Yuan, and S. J. Qin, "Bi-level demand response game with information sharing among consumers," *IFAC-PapersOnLine*, vol. 49, no. 7, pp. 663–668, 2016. DOI: [10.1016/j.ifacol.2016.07.252](https://doi.org/10.1016/j.ifacol.2016.07.252). [Online]. Available: <https://doi.org/10.1016/j.ifacol.2016.07.252> (Go back).
- [37] F.-L. Meng and X.-J. Zeng, "A bilevel optimization approach to demand response management for the smart grid," in *2016 IEEE Congress on Evolutionary Computation (CEC)*, IEEE, Jul. 2016. DOI: [10.1109/cec.2016.7743807](https://doi.org/10.1109/cec.2016.7743807). [Online]. Available: <https://doi.org/10.1109/cec.2016.7743807> (Go back).
- [38] A. Kovacs, "Bilevel programming approach to optimizing a time-variant electricity tariff for demand response," in *2016 IEEE International Conference on Smart Grid Communications (SmartGridComm)*, IEEE, Nov. 2016. DOI: [10.1109/smartgridcomm.2016.7778839](https://doi.org/10.1109/smartgridcomm.2016.7778839). [Online]. Available: <https://doi.org/10.1109/smartgridcomm.2016.7778839> (Go back).
- [39] M. Zugno, J. M. Morales, P. Pinson, and H. Madsen, "A bilevel model for electricity retailers' participation in a demand response market environment," *Energy Economics*, vol. 36, pp. 182–197, Mar. 2013. DOI: [10.1016/j.eneco.2012.12.010](https://doi.org/10.1016/j.eneco.2012.12.010). [Online]. Available: <https://doi.org/10.1016/j.eneco.2012.12.010> (Go back).
- [40] S. Mhanna, A. C. Chapman, and G. Verbic, "A fast distributed algorithm for large-scale demand response aggregation," *IEEE Transactions on Smart Grid*, vol. 7, pp. 2094–2107, 2016 (Go back).
- [41] J. Chen and Q. Zhu, "A stackelberg game approach for two-level distributed energy management in smart grids," *CoRR*, vol. abs/1608.08253, 2016 (Go back).
- [42] S. Kim, *Game Theory Applications in Network Design*, ser. Advances in Wireless Technologies and Telecommunication. Information Science Reference, 2014 (Go back).
- [43] L. G. Swan and V. I. Ugursal, "Modeling of end-use energy consumption in the residential sector: A review of modeling techniques," *Renewable and Sustainable Energy Reviews*, vol. 13, no. 8, pp. 1819–1835, Oct. 2009. DOI: [10.1016/j.rser.2008.09.033](https://doi.org/10.1016/j.rser.2008.09.033). [Online]. Available: <https://doi.org/10.1016/j.rser.2008.09.033> (Go back).
- [44] A. Sa, R. A. Lopes, and J. Martins, "Design of an agent-based simulator for real-time estimation of power consumption/generation in residential buildings," in *IECON 2015 - 41st Annual Conference of the IEEE Industrial Electronics Society*, IEEE, Nov. 2015. DOI: [10.1109/iecon.2015.7392698](https://doi.org/10.1109/iecon.2015.7392698). [Online]. Available: <https://doi.org/10.1109/iecon.2015.7392698> (Go back).
- [45] I. Richardson, M. Thomson, D. Infield, and C. Clifford, "Domestic electricity use: A high-resolution energy demand model," *Energy and Buildings*, vol. 42, no. 10, pp. 1878–1887, Oct. 2010. DOI: [10.1016/j.enbuild.2010.05.023](https://doi.org/10.1016/j.enbuild.2010.05.023). [Online]. Available: <https://doi.org/10.1016/j.enbuild.2010.05.023> (Go back).

- [46] C. Sandels, J. Widen, and L. Nordstrom, “Forecasting household consumer electricity load profiles with a combined physical and behavioral approach,” *Applied Energy*, vol. 131, pp. 267–278, Oct. 2014. DOI: [10.1016/j.apenergy.2014.06.048](https://doi.org/10.1016/j.apenergy.2014.06.048). [Online]. Available: <https://doi.org/10.1016/j.apenergy.2014.06.048> (Go back).
- [47] R. Castro, “Energia solar fotovoltaica,” in *Uma Introdução às Energias Renováveis: Eólica, Fotovoltaica, Mini-Hídrica*, ed. by ISTPress. 2012, pp. 363–373 (Go back).
- [48] R. Castanho, “Análise de sensibilidade da capacidade de transporte da rede elétrica ao aumento da produção renovável distribuída: Desenvolvimento de modelos de otimização,” Dissertação de Mestrado, Faculdade de Ciências da Universidade de Lisboa, 2017 (Go back).
- [49] B. M. Zagros Shahooei Guna R. Bharati, *Economic load dispatch and optimal power flow in power system - numerical optimization final project*, 2013. [Online]. Available: www.math.mtu.edu/~struther/Courses/.../MA5630_FinalProject_Optimization.pdf (Go back).
- [50] I. Apolinario, N. Felizardo, A. Garcia, P. Oliveira, A. Trinidad, and P. Verdelho, “Determination of time-of-day schedules in the portuguese electric sector,” in *2006 IEEE Power Engineering Society General Meeting*, IEEE, 2006. DOI: [10.1109/pes.2006.1709487](https://doi.org/10.1109/pes.2006.1709487). [Online]. Available: <https://doi.org/10.1109/pes.2006.1709487> (Go back).
- [51] B. Dupont, C. D. Jonghe, K. Kessels, and R. Belmans, “Short-term consumer benefits of dynamic pricing,” in *2011 8th International Conference on the European Energy Market (EEM)*, IEEE, May 2011. DOI: [10.1109/eem.2011.5953011](https://doi.org/10.1109/eem.2011.5953011). [Online]. Available: <https://doi.org/10.1109/eem.2011.5953011> (Go back).
- [52] T. K. Wijaya, T. G. Papaioannou, X. Liu, and K. Aberer, “Effective consumption scheduling for demand-side management in the smart grid using non-uniform participation rate,” in *2013 Sustainable Internet and ICT for Sustainability (SustainIT)*, IEEE, Oct. 2013. DOI: [10.1109/sustainit.2013.6685188](https://doi.org/10.1109/sustainit.2013.6685188). [Online]. Available: <https://doi.org/10.1109/sustainit.2013.6685188> (Go back).
- [53] varios. (2017). General algebraic modeling system, [Online]. Available: www.gams.com (Go back).
- [54] N. A. (auth.), *Nonlinear Optimization Applications Using the GAMS Technology*, ser. Springer Optimization and Its Applications 81. Springer US, 2013 (Go back).
- [55] B. A. McCarl, *Mccarl gams user guide*, 2008 (Go back).
- [56] P. Nunes, “Enabling solar electricity with electric vehicles in future energy systems,” Tese de doutoramento, Sistemas Sustentáveis de Energia, Universidade de Lisboa, Faculdade de Ciências, 2015 (Go back).
- [57] M. O. Panão, S. Camelo, and H. Gonçalves, “Cost-optimal study for new residential buildings in portugal,” Direção Geral de Energia e Geologia, Relatório, 2013 (Go back).
- [58] M. Almeida, *Cost-optimal solutions for portugal residential buildings*, Presentation, 2015 (Go back).
- [59] DGEG, “Inquérito ao consumo de energia no sector doméstico 2010,” Statistical Report, 2011 (Go back).

- [60] ERSE. (2017). Perfis de consumo, [Online]. Available: <http://www.erse.pt> (Go back).
- [61] S. Fonseca, “Caracterização do consumo de energia no sector residencial em portugal,” Dissertação de Mestrado, Instituto Superior Técnico, 2015 (Go back).
- [62] EDP. (2017). Tarifas transitórias, [Online]. Available: <https://www.edpsu.pt/pt/particulares/tarifasehorarios/BTN/Pages/TarifasBTNate20.7kVA.aspx> (Go back).
- [63] I. N. de Estatística, “Estatísticas da construção e habitação 2010,” Statistical Report, 2011 (Go back).
- [64] IRENA. (2016). Irena data and statistics - lcoe 2010-2016, [Online]. Available: <http://resourceirena.irena.org/gateway/dashboard/?topic=3&subTopic=1057> (Go back).
- [65] ERSE, “Tarifas e preços para a energia elétrica e outros serviços em 2017,” ERSE, Tech. Rep., 2016 (Go back).
- [66] OMIE. (2017). 29 june 2017 hourly electricity prices, [Online]. Available: <http://www.omel.es/files/flash/ResultadosMercado.swf> (Go back).
- [67] A. N. Laboratory. (2016). Repast simphony, [Online]. Available: https://repast.github.io/repast_simphony.html (Go back).
- [68] P. M. Team. (2016). Mesa: Agent-based modeling in python 3+, [Online]. Available: <https://mesa.readthedocs.io/en/latest/> (Go back).
- [69] FMC. (2017). Fundamental modeling concepts, [Online]. Available: <http://www.fmc-modeling.org/> (Go back).
- [70] A. Knöpfel, *Fmc quick introduction*, 2007. [Online]. Available: <http://www.fmc-modeling.org/download/quick-intro/FMC-QuickIntroduction.pdf> (Go back).
- [71] R. Apfelbacher and A. Rozinat. (2003). Fundamental modeling concepts (fmc) notation reference, [Online]. Available: http://www.fmc-modeling.org/download/notation_reference/FMC-Notation_Reference.pdf (Go back).
- [72] R. Apfelbacher. (2005). Compositional structures block diagrams - reference sheet, [Online]. Available: http://www.fmc-modeling.org/download/notation_reference/Reference_Sheet-Block_Diagram.pdf (Go back).
- [73] R. Apfelbacher and A. Rozinat. (2005). Dynamic structures petri nets (1/2) - basic reference sheet, [Online]. Available: [http://www.fmc-modeling.org/download/notation_reference/Reference_Sheet-Petri_Net_\(1\).pdf](http://www.fmc-modeling.org/download/notation_reference/Reference_Sheet-Petri_Net_(1).pdf) (Go back).
- [74] T. L. Bergman, A. S. Lavine, F. P. Incropera, and D. P. DeWitt, “Fundamentals of heat and mass transfer,” in, 7th ed. John Wiley & Sons, Inc., 2011, ch. 5.1, p. 280 (Go back).
- [75] F. M. da Silva, *Apontamentos de disciplina de aerodinamica (fcul/lneg)*, 2016 (Go back).
- [76] H. Pina, *Metodos Numéricos*. McGraw-Hill Portugal, 1995, p. 79 (Go back).
- [77] N. P. S. Corp, *Northwind 100 technical specification*, 2018 (Go back).
- [78] S. Frank, I. Steponavice, and S. Rebennack, “Optimal power flow: A bibliographic survey i,” *Energy Systems*, vol. 3, no. 3, pp. 221–258, Apr. 2012. DOI: [10.1007/s12667-012-0056-y](https://doi.org/10.1007/s12667-012-0056-y). [Online]. Available: <https://doi.org/10.1007/s12667-012-0056-y> (Go back).

- [79] M. Ferris, R. Jainy, and S. Dirkse, “Gdxmlrw: Interfacing gams and matlab,” *Renewable and Sustainable Energy Reviews*, 2010. [Online]. Available: <http://pages.cs.wisc.edu/~ferris/matlab/gdxmlrw.pdf> (Go back).
- [80] (2017). Optimization with gams, [Online]. Available: <http://www.gamsoptimization.com/gams-and-matlab/> (Go back).
- [81] J. Dorfner. (2017). Gams and how to use it from matlab. version 0.1, Institute for Renewable and Sustainable Energy Systems, Technische Universität München, [Online]. Available: <https://gams-matlab.readthedocs.io/en/latest/index.html> (Go back).
- [82] OpenRenewables, *Open 2xx-pm60 datasheet*, 2018 (Go back).
- [83] DEGGE, *Meteorological station campus solar fcul*, Departamento de Engenharia Geográfica, Geofísica e Energia. [Online]. Available: <https://ciencias.ulisboa.pt/pt/esta%C3%A7%C3%A3o-meteorol%C3%B3gica> (Go back).
- [84] G. C. da Graça, A. Augusto, and M. M. Lerer, “Solar powered net zero energy houses for southern europe: Feasibility study,” *Solar Energy*, vol. 86, no. 1, pp. 634–646, Jan. 2012. DOI: 10.1016/j.solener.2011.11.008. [Online]. Available: <https://doi.org/10.1016/j.solener.2011.11.008> (Go back).
- [85] EDP. (2018). Perfis de consumo, de produção e de autoconsumo para o ano de 2018, [Online]. Available: https://www.edpdistribuicao.pt/pt/comercializador/DisponibilizacaoDadosdeEnergia/Dados/EDP_Digital_Consumo_2018.xls (Go back).

Chapter 6

Annexes

6.1 Fundamental Modeling Concepts

Fundamental Modeling Concepts [69] is a way to think and communicate about complex systems and a framework for the comprehensive description of software intensive systems. It presents an universal graphical notation towards the visualization of modeling concepts and structures [70],[71]. FMC distinguishes three structure types namely, *Compositional*, *Dynamic* and *Value-Range* structures. For that uses *Block-Diagrams*, *Petri-Nets* and *Entity-Relationship Diagrams*. FMC is a formal way to model and think agent-based systems architecture.

Compositional Structures with Block Diagrams FMC block diagrams show the compositional structures as a composition of collaborating components. *Agents* are active system components represented by squares. Storage and channels are passive systems components and are represented by ellipses. Active components may have read or write access to passive ones in order to store data. Channels are represented by arrows and are used to communicate data. Storage and channels are virtual locations where information can be observed. In [72] the reference sheet for block diagrams may be consulted

Dynamic Structures with Petri-Nets FMC Petri-Nets represent the system behavior over time depicting the actions performed by agents. The simplest notation uses squares for transitions, i.e, an action, an event or operation taking place at a given point in time. Circles are used for places, which means a control state or point in the time line. Directed arcs connect transitions and places. Petri nets are used to visualize the behavior of a system over time corresponding to a block-diagram. In [73] the reference sheet for FMC dynamic structures may be consulted.

6.2 Abstraction layers

Functional layer compositional structure represents each agent internal structure from a functional point of view. In Figure 6.1 it is shown the three main blocks of agents involved. K \mathcal{A}_k agents, where we are using the index $k = 1, \dots, K$, one \mathcal{A}_N agent and one \mathcal{A}^0 agent. The internal agent structure is composed by data storage location, data sensor and data processor agents. Data input agents only have write access to storage but processor agent has read/write access. It is a simple structure that highlights what a model's agent need to operate: gather,

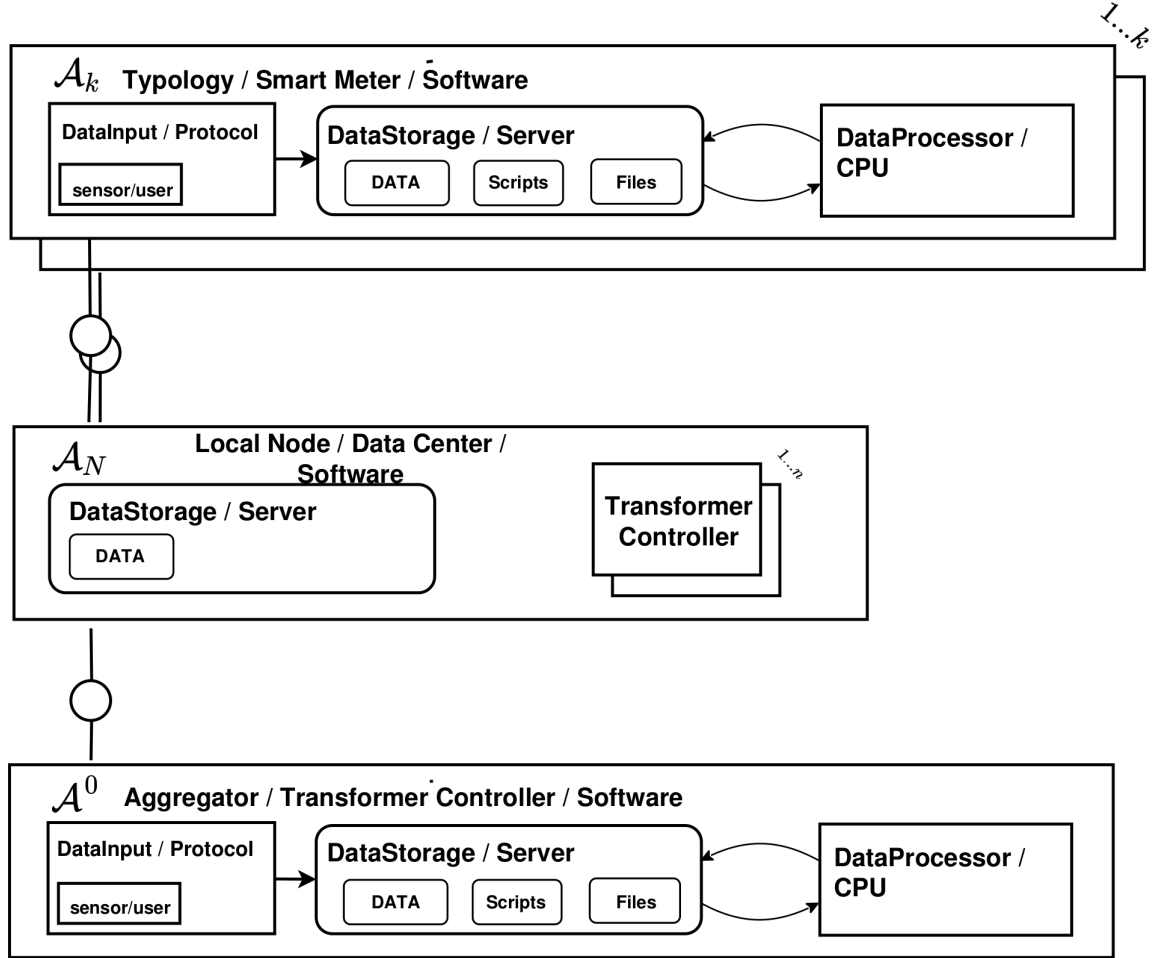


Figure 6.1: Agent framework's compositional structure block diagram

storage, process and output data. Each \mathcal{A}_k function is to compute an individual solutions for DSM model, \mathcal{M}_k , and output day-ahead optimal load diagram but also to communicates with \mathcal{A}_N . This latter agent has the main function of aggregating solutions from typology agents and compute an aggregated load diagram with its \mathcal{M}_N model. Internally it is composed by N agents which represent power grid nodes. \mathcal{A}_N must also evaluate when communication and computing between other agents must stop and solutions must be presented which means that it acts as a mediation or negotiation agent between the other two agents. Agent \mathcal{M}^0 has, essentially, the same internal structure as \mathcal{A}_k but it solves its model \mathcal{M}^0 with its own objectives and it represents a different point in the power grid.

Physical layer represents the actual implementation of the general model in a physical real grid, i.e, where agents would actually "live". Agent \mathcal{A}_k are now implemented in power consuming points at residential, commercial or industrial types. Node agent represents a group of transformers so it could be a computational. It is responsible for managing the aggregated behavior of the N transformers between Aggregator higher voltage levels and typologies lower voltage levels. However, since we are not making a nodal analysis we conceive \mathcal{A}_N as representing a group of

transformers. This agent aggregates data from all the transformers in between levels and for that it needs privileged access to grids information. The agents architecture allows to easily model the case of a single transformer. Agent \mathcal{A}_N is not performing power flow calculations and it acts as an intermediary so it is in direct connection with local transformers. At this point we get to see that voltage levels within a grid are being stepped-up between levels coming from low tensions at typologies levels to higher voltages on upper levels. Agent \mathcal{A}^0 is implemented in the stepping down transformer's controller device, like a distribution grid substation, since it is supposed to control grid operation with \mathcal{M}^0 . It is also a price setting entity or a system operator. Internally all agents follow an approximate similar structure being composed by active inner agents, namely CPU units to perform calculations, sensors and I/O devices and passive locations such as data storages. *Cybernetic layer* is centered on software processes and data types, on one side, and communication processes, on the other. The model's main activity is to gather data from sources, processing it and computing mathematical models solutions from that data. At this point it is important to see that the data formats are data series that should be encoded in signals. In the agents internal structure software modules, protocols, scripts, files and models can be seen.

6.3 Information and privacy in agent-based systems

In the present work the tone is placed on the engineering optimization problems of power grids rather than in the computing and information network problem. However, the proposed methodology makes use of an approach with clear and direct connections to a computer network discussion. The model is a Input/Output one and this means that data and information is inserted into a set of equations, code routines or model solvers, and more information is computed. The results of this computing is sent to agents that, in turn, compute more information through their models. This is the case of some device characteristics, load profiles or climate data forecasts like wind speed or temperatures. In general, real number time-series and real parameters are expected to travel around between agents. Nevertheless, it is understandable that, for a computer network engineer, major technical challenges arise when confronted with the transmission of high volumes on information and data such as, for example, one-minute discretized time-series. The problem becomes hard to handle when a real network is considered with a big number of power grid buses and thousands of smart-meters in communication with each other. The focus, obviously is not on this domain and the agent model will be addressed from a strictly mathematical and physical perspective making use of the data that better fits the problem and formulation. Although the focus is not "how much" information travels through the network the question of "what" information cannot be avoided. The coexistence of different models controlled by different agents that are placed in specific points in the power grid means that agents will access different datasets. Inevitably in a real world implementation of the proposed model there will be information asymmetries since not all information and data-sets are available, at all times, to all agents, since that would raise privacy issues. Data sets such as smart-meter user-defined working schedules, typologies appliances specific data or informations like the number of people in a household are all data that will feed lower level physical models while aggregator agent, for example, have no access to it. As a consequence the agent architecture and the solution approach must be conceived in a way that models don't need all the information at all system's points.

More than that, they should be able to compute solutions using the minimum possible subsets of data. This design requisite reduces the quantity of data that agents must exchange between them in order to cooperate. The communication process between agents must, therefore, take *privacy* as a design feature. Inevitably, questions will arise concerning the impact of such a design feature in the quality and form of the solutions

6.4 Thermal Models

The problem is a transient heat problem since we want to evaluate the thermal dynamics of a certain system in time when some control action, like turning the HVAC system on or off, suddenly takes place. This model should be applicable to any system that fits into its assumptions and in the present case it will be applied to a set of predefined typologies. For that, some assumptions and simplifications must be made concerning the building or refrigerator compartment characteristics that will be called the *thermal volume*. The first assumption is that thermal volumes will be treated as a uniform and continuous volume and that the temperature inside that volume is spatially uniform at any instant during the transient process. Dwellings or refrigeration compartment are, geometrically, a box with a unified volume. This means that the temperature gradients inside that volume are very small and can be neglected or at least assumed to have a very small resistance to conduction inside the volume when compared with external resistance to convection between the volume and its surroundings. This is the basis for the application of *Lumped Capacitance Method* and is extensively described in [74].

The approach must start by considering an overall energy balance inside the volume where it is stated that the rate of change in internal energy, \dot{E}_{int} , must equal the rate of heat transfer through its surface plus the thermal energy that is generated:

$$\dot{E}_{int} = \dot{E}_{th} - \dot{E}_{out} \quad (6.1)$$

The only two factors influencing the temperature inside the volume are the thermal power extracted or inserted, on one hand, and the transfer with external environment, on the other. This means that only HVAC or fridge compressor through exchanges with volume's walls will be influencing temperature. Expanding both sides in the above equation it follows

$$\rho V c \frac{dT}{dt} = p^{th} + \frac{k^{th} A}{L} (T - T^o) \quad (6.2)$$

where p^{th} is the thermal power that HVAC system will put or take from the household or the thermal power that fridge compressor will take from the chamber. Making a variable change $\theta = T - T^o$ and considering that $\frac{d\theta}{dt} = \frac{dT}{dt}$ it follows

$$mc \frac{d\theta}{dt} = p^{th} + \frac{k^{th} A}{L} \theta \quad (6.3)$$

Separating variables and setting $a = \frac{p^{th}}{mc}$ and $b = -\frac{k^{th} A}{mcL}$ it follows

$$\frac{d\theta}{dt} = a - b\theta \quad (6.4)$$

and can integrate between variable limits.

$$\int_{\theta_0}^{\theta_f} \frac{d\theta}{a - b\theta} = \int_{t_0}^{t_f} dt \quad (6.5)$$

Solving the integral it follows

$$-\frac{1}{b} \log\left(\frac{a - b\theta}{a - b\theta_0}\right) = t_f - t_0 \quad (6.6)$$

$t_f - t_0$ is the time period between the two integration limits where the transient analysis is applied. This model to is applied to each timeslot in the time discretization so the definite integral's limits define the time span between two timeslots, i.e the timestep of the discrete-time model. Making $\Delta t = t_f - t_0$ and setting $\tau = \frac{mc}{k^{th}L}$ it follows

$$\frac{a - b\theta}{a - b\theta_0} = e^{-\frac{\Delta t}{\tau}} \quad (6.7)$$

Further defining $\varepsilon = e^{-\frac{\Delta t}{\tau}}$ and arranging equations it follows

$$T_{t_f}^{in} = \varepsilon T_{t_0} + (1 - \varepsilon)(T_{t_f}^o + \beta p^{th}) \quad (6.8)$$

All the parameters defined in equation (6.8) have clear physical meanings and determine the evolution of the system. τ is the system's thermal time-constant which is defined as the time that the system take to reach equilibrium with its surroundings. It is defined as $\tau = \frac{mc}{k^{th}L}$ where m is the mass of the volume we are considering in Kg , c_p the specific heat capacity in $J/Kg^\circ C$ ($m_c = mc_p$ is the Heat capacity or thermal capacitance in $J/^\circ C$), k is the volume thermal conductivity in $W/m^\circ C$ and L the wall thickness in *meters*. $\beta = \frac{1}{k^{th}L}$ is a measure of the temperature change while thermal power is injected or extracted from the solid during one timeslot, i.e the inverse of thermal conductance. β may be also calculated using the overall heat transfer coefficient, U-value, in $W/m^2^\circ C$, a more common technical insulation parameter. ε is the dimensionless systems inertia, a measure of the resistance that the systems shows towards temperature change. Its exponential decay sets the shape of the temperature time evolution.

6.4.1 HVAC characteristics

Table 6.1: HVAC system characteristics

E_k^{cb}	$\eta_{\omega,h}^H$	$\eta_{\omega,c}^H$	$p_{\omega,max}^H$ (W)
ω^H	3.4	3	[100,400,500]

6.4.2 Refrigerator

For a refrigerator $\omega \in E_k^{cb} \subseteq \Omega_k$ the following expression must be considered where the minus sign of the last right-side term indicates that heat is being taken out of the chamber

$$T_{t+1}^{Fr} = \varepsilon^{Fr} T_t^{Fr} + (1 - \varepsilon^{Fr})(T_t^{Fr} - y_{\omega,t}^{Fr} \beta \eta_{\omega}^{Fr} p_{\omega}^{Fr}) \quad (6.9)$$

However in refrigerator the optimal instant power consume is not determined but only optimal sequence of On/Off states that the refrigerator compressor would experience. The objective of refrigerator is to maintain refrigerator chamber temperature (food) within a certain band and

to accomplish that it must work with setpoints $T_{\omega,-}^{Fr}$ and $T_{\omega,+}^{Fr}$. Therefore the following binary variable must be considered

$$y_{\omega,t}^{Fr} = \begin{cases} 1 & \text{if fridge is ON} \\ 0 & \text{if fridge is OFF} \end{cases} \quad (6.10)$$

in order to model the ON/OFF states. The electrical power input p_{ω}^{Fr} is now a design parameter from a particular fridge for a typology. If the refrigerator is at a OFF state in a certain timeslot its power consume will be zero but if it is at a ON state it will be a constant value of p^F during that timeslot. The refrigerator load at each time-slot is given by

$$p_{\omega,t}^{Fr} = y_{\omega,t}^{Fr} p_{\omega}^{Fr} \quad (6.11)$$

6.4.2.1 Refrigerator parameters

The fridge has the following characteristics

Table 6.2: Fridge characteristics

E^{cb}	ω^{Fr}
$V_{\omega}^{Fr} (m^3)$	0.213
$P_{\omega}^{Fr} (W)$	50
η_{ω}^{Fr}	3
$C_{\omega}^{Fr} (J/^{\circ}C)$	2.73×10^4
$K_{\omega}^{Fr} (W/^{\circ}C)$	4.10
$U_{\omega}^{Fr} (W/m^2 \text{ }^{\circ}C)$	0.34
$\tau_{\omega}^{Fr} (s)$	6.6×10^3
$T_{\omega,+}^{Fr} (^{\circ}C)$	5
$T_{\omega,-}^{Fr} (^{\circ}C)$	1
$\varepsilon_{\omega}^{Fr}$	0.91

6.5 Residential storage

For prosumers residential storage will act as an energy management system since we may be considering grid-connected dwellings with commercially available storage technologies. They may be used as a way to lower user electricity bill charging during low-prices time periods or renewable resource abundance, or discharged during high-prices periods or renewable production scarcity. Let $b \in B_k$ be a storage system present in a typology. \mathcal{M}_k must output a solution to the day-ahead charging-discharging strategy of the storage system. Two main variables will be present, $r_{b,t}^c$ and $r_{b,t}^d$, namely charge and discharge rates at each timeslot. A binary variable is defined as:

$$x_{b,t} = \begin{cases} 1 & \text{if } b \text{ is charging at } t \\ 0 & \text{if } b \text{ is discharging at } t \end{cases} \quad (6.12)$$

And they are subjected to the following constraints

$$\begin{cases} 0 \leq r_{b,t}^c \leq r_{b,max}^c x_{b,t} \\ 0 \leq r_{b,t}^d \leq r_{b,max}^d (1 - x_{b,t}) \end{cases} \quad (6.13)$$

(6.13) prevents the storage system to be simultaneously in a charge and discharge state. From the constraint we can see that they cannot be simultaneously positive. It also imposes an upper limit to charging and discharging power through the systems specific parameters $r_{c,max}^b$ and $r_{d,max}^b$. Storage systems also need a State-of-Charge given by

$$SOC_{b,t} = SOC_{b,t-1} + \mu' \left(\eta_b^c r_{b,t}^c - \frac{r_{b,t}^d}{\eta_b^d} \right) \quad (6.14)$$

Where η_b^c e η_b^d are respectively, charge and discharge efficiency. In the beginning of a day some energy must exist in the storage system that could have remained from day before so it needs a initial SOC for $t = 1$

$$SOC_{b,t=1} = SOC_{b,0} \quad (6.15)$$

Optimal operation of storage system imposes that $SOC_{b,t}$ is limited by

$$SOC_{b,min} \leq SOC_{b,t} \leq SOC_{b,max} \quad (6.16)$$

where $SOC_{b,min} = DOD_b SOC_{b,max}$ At the end of the day a certain quantity of energy is available.

$$SOC_{b,t=H} = SO_{b,H} \quad (6.17)$$

$SOC_{b,H}$ may be set to fulfill technical operation standards setting it to $SOC_{b,H} = SOC_{b,min}$ but it can be used to model user preferences, for example, to save a certain quantity of energy for next day.

6.6 Production - Wind power production

To account for decentralized renewable electricity production in \mathcal{M}^0 the power output of one WT will be modeled. The approach will depend on the existence of wind speed time series v_t and the availability of a Power-Curve for WT p_s^{WTPC} . The active power output from a single WT is just

$$P_t^{WT} = p^{WTPC}(v_t^{wt}) \quad (6.18)$$

where v_t^{wt} its the wind speed in m/s measured at the WT hub height z^{wt} , computed using the following *Wind Profile Power Law* taken from [75]

$$v_t^{wt} = v_t^0 \left(\frac{z^{wt}}{z_0} \right)^\alpha \quad (6.19)$$

$$\alpha = a \log(z_0) + b \log(z_0)^2 + c \quad (6.20)$$

Power law is a correction to wind speed measured at one height to a higher high considering reference speed v_t^0 at reference height z_0 . α is a coefficient that depends on atmosphere stability. We want to be able to compute the power output for any wind speed value that shows in time-series. However p_s^{WTPC} is only defined for integer values between $0 \leq s \leq 25$. The solution is to interpolate non-existent values by a first order polynomial using an adaptation of the expression presented in [76]

$$P_t^{WT}(v_t^{wt}) = p_s^{WTPC} \left(\frac{v_{s+1}^{wtPC} - v_t^{wt}}{h_s} \right) + p_{s+1}^{WTPC} \left(\frac{v_t^{wt} - v_s^{wtPC}}{h_s} \right) \quad (6.21)$$

$$v_s^{wtPC} \leq v_t^{wt} \leq v_{s+1}^{wtPC} \quad (6.22)$$

Where $h_s = v_{s+1}^{wtPC} - v_s^{wtPC}$

6.6.1 Wind Power Park

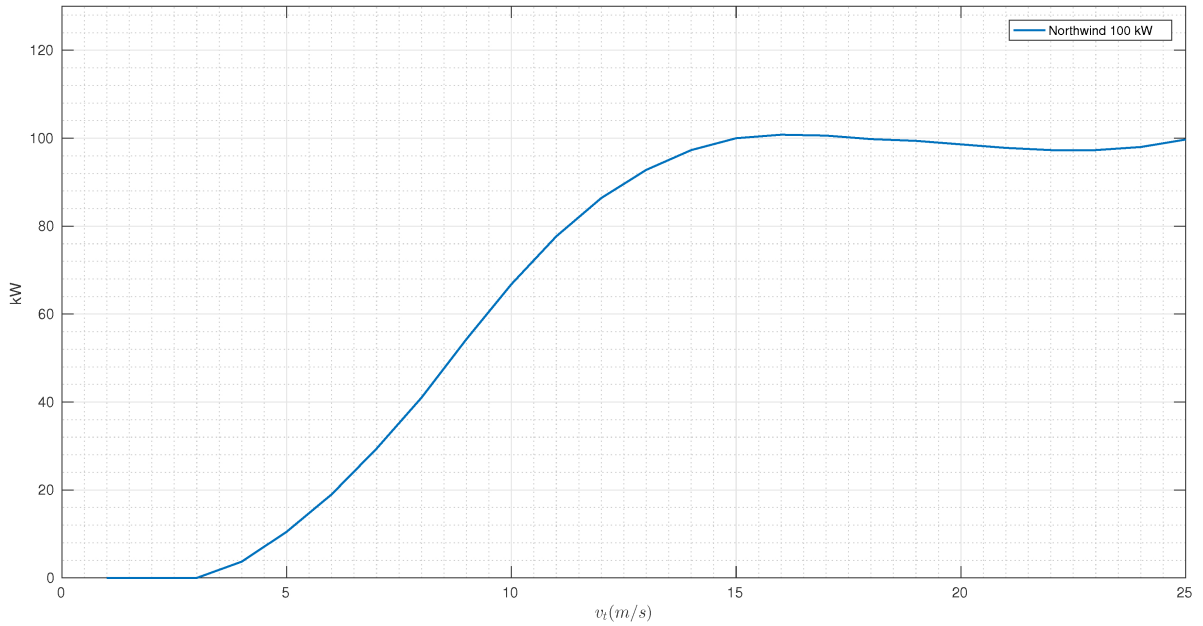


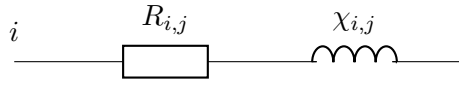
Figure 6.2: NorthWind 100 Power Curve [77]

Table 6.3: NorthWind 100 characteristics [77]

z_{wt} (m)	v_{in}^{wt} (m/s)	v_{out}^{wt} (m/s)	z^{wt} (m)
37	3.5	25	21

6.7 Line model

Considering the simple line model in Figure 6.7



The complex *impedance* from node i to node j is given by $Z_{ij} = R_{ij} + \mathbf{j}\chi_{ij}$, where $\mathbf{j} = \sqrt{-1}$. Considering *admittance* $Y_{ij} = Z_{ij}^{-1}$ we get

$$Y_{ij} = \frac{1}{R_{ij} + \mathbf{j}\chi_{ij}}$$

Considering the line *resistance* R_{ij} and *reactance* χ_{ij} we can multiply and divide by $R_{ij} - \mathbf{j}\chi_{ij}$ we get

$$Y_{ij} = \frac{R_{ij} - \mathbf{j}\chi_{ij}}{(R_{ij} + \mathbf{j}\chi_{ij})(R_{ij} - \mathbf{j}\chi_{ij})} = \frac{R_{ij}}{R_{ij}^2 + \chi_{ij}^2} - \mathbf{j} \frac{\chi_{ij}}{R_{ij}^2 + \chi_{ij}^2}$$

Defining *conductance* G_{ij} and *susceptance* B_{ij} as

$$G_{ij} = \frac{R_{ij}}{R_{ij}^2 + \chi_{ij}^2} \quad (6.23)$$

$$B_{ij} = \frac{\chi_{ij}}{\chi_{ij}^2 + R_{ij}^2} \quad (6.24)$$

both in *Siemens* it follows

$$Y_{ij} = G_{ij} + \mathbf{j}B_{ij}$$

where G_{ij} and B_{ij} are the real and complex components of Y_{ij}

6.8 General Optimal Power Flow

Power transmission at a given timeslot is given by the following equations

$$P_{t,i,j} = V_{t,i}V_{t,j}(G_{ij} \cos(\theta_{t,i} - \theta_{t,j}) + B_{ij} \sin(\theta_{t,i} - \theta_{t,j})), \quad \forall ij : \mathbf{a}_{ij} = 1 \quad (6.25)$$

$$Q_{t,i,j} = V_{t,i}V_{t,i}(B_{ij} \cos(\theta_{t,i} - \theta_{t,j}) - G_{i,j} \sin(\theta_{t,i} - \theta_{t,j})), \quad \forall ij : \mathbf{a}_{ij} = 1 \quad (6.26)$$

where $P_{t,i,j}$ is the active power and $Q_{t,i,j}$ the reactive power. This is a rather simple case and enough for our purposes. At each node, power production, consumption and transit must be balanced at all timeslots

$$\sum_g P_{t,i,g} - \sum_l P_{t,i,l} - \sum_{j:\mathbf{a}_{ij}=1} P_{t,i,j} - \sum_{j:\mathbf{a}_{ij}=1} P_{t,j,i} = 0 \quad \forall ij : \mathbf{a}_{ij} = 1 \quad (6.27)$$

$$\sum_g Q_{t,i,g} - \sum_l Q_{t,i,l} - \sum_{j:\mathbf{a}_{ij}=1} Q_{t,i,j} - \sum_{j:\mathbf{a}_{ij}=1} Q_{t,j,i} = 0 \quad \forall ij : \mathbf{a}_{ij} = 1 \quad (6.28)$$

where $P_{t,i,g}$ and $Q_{t,i,g}$ are the active and reactive generated power by generator g at node i and $P_{t,i,l}$ and $Q_{t,i,l}$ are respectively the active and reactive consumed by load l at node i . Variables assume the following constraints.

$$P_{t,i,j}^{min} \leq P_{t,i,j} \leq P_{t,i,j}^{max} \quad (6.29)$$

$$Q_{t,i,j}^{min} \leq Q_{t,i,j} \leq Q_{t,i,j}^{max} \quad (6.30)$$

$$V_{t,i}^{min} \leq V_{t,i} \leq V_{t,i}^{max} \quad (6.31)$$

$$\delta_{i,j} = \theta_{t,i} - \theta_{t,j} \quad (6.32)$$

$$-\frac{\delta_{i,j}^{max}}{\pi/180} \leq \delta_{t,i,j} \leq \frac{\delta_{i,j}^{max}}{\pi/180} \quad (6.33)$$

This set of equations constitute the constraints for the general form of the *Optimal Power Flow* in the polar form. As a non-linear, non-convex optimization problem the solutions output will depend on the objective function considered [48, pag. 7]. The Most common objectives are the minimization of the power production cost, $C(P_{t,i,g}, Q_{t,i,g})$ a function of the generators power output. For most of the formulations, as is the case of thermal generators, C is a quadratic function or a linear step-wise function [78]. Other objectives, such as minimizing power losses or maximization of the power quality may be considered. There is a plethora of different OPF formulations. In [78] an extensive review not only on different formulations but on solution methods is presented.

6.9 Numerical implementation annexes

6.9.1 Software workflow algorithm

```

1 MatLab General Model Function
2    $\mathcal{M}_k$ 
3     Read DataInput.xls .m .csv                                ▷ Read DataSeries and Parameters
4     Run Scripts.m      ▷ Scripts and functions for physical models; DataSeries processing
5     Write DataToGAMS.gdx                                ▷ Create input file to GAMS
6     GAMS as a MATLAB process
7       Read DataToGAMS.gdx
8       Run Model.gms                                       ▷ CPLEX solves the MIP models
9       Write DataToMat.gdx
10    Read DataToMat.gdx
11    Run Data.m                                           ▷ Process solutions, prepare signals to next model
12   $\mathcal{M}_N$ 
13    Read Data.m
14    Run Model.m                                           ▷ Matrix operations
15   $\mathcal{M}^0$ 
16    Read DataInput.xls .m .csv
17    Run Scripts.m
18    write DataToGAMS.gdx
19    GAMS as a MATLAB process
20      Read DataToGAMS.gdx
21      Run Model.gms                                       ▷ CONOPT solves de NLP model
22      Write DataToMat.gdx
23    Read DataToMat.gdx
24    Run Scripts.m                                       ▷ Process solutions; prepare data to re-enter the cycle
25   $\mathcal{M}_N$  Acting as a mediator
26    if convergence then
27      Run results.m                                       ▷ present plots;tables;figures
28    else if no convergence then
29      go to line 4

```

GAMS reads *GAMS data exchange* (.gdx) files, a platform independent file that stores symbols such as sets, variables and parameters in binary format. However they don't store the model formulation or executable statements [55]. The communication between MATLAB and GAMS is based in the exchange of GDX files. GAMS users created utilities to import and export data through the GDXMRW routines which read and write Matlab variables in to a GDX file after converting into structures [79]. However, GAMS has no visualization features and using the GDXMRW routines alone may be a time consuming task for a dynamic sensitivity analysis and data manipulation. Therefore two sets of freely available, *open source* GDXMRW based MATLAB functions (.m) fulfill these needs. First, the functions available at [80] are specific

MATLAB functions that allow the control of the interaction not only between Matlab and GAMS but also with Microsoft Excell using an easy syntax. GAMS solving process is called as a command line process inside Matlab. Second, the *GAMS.m* [81] is a utility wrapper class for MATLAB that allows for data manipulation and executing GAMS models as MATLAB objects. Both these tools highly increase the potentiality of model building since the MATLAB data treatment capabilities can be coupled with GAMS potential for large scale model solving.

6.9.2 PV production

Table 6.4: PV module characteristics and model parameters [82]

P^{PV} (W)	I^{rcc} (A)	V^{rOC} (V)	I^{rMP} (A)	V^{rMP} (V)	A^{PV} (m^2)	$NOCT$ ($^{\circ}C$)	m	ε
265	8.95	37.85	8.60	30.70	1.6396	48	1.3	1.12

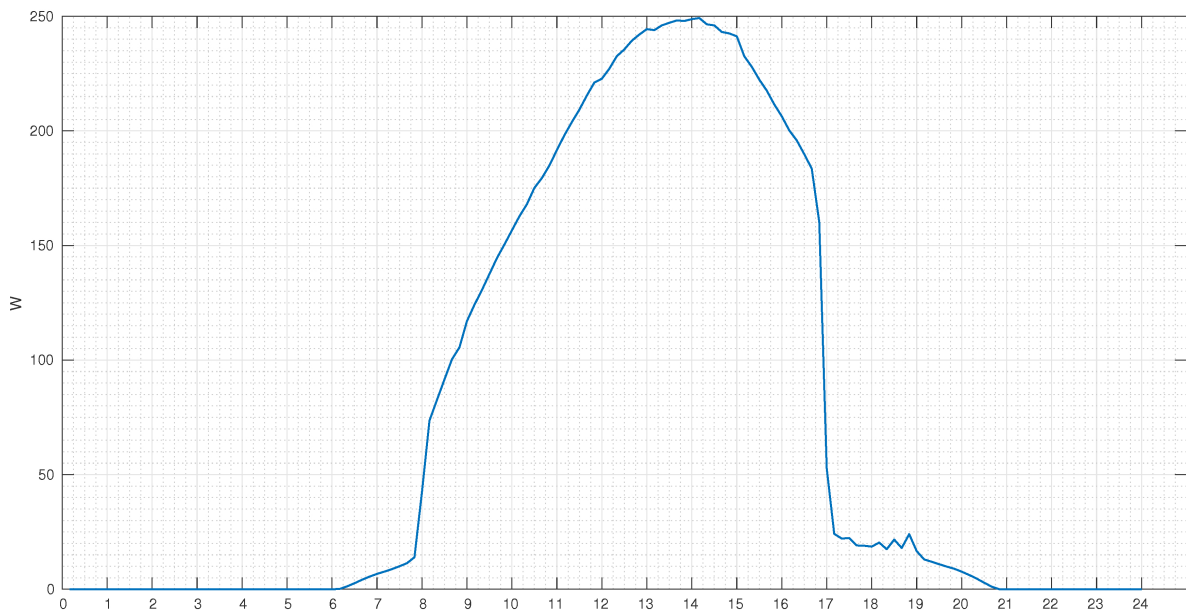


Figure 6.3: 265 W Open Renewables PV module output

6.9.3 Meteorological data

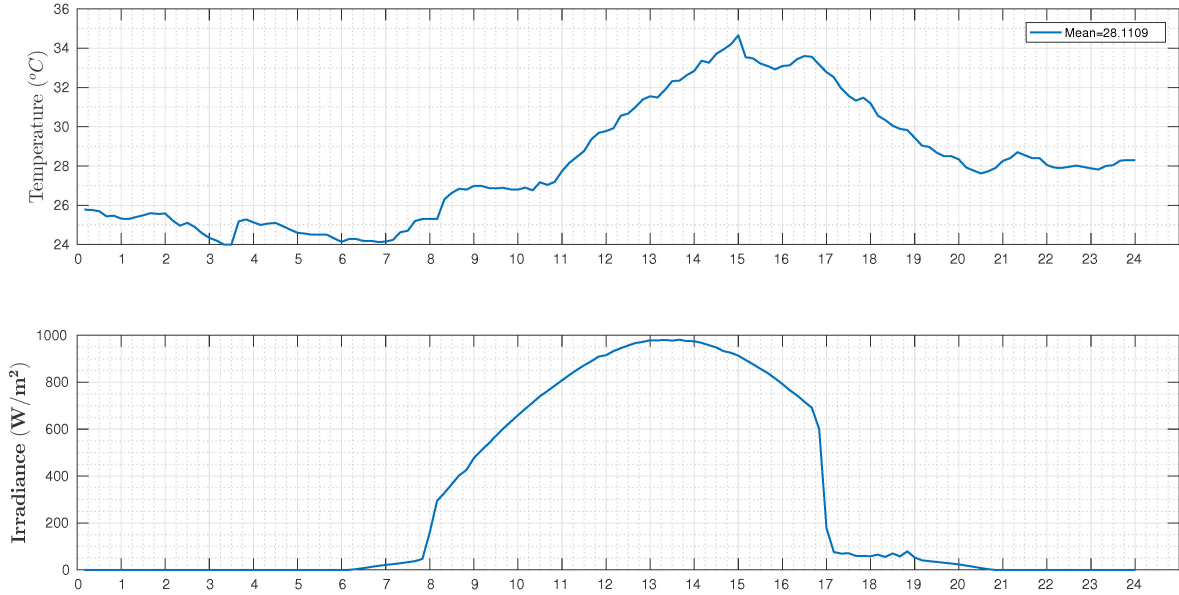


Figure 6.4: Temperature and irradiance time series for a day (font: [83])

6.9.4 Wind speed scenarios

The following plot shows two scenarios for wind speed at the hub height computed using equations (6.19) and (6.20) in Annex 6.6 with the following parameters

Table 6.5: Wind power law parameters(source: [75])

z_0	a	b	c
120×10^{-2}	0.096	0.016	0.24

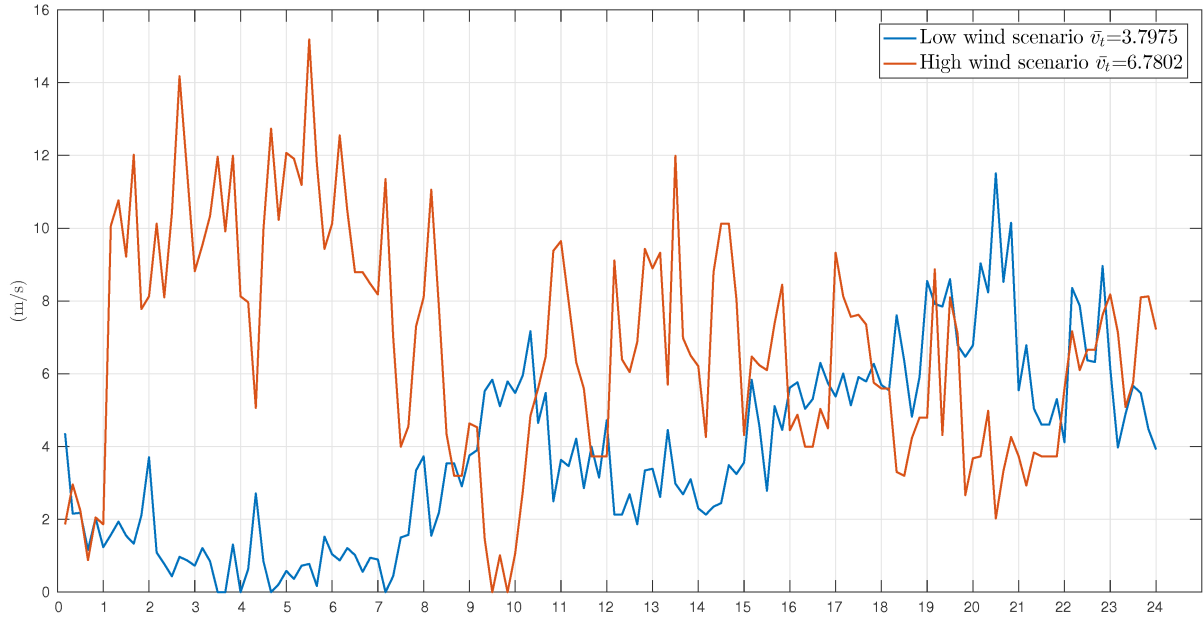


Figure 6.5: Wind resource scenarios at hub height for a general day

6.9.5 Typologies summary

Table 6.6: Typologies physical and thermal characteristics

k (Typology)	1	2	3	4	5	6 (commercial)
Source	[46]	2 story house [57]	Apartment [57]	[84]	[84]	[57]
E_k^F (kWh)	7,58	6,44	7,07	8,03	8,29	10,93
Fixed Load Source [85]	BTN C	BTN A	BTN B	BTN A	BTN B	MT
$E_k^{H_{ele}}$ (kWh)	-	-	-	1,49	1,67	2,89
$E_k^{H_{th}}$ (kWh)	-	-	-	4,48	5,00	8,68
$t_{k,start}^S$ (tslot)	1	1	1	1	1	1
$t_{k,end}^S$ (tslot)	144	144	144	144	144	144
$T_k^{H_{ref}}$	21,00	21,00	21,00	21,00	21,00	21,00
ΔT_k^H	4,00	4,00	4,00	4,00	4,00	4,00
K_k^H ($W/^\circ C$)	30,94	87,84	61,64	30,97	30,97	87,84
η_k^H	0,94	0,96	0,90	0,95	0,95	0,96
C_k^H ($J/^\circ C$)	292382,45	1157834,50	368401,89	385944,83	385944,83	1157834,50
m_k^H (Kg)	290,35	1149,79	365,84	383,26	383,26	1149,79
τ_k^H (s)	9449,98	13180,56	5976,41	12462,70	12462,70	13180,56
$p_{k,max}^H$ (W)	.	-	-	100,00	100,00	500,00
V_k^H (m^3)	250,00	990,00	315,00	330,00	330,00	990,00
$U_{k,floor}^H$ ($W/m^2\ ^\circ C$)	0,40	0,77	0,40	0,41	0,41	0,77
$A_{k,floor}^H$ (m^2)	100,00	165,00	105,00	110,00	110,00	165,00
$U_{k,roof}^H$ ($W/m^2\ ^\circ C$)	0,25	0,56	0,43	0,23	0,23	0,56
$A_{k,roof}^H$ (m^2)	100,00	165,00	105,00	110,00	110,00	165,00
$U_{k,win}^H$ ($W/m^2\ ^\circ C$)	3,00	3,80	3,00	1,80	1,80	3,80
$A_{k,win}^H$ (m^2)	20,00	33,00	21,00	23,00	23,00	33,00
$U_{k,door}^H$ ($W/m^2\ ^\circ C$)	1,50	1,50	1,50	1,50	1,50	1,50
$A_{k,door}^H$ (m^2)	4,00	8,00	8,00	8,00	8,00	8,00
$U_{k,wall}^H$ ($W/m^2\ ^\circ C$)	0,30	0,42	0,34	0,32	0,32	0,42
$A_{k,wall}^H$ (m^2)	79,00	196,12	429,60	97,00	97,00	196,12

6.9.6 Mean conductance for each typology

To compute mean conductance for each typology the following matrices must be considered

$$U_{k,m} = \begin{bmatrix} U_{1,floor}^H & U_{1,roof}^H & U_{1,win}^H & U_{1,door}^H & U_{1,wall}^H \\ U_{2,floor}^H & U_{2,roof}^H & U_{2,win}^H & U_{2,door}^H & U_{2,wall}^H \\ \vdots & \vdots & \vdots & \vdots & \vdots \\ U_{k,floor}^H & U_{k,roof}^H & U_{k,win}^H & U_{k,door}^H & U_{k,wall}^H \end{bmatrix}$$

for heat transfer coefficients, and

$$A_{k,m} = \begin{bmatrix} A_{1,floor}^H & A_{1,roof}^H & A_{1,win}^H & A_{1,door}^H & A_{1,wall}^H \\ A_{2,floor}^H & A_{2,roof}^H & A_{2,win}^H & A_{2,door}^H & A_{2,wall}^H \\ \vdots & \vdots & \vdots & \vdots & \vdots \\ A_{k,floor}^H & A_{k,roof}^H & A_{k,win}^H & A_{k,door}^H & A_{k,wall}^H \end{bmatrix}$$

for construction element's area, where $m = \{floor, roof, win, door, wall\}$. With these two matrices a thermal conductance can be computed for each construction element given by the Hadamard matrix product

$$\mathbf{K}_{k,m}^{th} = U_{k,m} \circ A_{k,m} = \begin{bmatrix} K_{1,floor}^{th} & K_{1,roof}^{th} & K_{1,win}^{th} & K_{1,door}^{th} & K_{1,wall}^{th} \\ K_{2,floor}^{th} & K_{2,roof}^{th} & K_{2,win}^{th} & K_{2,door}^{th} & K_{2,wall}^{th} \\ \vdots & \vdots & \vdots & \vdots & \vdots \\ K_{k,floor}^{th} & K_{k,roof}^{th} & K_{k,win}^{th} & K_{k,door}^{th} & K_{k,wall}^{th} \end{bmatrix}$$

The thermal conductance for each typology is then given by the mean of all construction element, i.e the mean along each line of $K_{k,m}^{th}$

$$\mathbf{K}_k^{th} = \left[K_1^{th} \quad K_2^{th} \quad K_3^{th} \quad K_4^{th} \quad K_5^{th} \quad K_6^{th} \right]^T$$

6.9.7 Adjacency and connection matrices

$$\mathbf{a}_{i,j} = \begin{bmatrix} 0 & 1 & 1 & 1 & 1 \\ 1 & 0 & 0 & 0 & 0 \\ 1 & 0 & 0 & 0 & 0 \\ 1 & 0 & 0 & 0 & 0 \\ 1 & 0 & 0 & 0 & 0 \end{bmatrix} \quad (6.34)$$

$$\mathbf{a}_{l,i}^{load} = \begin{bmatrix} 0 & 1 & 0 & 0 & 0 \\ 0 & 0 & 1 & 0 & 0 \\ 0 & 0 & 0 & 1 & 0 \\ 0 & 0 & 0 & 0 & 1 \end{bmatrix} \quad (6.35)$$

Wind generators connection matrix comes

$$\mathbf{a}_{i,g^{wt}}^{wt} = \begin{bmatrix} 0 \\ 1 \\ 0 \\ 0 \\ 0 \end{bmatrix} \quad (6.36)$$

Power plant connection matrix comes

$$\mathbf{a}_{i,g^{pv}}^{pv} = \begin{bmatrix} 0 \\ 0 \\ 1 \\ 0 \\ 0 \end{bmatrix} \quad (6.37)$$

6.9.8 Aggregation bus example

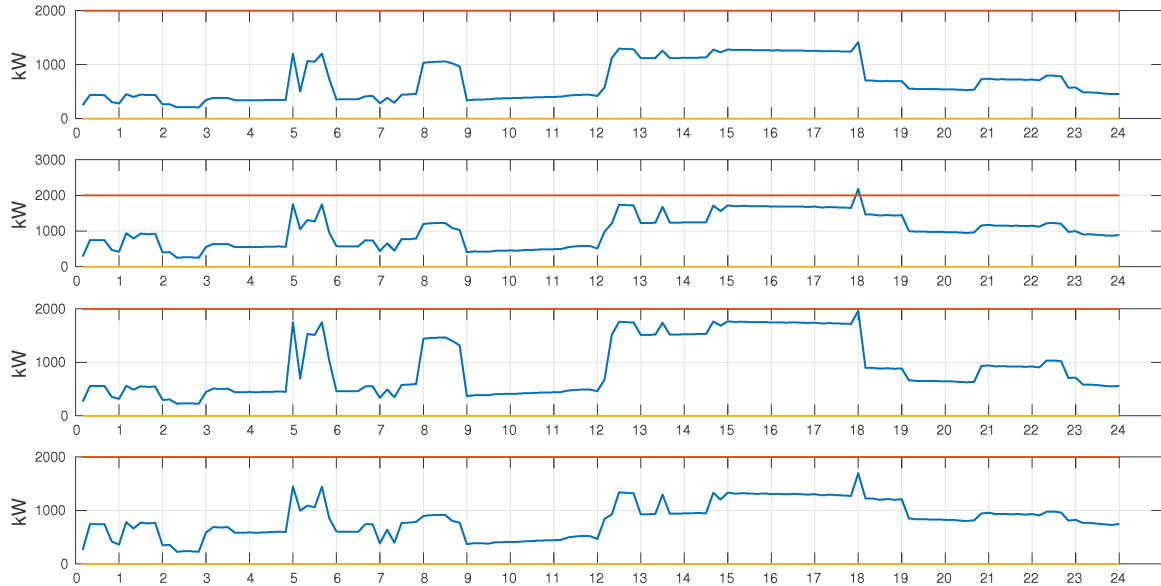


Figure 6.6: Aggregated load at grid buses

In the plot in Figure 6.6 we notice a violation of the maximum transformer capacity at 18h in bus 3 consequence of a peak in load requests. The present implementation of the model does not account for mechanism to deal with violations of the operational limits of the power grid. This means that lower level power requests are not limited and therefore subsequent OPF solve in \mathcal{A}^0 may return unfeasible. Power imports in typologies is limited by $P_k^{LimGrid}$ and nodes are limited by MT-LT transformers installed capacity which can be reached if all typologies elements request the maximum. This situation is never reached because the specific numerical implementation of the present model uses parameters and data sets do not allow. Future implementations of the model must account for some mechanism to deal with infeasibilities in OPF.

6.9.9 Scenarios

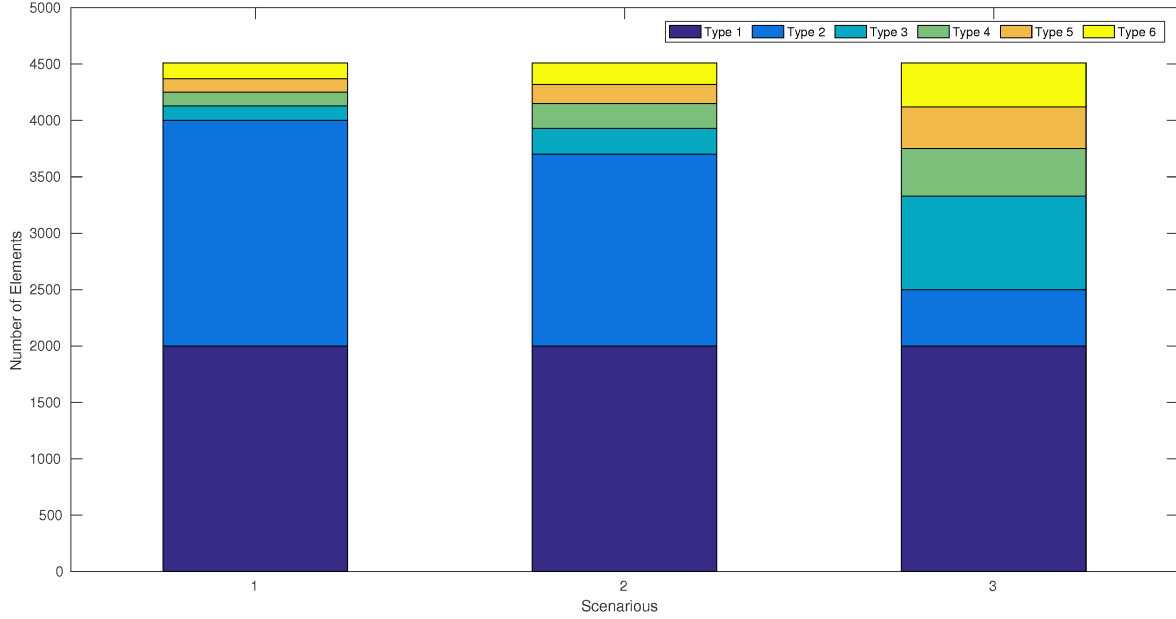


Figure 6.7: Typologies mix for different scenarios

The scenarios increase the variable part of total load. This approach allows to study situations with just a few percentage of the dwellings participating in DR programs or to study the penetration rates of EV's or other technological device.

6.9.9.1 Typologies mix matrices

The corresponding typologies mix matrices for the considered scenarios are the following

$$N_{l,k}^{Vlow} = \begin{bmatrix} 500 & 500 & 0 & 0 & 0 & 0 \\ 500 & 500 & 50 & 60 & 60 & 100 \\ 500 & 500 & 50 & 30 & 30 & 20 \\ 500 & 500 & 30 & 30 & 30 & 20 \end{bmatrix}$$

$$N_{l,k}^{low} = \begin{bmatrix} 500 & 300 & 50 & 50 & 50 & 50 \\ 500 & 400 & 100 & 110 & 60 & 100 \\ 500 & 500 & 50 & 30 & 30 & 20 \\ 500 & 500 & 30 & 30 & 30 & 20 \end{bmatrix}$$

$$N_{l,k}^{central} = \begin{bmatrix} 500 & 200 & 200 & 50 & 50 & 50 \\ 500 & 100 & 200 & 160 & 110 & 150 \\ 500 & 100 & 300 & 80 & 80 & 70 \\ 500 & 100 & 130 & 130 & 130 & 120 \end{bmatrix}$$

6.9.10 Tariffs

General distribution grid access tariff (€/kWh)	τ^{dist}	0.0495	Simple grid access tariff for normal Low tension consumers with contracted $P^{LimGrid} \leq 20.7kVA$
Fixed distribution grid access tariff (€/day)	τ^{fix}	0.2979	Fixed grid access tariff for normal Low tension consumers with contracted power $P^{LimGrid} = 6.9kVA$
Fixed distribution grid access tariff (€/day)	τ^{fix}	0.1986	Fixed grid access tariff for normal Low tension consumers with contracted power $P^{LimGrid} = 4.6kVA$
Active Power commercialization tariff (€/kWh)	τ_A^{com}	0.0030	Commercialization Tariff applied by retailer for normal Low tension consumers
Fixed daily commercialization tariff (€/day)	τ^{com}	0.0176	Commercialization fixed Tariff applied by retailer for normal Low tension consumers

General High Tension grid access tariff (€/kWh)	τ_A^{HT}	0.0246	High Tension grid access tariff for Substation access to High Tension grid
High tension Contracted power tariff (€/kW)	τ^{HTpc}	0.0227	Fixed contracted power grid
High tension Contracted power tariff (€/tslot)	τ_{ts}^{HTpc}	1.5764	Fixed contracted tariff for 10000 kW substation per timeslot $\tau^{HTpc} \times 10000 \frac{dt}{24 \times 60}$